ISBN: 978-3-00-042655-1

Herausgeber:
Bauhaus-Universität Weimar
F. A. Finger-Institut für Baustoffkunde
Professur Werkstoffe des Bauens
Direktor: Prof. Dr.-Ing. Horst-Michael Ludwig

Metakaolin as an Additive in Composite Cement

A thesis presented for the Degree of Doctor of Engineering
At the Faculty of Civil Engineering of the Weimar Bauhaus University

By Thu-Ha Phung-Thi from Hanoi, Vietnam
Master of Engineering, National University of Civil Engineering

Examiners:
Prof. Dr. -Ing. Horst-Michael Ludwig
Prof. Dr.-Ing. habil. Jochen Stark
Prof. Dr.-Ing. Wolfgang Breit

Date of submission: 30.11.2012
Date of examination: 08.05.2013

I would like to express my sincere gratitude to my supervisor Prof. Dr. -Ing. Horst-Michael Ludwig for his excellent and worthy advice to this thesis.

Moreover, I would like to thank all other members in the FIB for experiment supports; especially Dr. rer. nat. Holger Kletti for his excellent and useful discussions; furthermore, Vietnamese and German friends for their helps in English proofreading; especially Dr.-Ing Phuong Nguyen-Thanh and Helen Hoper.

In addition, I extend thanks to MOET, FIB, and DAAD as the three crucial sources for my thesis work.

Last but not least, I dedicate this dissertation to my parents Tho Phung-Van and Dan Le-Thi as well as my mother-in-law Margaretha Giese, my husband Andreas Giese and especially my daughter Esther Giese who are always by my side and encourage me with love and support.

..*Nhoc Giese*…I am sorry.

Weimar, 4.2012

Thu-Ha Phung-Thi

Table of contents

List of Abbreviations

ASR	Alkali Silica Reaction (alkali aggregate reaction)
BET	BET method (Brunauer, Emmett and Teller, 1938)
BET surface	Specific surface area assessed by BET method
CSI	Compressive Strength Index
DSC	Differential Scanning Calorimetry
DTA	Differential Thermal Analysis
HPC	High Performance Concrete
HPM	High Performance Mortar
LOI_{1000}	Loss On Ignition at 1000 ^{o}C
mCh	Modified Chapelle test
SCM	Supplemental Cementitious Material
SEM	Scanning Electron Microscope
SEM-SE	Scanning Electron Microscope – Secondary Electrons
SSA	Specific Surface Area
PSD	Particle Size Distribution
RH	Relative Humidity
TGA	Thermo Gravimetric Analysis
TGA-CaO method	Free lime consumption is calculated by using TGA
UHPC	Ultra-High Performance Concrete
w/b	water to blend (cementitious materials) ratio
w/c	water to cement ratio
Wt.-%	weight percentage
XRD	X-Ray Diffraction
XRD-Rietveld	Quantitive of X-Ray Diffraction with the Rietveld software package TOPAS 4.2
DQKa00	DQK kaolin is calcinated at a00 ^{o}C
DQK*xy*	DQK kaolin is calcinated at 100*x* ^{o}C of the calcinations for *y* hours
HTK*xy*	HTK kaolin is calcinated at 100*x* ^{o}C of the calcinations for *y* hours
HTKa00	HTK kaolin is calcinated at a00 ^{o}C
Free lime	CaO
Lime consumption	Free lime is consumed by the pozzolanic reaction of metakaolin
Lime paste	Free lime or Portlandite + metakaolin + water

List of Symbols

A	aluminium - Al_2O_3
Al^{3+}	aluminium / alumino releasing from metakaolin during pozzolanic reaction
$Al(OH)^-_4$	aluminium releasing during cement hydration process
AS_2	aluminium / alumino, metakaolinite, amorphous phase - $Al_2O_3 \cdot 2SiO_2$
C	calcium oxide, lime or free lime - CaO
CH	calcium hydroxide, portlandite - $Ca(OH)_2$
C-S-H	calcium silicate hydrate - $xCaO \cdot ySiO_2 \cdot zH_2O$
$C_3A \cdot 3C\bar{S} \cdot H_{32}$	ettringite – $Ca_6Al_2(SO_4)_3(OH)_{12} \cdot 26H_2O$ or $3CaO \cdot Al_2O_3 \cdot 3CaSO_4 \cdot 32H_2O$
C_2ASH_8	hydrated gehlenite, stratlingite – $Ca_2Al_2SiO_2(OH)_{10} \cdot 3H_2O$ or $2CaO \cdot Al_2O_3 \cdot SiO_2 \cdot 8H_2O$
C_4AH_{13}	tetracalcium aluminate hydrate - $4CaO \cdot Al_2O_3 \cdot 13H_2O$
$C_3SC–S–H_{15}$	thaumasite - $CaSiO_3 \cdot CaCO_3 \cdot CaSO_4 \cdot 15H_2O$ or $Ca_3Si(OH)_6(CO_3)(SO_4) \cdot 12H_2O$
C_3AH_6	tricalcium aluminate hydrate, hydrogarnet - $3CaO \cdot Al_2O_3 \cdot 6H_2O$
$C_4A\bar{C}H_{11}$	mono-carbonate - $3CaO \cdot Al_2O_3 \cdot CaCO_3 \cdot 11H_2O$
$C_4A\bar{C}_{0.5}H_{11}$	hemi-carbonate - $3CaO \cdot Al_2O_3 \cdot 0.5CaCO_3 \cdot 11H_2O$
$C_3A\bar{S}H_{12}$	mono-sulfate - $3CaO \cdot Al_2O_3 \cdot CaSO_4 \cdot 12H_2O$
H	dihydro oxygen, water - H_2O
S	silicon dioxide - SiO_2
Si^{4+}	silicon releasing from metakaolin during pozzolanic reaction
$Si(OH)^-_5$	silicon releasing during cement hydration process
α	de-hydroxylation degree

Abstract of the study

Metakaolin made from kaolin is used around the world but rarely in Vietnam where abundant deposits of kaolin is found. The first studies of producing metakaolin were conducted with high quality Vietnamese kaolins. The results showed the potential to produce metakaolin, and its effect has on strength development of mortars and concretes. However, utilisation of a low quality kaolin for producing Vietnamese metakaolin has not been studied so far.

The objectives of this study were to produce a good quality metakaolin made from low quality Vietnamese kaolin and to facilitate the utilisation of Vietnamese metakaolin in composite cements.

In order to reach such goals, the optimal thermal conversion of Vietnamese kaolin into metakaolin was carried out by many investigations, and as such the optimal conversion is found using the analysis results of DSC/TGA, XRD and CSI. During the calcination in a range of 500 – 800 ^{o}C lasting for 1 – 5 hours, the characterisation of calcinated kaolin was also monitored for mass loss, BET surface, PSD, density as well as the presence of the residual water. It is found to have a well correlation between residual water and BET surface.

The pozzolanic activity of metakaolin was tested by various methods regarding to the saturated lime method, mCh and TGA-CaO method. The results of the study showed which method is the most suitable one to characterise the real activity of metakaolin and can reach the greatest agreement with concrete performance. Furthermore, the pozzolanic activity results tested using methods were also analysed and compared to each other with respect to the BET surface.

The properties of Vietnam metakaolin was established using investigations on water demand, setting time, spread-flowability, and strength. It is concluded that depending on the intended use of composite cement and weather conditions of cure, each Vietnamese metakaolin can be used appropriately to produce (1) a composite cement with a low water demand (2) a high strength of composite cement (3) a composite cement that aims to reduce CO_2 emissions and to improve economics of cement products (4) a high performance mortar.

The durability of metakaolin mortar was tested to find the needed metakaolin content against ASR, sulfat and sulfuric acid attacks successfully.

1. Introduction

The reduction of CO_2 emissions in the cement industry is currently one of the most important tasks. Replacement of cement clinker by using SCM such as metakaolin to reduce CO_2 is an effective method that is well-known in the world.

Kaolin quality is influenced by different mineral compositions it contains, which in turn affects its color. As such, the whiteness of kaolin is an important factor when considering its role in the ceramic industry. Low quality kaolin, i.e. possessing a low whiteness, is low-cost. High quality metakaolin is expensive whereas metakaolin made using low quality kaolin is economical.

Vietnam has abundant deposits of kaolin with varying amounts of other minerals resulting in many different levels of whiteness. The utilisation of a low quality kaolin for producing Vietnamese metakaolin has not been studied so far. Furthermore, the addition of Vietnamese metakaolin in composite cement and the influence of Vietnamese metakaolin on durability fields of concrte have as yet not been considered in details.

The thermal treatment processs of kaolin to prepare metakaolin is one factor in facilitating the production of very high quality (i.e. pozzolanic activity) metakaolin. The pozzolanic activity of metakaolin can only be achieved a maximal value during an optimal thermal treatment process. A number of investigations for pozzolanic activity are needed to determine the optimal process. The pozzolanic activity of metakaolin can be determined by several testing methods. An appropriate testing method provides the real value of pozzolanic activity however, which method is the most suitable one to show the real pozzolanic activity has as yet not been determined.

Studying the utilisation of low quality kaolin for manufacturing metakaolin as an additive in composite cement will provide some fundamental answers to the following topics:

Firstly, is low quality Vietnamese kaolin suitable to produce a good quality metakaolin?

Secondly, which test of pozzolanic activity for metakaolin is most suitable to characterise its real activity and to reach the greatest agreement between it and cement performance?

Thirdly, what are properties of Vietnamese metakaolin as compared to commercial metakaolin?

Finally, can Vietnamese metakaolin be combined with a highly alkaline clinker, thereby reducing the risk of ASR? Whether can composite cement containing Vietnamese metakaolin resist SO_4^{2-} attack coming from the chemical environment (e.g. sea water)?

2. Motivation and objectives

2.1 Motivation

In Vietnam exacerbated environmental pollution, namely from the release of CO_2, is a direct result of producing clay brick; which is partly made from low quality kaolin that has abundant deposits. The Vietnamese Government issued a decision (567/QD-TTg, 2010) and directive (10/CT-TTg, 2012) on the approval of developing a program of non-heating construction materials [1, 2]. One of the objectives of this decision was to reduce the use of clay brick which has caused 0.57 million tons of CO_2 per 1 billion of clay brick to be released into the atmosphere, and to replace it by other advanced materials. Therefore, studying a new utilisation method for low quality kaolin is essential.

Previous studies on Vietnamese metakaolin production [3, 4, 5, 6] showed that a high temperature treatment (750 - 800 ^oC) is required to acheive the optimal conversion rate to turn kaolin into metakaolin. Thus, an open question is if a lower temperature treatment is sufficient for making a good quality Vietnamese metakaolin?

The influence of Vietnamese metakaolin on durability needs to be considered due to the following factors. *Firstly*, previous studies mainly showed the effect of metakaolin on strength [3, 6]. One study about the influence of Mg_2SO_4 on the strength and mass of mortars has already been carried out [7]. *Secondly*, the clay in the central and southern regions of Vietnam possesses a highly alkaline content (3.4–4.4 Wt.-%) [8], which is higher than the threshold value according to the Vietnamse standard TCVN 6071:1995 (≤ 3 Wt.-%) for raw clay material in producing clinker [9]. This might lead to a reduction of durability in concrete with respect to ASR. *Thirdly*, thanks to a long coastline, which is approximately 3.444 km [10], Vietnam building constructions are always faced with an aggressive environment, such as attack from sulfate ions (SO_4^{2-}). *Finally*, in Vietnam there is a high demand (ca.130 million tons in 2030) for good quality cement (resisting corrosions) and the need for greater environmental protection [11].

2.2 Objectives

Objectives of this study were to produce a good quality metakaolin made using low quality Vietnamese kaolin and to assess the test methods for pozzolanic activity. The purpose was also to discover a successful case using Vietnamese metakaolin in composite cements. As such, investigations that examined strength and durability properties of metakaolin were carried out.

3. Literature review

The utilisation of metakaolin as a pozzolanic material for mortar and concrete products has received considerable attention in recent years [12]. Many studies on the usage of metakaolin as SCM have been carried out, and there were several published reviews as reference documents [13, 14, 15, 16, 12, 17]. For this reason, this section provides a short description of the stages of production for metakaolin as well as the pozzolanic properties of the produced cementitious materials. Since the factors that affect the pozzolanic activity and qualitative characterisation of metakaolin have not been considered, they will be analysed in detail in this section.

3.1 Kaolin and metakaolin

3.1.1 Kaolin in the world and Vietnamese kaolin

The term kaolin has three different meanings namely that it is a rock term, kandites, or an industrial mineral commodity [15]. The main component of kandites is kaolinite [18, 19], whose chemical formula is $A1_2Si_2O_5(OH)_4$ which can also be written as $A1_2O_3{\cdot}2SiO_2{\cdot}2H_2O$ (AS_2H_2). The crystalline structure of kaolinite is classified as a two-layered sheet silicate. One layer contains aluminate groups ($AlO_4(OH)_2$-octahedrons), and the other contains silicates (SiO_4-tetrahedrons) as seen in Figure 3.1.

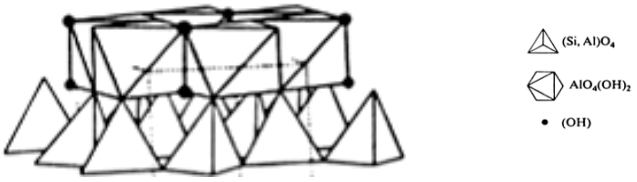

Figure 3.1 Crystal structure of kaolinite, [20]

The adjacent layers are linked by hydrogen bonding involving aluminol (Al–OH) and siloxane (Si–O) groups [21]. In well crystallized kaolinite, almost hexagonal platelets have been found by transmission electron microscopy [22]. Vietnamese kaolin analysed by SEM (Nova NanoSEM 230, FEI, Netherlands) showed a hexagonal layer mophology with single nano-size particles and coarser agglomerated stacks as seen in Figure 3.2. As seen, particles of hexagonal layer tend to re-aggregate and form coarser particles of stacks. Kaolinite possesses a low hardness about 2 – 2,5 on the Mohs scale [23].

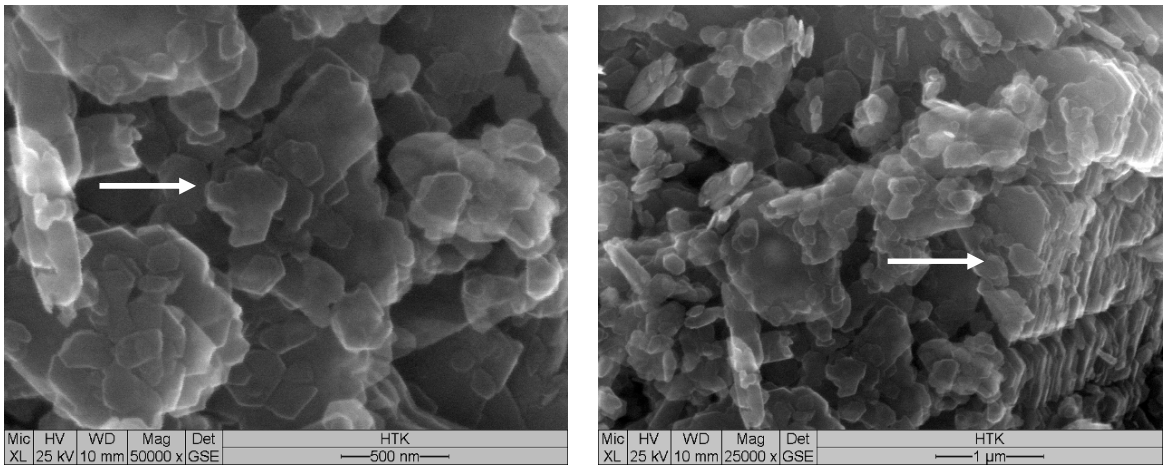

(a) single particles (b) coarser particles

Figure 3.2 Microstructure of kaolin HTK imaged by SEM-SE imaging technique.

Kaolinite formation is one of clay mineral formations. It is known that, their formation is operated by geological environments such as weathering, sedimentary, and diagenetic-hydrothermal; and their mechanisms are inheritance, neoformation and transformation [24, 25]. In addition, due to the characteristic formation of natural kaolinite, a great amount of kaolinite can only be found in some countries. Kaolinite can be also synthesized from the dissolution of metakaolin in the condition of low pH value, high temperature, and under the equilibrium water pressure [26].

The chemical and mineralogical compositions of kaolinite rocks (i.e. kaolin in the following) vary in some countries as listed in Appendix 13.1. The oxide composition of (Al_2O_3 + SiO_2 + Fe_2O_3) ranges from 75 to 97 Wt.-%. Commonly minerals such as quartz, muscovite and orthoclase are found in kaolin. Vietnam has abundant deposits of kaolin that is widely distributed over many parts of the territory (see Appendix 13.1). The total reserve of kaolin is approximately 900 million tons, mainly located in the northeast, the central highlands and the southeast of the country [27]. Sixty seven kaolin mines are geologically reconnoitred with 196 million tons of metamorphosed sedimentary kaolin and 71 million tons of the heat solution kaolin [28]. The whiteness plays an important role for a quality assessment of kaolin and its utilisation. The metamorphosed sedimentary kaolin with a whiteness under 70 (e.g, gabbro weathering kaolin) is considered as a low quality kaolin that can only be used in manufacturing conventional ceramic [29]. The chemical composition of Vietnamese kaolin varies from 55 to 83 Wt.-% of (Al_2O_3 + SiO_2 + Fe_2O_3) as shown in Appendix 13.1. Currently, Vietnamese kaolin is used primarily in manufacturing ceramics, refractory and glass materials. Furthermore, a small proportion is used

in the paper and paint industries [29,4]. The deposits of high quality kaolin have facilitated the development of the glass and ceramic industry in Vietnam for centuries [30]. The idea to use kaolinite for manufacturing Vietnamese metakaolin as SCM has only just been addressed in recent years. However, Vietnamese metakaolin has as not yet been utilised in composite cement and concrete products.

The quality of kaolin around the world varies as listed in Appendix 13.1. The kaolin for producing metakaolin is termed high quality kaolin when it can be transformed into a highly-reactive metakaolin with the following properties [31, 32]:

- A Hunter L whiteness value greater than 90, an average particle size of less than 2 μm and a specific gravity of approximately 2.5 g/cm^3.
- The reported oxide composition ($Al_2O_3 + SiO_2 + Fe_2O_3$) is approximately 95 Wt.-%.
- The resulting anhydrous aluminium/alumino-silicate ($Al_2O_3.2SiO_2$) is mainly amorphous material, which behaves as a highly reactive artificial pozzolan.

Depending on these definitions, a highly-reactive metakaolin made from a low quality kaolin is probably impossible. For example, the whiteness of kaolin is low when muscovite mineral is present in kaolin compositions. In fact, muscovite as an impurity is always coexistent together with a kaolinite mineral [33]. As muscovite is one of the unwanted minerals in glass and ceramic productions because of its various colors (e.g, gray), its presence can be seen as an index of the low quality of kaolin.

Based on the database concerning the quality and quantity of kaolin resources in Vietnam (see Appendix 13.1), Lam Dong kaolin, which is abundant source of kaolin has been chosen to be the sample for the present study due to the following reasons: (1) The expected resource was predicted to be large, i.e. estimated 520 million tons which exceeds other resources in Vietnam. (2) The low quality kaolin in Lam Dong has not yet been studied for producing metakaolin in Vietnam.

3.1.2 Metakaolin

Metakaolin is made from very pure kaolin clay (kaolin with a high content of kaolinite) by low-temperature calcination up to temperatures of 700 - 800 ^oC [34]. The transformation of kaolinite

into metakaolinite can be understood in simple terms as the removal of water from kaolinite [35, 36]:

$$AS_2H_2 \rightarrow AS_2 + 2H \text{ (vapour)}. \qquad \text{Equation 3.1}$$

Depending on the increase in the heating temperature, the removal stages of H_2O^- and H_2O^+/OH^- are the following [37, 38, 39, 40, 41, 42]:

(a) 100 – 120 ^oC: release of moisture and absorbed water (H_2O^-);

(b) 120 – 400 ^oC: mass loss (H_2O^- , H_2O^+/OH^-) correlated with a pre-dehydration process which takes place as a result of the reorganisation in the octahedral layer and first occurring at the OH^- group at the surface;

(c) 400 – 650 ^oC: de-hydroxylation of kaolinite and formation of metakaolinite according to the reaction: $Al_2Si_2O_5(OH)_4 \rightarrow Al_2Si_2O_5(OH)_xO_{2-x}+(2-x/2)H_2O$ with a low value of x (about 10% of residual hydroxyl groups in metakaolinite);

(d) 900 – 1000 ^oC: metakaolinite decomposes and then crystallizes to form mullite or cristobalite, or both.

Metakaolin consists of a non-crystalline aluminosilicate phase (also called a metakaolinite mineral or an amorphous phase - AS_2) that is obtained from the kaolinite mineral. During the calcination of kaolinite (up to 700 - 800 ^oC), the crystallography of calcinated kaolin is affected as follows:

- the gradual loss of OH^- groups [39, 36]. The majority of these ions are located on the interlayer surface of the octahedral sheet of alumina trapped between two sheets of silicon tetrahedrons [21].
- the gradual change of octahedral AI-O(OH) layer [43] and the coordination sites of $Al^{3+[VI]}$ to $Al^{3+[V]}$ and $Al^{3+[IV]}$ [36, 21]. However, the tetrahedral Si-0 layer (SiO_4) of kaolinite is remained in metakaolinite [36, 43].
- the collapse of kaolinite layers (7.15 A^o, crystalline structure) to become metakaolinite (6.3 A^o, amorphous structure) [43].
- the lattice parameters *a* and *b* of kaolinite are retained more or less unchanged in metakaolin, but c-axis periodicity disappears [43].

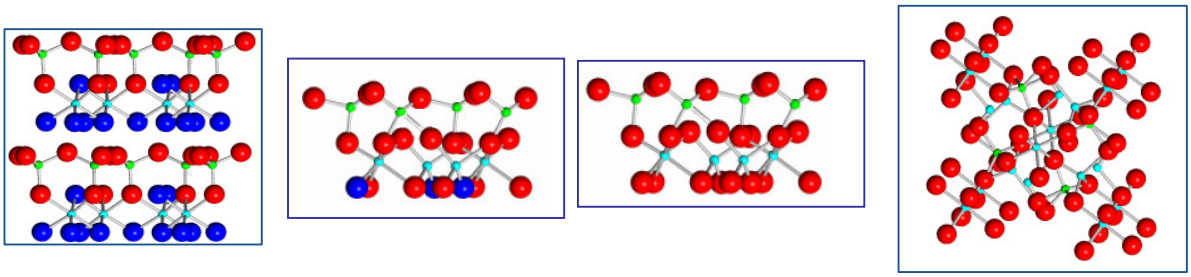

(a)	(b)	(c)	(d)
Natural kaolinite $Al_2O_3{\cdot}2SiO_2{\cdot}2H_2O$ [44]	Calcinated kaolinite during pre-dehydration $Al_2O_3{\cdot}2SiO_2{\cdot}xH^+{\cdot}yO^{-2}$	Calcinated kaolinite during de-hydroxylation $Al_2O_3{\cdot}2SiO_2$	Calcinated kaolinite after de-hydroxylation $3Al_2O_3{\cdot}2SiO_2$ [45, 46]

Figure 3.3 Schematic change of structure of kaolinite during calcination.
● : Al, ●: Si, ●: O, ●: H

These above changes in calcinated kaolinite are described in Figure 3.3. The crystalline structure of natural kaolinite is stable with nine oxygen ions and four hydrogen ions from the octahedral sheet of alumina and tetrahedral sheet of silicon (see Figure 3.3.a). In this structure, no cation exchange (such as pozzolanic reactions) takes place, but cation adsorption (as swelling on the surface) is possible [47]. Pre-dehydration of kaolinite at 400 – 500 ^oC causes the lose of some oxygen hydrogen ions from the octahedral sheet of alumina as a pattern shown in Figure 3.3.b. Thus, the pre-dehydrated kaolinite is able to exchange cation ions in pozzolanic reaction. When de-hydroxylation is occurred completely (at temperatures between 700 – 800 ^oC), calcinated kaolinite loses two oxygen ions and four hydrogen ions, becoming metakaolinite as described by a pattern shown in Figure 3.3.c. Metakaolinite like other pozzolana (e.g, silica fume) is able to react strongly with free lime (C) / portlandite (CH) to form C-S-H, CAH and CASH phases [48, 49] as seen in Figure 3.4. Calcinated at 950 - 1000^oC, metakaolinite decomposes and then crystallizes to form mullite (see Figure 3.3.d), which has no pozzolanic activity.

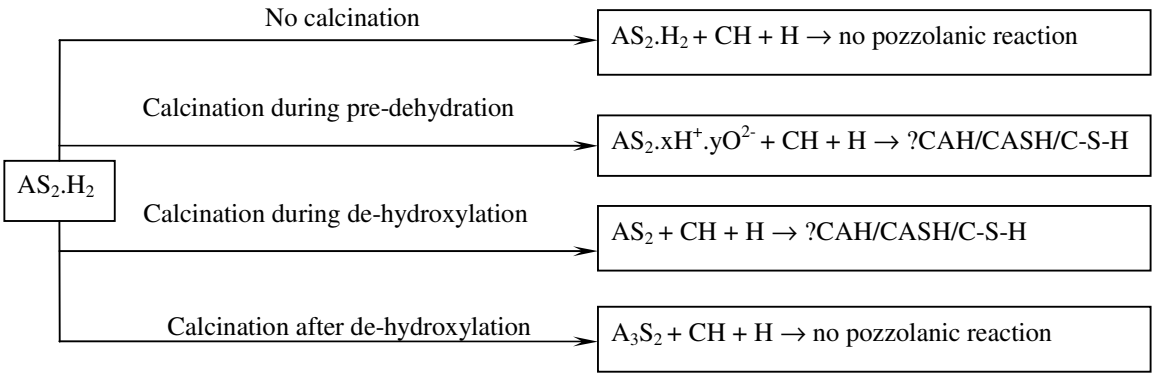

Figure 3.4 Calcination of kaolinite and the pozzolanic reactions of calcinated kaolin

In summary, kaolinite mineral is not completely transformed into metakaolin during the pre-dehydration process. At approximately 500 ^{o}C, calcinated kaolinite loses most of its ***crystal water*** (H_2O^+/OH^-), but there are still H_2O^+/OH^- groups in its structure. These remaining H_2O^+/OH^- groups are called ***residual water*** in structure of calcinated kaolin (metakaolin). A complete transformation to remove all of residual water without the formation of mullite is the critical step during calcination. Therefore, heating temperature and calcination duration for the thermal treatment process have to be optimised. As such, one of the input questions for producing metakaolin and its usage as SCM is what minimum heating temperature and minimum calcination duration are needed. In this context, it has also another open question if the residual water content in metakaolin can reduce its pozzolanic activity significantly and thus can decrease its ion consumption capability considerably.

It can be seen that, during the calcination the collapse of layers [43] could be a reason that leads to the reduction in BET surface [37, 50, 51, 52, 53, 54, 55]. The final open question is what the role of BET surface in pozzolanic activity of metakaolin is.

3.2 Pozzolanic activity of metakaolin

3.2.1 Qualitative classification of metakaolin

The quality of metakaolin for usage as SCM is mainly assessed by its pozzolanic activity, i.e. the reaction capability between metakaolin with free lime / portlandite produced during the cement hydration. Three possible alternative chemical reactions between calcium hydroxide and aluminosilicate phase (metakaolinite) may take place as follows [56, 57]:

$$AS_2 + 6CH + 9H \rightarrow C_4AH_{13} + 2C\text{-}S\text{-}H \qquad \text{Equation 3.2}$$

$$AS_2 + 5CH + 3H \rightarrow C_3AH_6 + 2C\text{-}S\text{-}H \qquad \text{Equation 3.3}$$

$$AS_2 + 3CH + 6H \rightarrow C_2ASH_8 + C\text{-}S\text{-}H \qquad \text{Equation 3.4}$$

In general, the specification requirements for the quality of pozzolana are normally dependent on the standards of EN ISO 3262-9 [58], ASTM C 618 [59]. There is no specification requirement for a special metakaolin, except an individual guideline DMS - 4635 from Texas Department of Transportation [32]. In fact, the ASTM C 618 standard and the DMS - 4635 guidelines refer to the specification requirement of strength activity whereby it has to be more than 75 – 85 % of the control sample. This is also the specification requirement in the Vietnamese specification standard applied for metakaolin TCVN 6882:2001 [60].

The EN ISO 3262-9 standard ignores the specification requirement of strength activity and also provides no information about the specification requirements of the capability of consuming lime. However, the lime consumption capability according to EN DIN 196-5 is required, whereby the CaO concentration and the OH^- concentration have to create a date point that is satisfied by EN DIN 196-5. It can be seen in Table 3.1 that, most experimental tests for the qualitative classification of metakaolin are dependent on both strength activity and lime consumption.

Table 3.1 The needed conditions for testing methods of pozzolanic activity.

	Direct testing methods (The analysis of lime consumption)				Indirect testing methods (The analysis of strength activity)	
	Saturated lime method (g)	mCh (g)	EN DIN 196-5 (g)	TGA-CaO method (Wt.-%)	Lime activity (Wt.-%)	CSI (Wt.-%)
Cement	-	-	16	75-90	-	80
Metakaolin	1-2	1	4	10-25 or 50[+]	50-70	20
CaO or $Ca(OH)_2$	-	1-2	-	or 50[+]	50	-
Sand	-	-	-	-	-	2.75-3
Water	75-100[++]	100-200	100	-	-	-
w/b	-	-	-	0.5-0.55 or 0.9-1[+]	0.75-1.25	0.48-0.6
Test age	7 - 30 days	16 hours	7-15 days	2 - 28 days	28 days	
Cure	at room temperature or 40 ^oC	90-100 ^oC	40 ^oC	20-60 ^oC: airtight condition	24 h: 20-23 ^oC in mould Other days: 20-38-40 ^oC in water/airtight condition	
Literature	[61, 62, 63, 64]	[65, 66, 38, 67, 68, 69]	[62, 70]	[71, 67, 52, 72, 73, 61]	[74, 56, 75, 76, 65, 67, 52, 77, 78]	[51, 74, 38, 61, 50, 62, 79, 80, 81]

[+] CaO or $Ca(OH)_2$ is replaced for cement in TGA test. [++] saturated lime solution

3.2.2 Testing methods for pozzolanic activity of metakaolin

In generally, there are two main groups for testing method to determine the pozzolanic activity of metakaolin as seen in Figure 3.5.

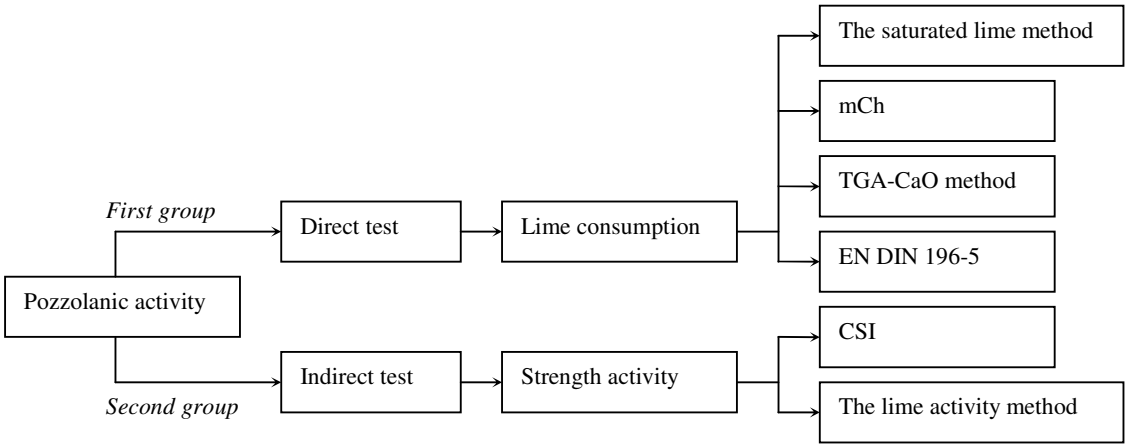

Figure 3.5 A summary of test methods for the pozzolanic activity of metakaolin.

The first group is to measure the consumption capability of free lime (CaO) and is called a direct test because it depends on the amount of free lime reacting directly with metakaolinite. The quantity of lime consumption is calculated from the remaining CaO amount, which is assessed by different ways for testing methods. In the saturated lime method, the remaining CaO amount in solution is determined using the indicator paper for analysis. ICP-OES is used for determing the quality of remaining Ca^{2+} content in solution for mCh and EN DIN 196-5. The quantity of remaining CaO amount in pastes is calculated from the endothermic peak (characteristic peak of portlandite) in TGA-CaO method. The needed conditions for testing methods are different too. The pozzolanic reaction of the saturated lime method and mCh is investigated by combining metakaolin and CaO or $Ca(OH)_2$. These reactions are investigated with pure phases, i.e. without the presence of other cement constituents. The reaction temperature of mCh is unrealistically high (90 - 100 ^{o}C). The pozzolanic reactions according to TGA-CaO method and EN DIN 196-5 are performed by mixing cement and metakaolin. However, the reaction temperature required in EN DIN 196-5 is higher (40 ^{o}C) than that in TGA-CaO method (20 ^{o}C). In conclusion, the pozzolanic activity results from the saturated lime method, mCh and EN DIN 196-5 provide no information regarding realistic reactions, which take place between metakaolin and cement. On the other hand, the pozzolanic activity result from TGA-CaO method produces realistic reaction information.

The second group aims to measure the relative compressive strength. This group is called an indirect test because it depends on the formation of hydration products (CAH, CASH and C-S-H) and the filler effect, which contribute to the increase in compressive strength (strength activity). The indirect test includes the lime activity method and CSI. The lime activity method characterises the pozzolanic activity of metakaolin under unreal reaction conditions between metakaolin and $Ca(OH)_2$ or CaO, while real reaction conditions between metakaolin and cement takes place in CSI. It is used to measure the relative compressive strength of metakaolin mortar bars in comparison with the control mortar bars. For these reasons, CSI is considered to be the reference test method in comparison with other direct testing methods [62].

It should be noted that in fact, the strength activity is a popular test as a reference test method in comparison with the direct test. This is due to a very good agreement between strength activity test and the performance of the cement and concrete products in application. Furthermore, the lime consumption value of metakaolin reflects a part of strength activity by showing an increased density structure due to its filler effect and pozzolanic activity that can form C-S-H, CAH and CASH phases. As such, the effect of lime consumption is an overall contribution of strength activity. Therefore, CSI should be used to assess the quality of metakaolin after the calcination.

A variable w/b for the control and pozzolanic mortars can be a reason for the unsuitable performance in concrete of ASTM C618, as strength activity defined by ASTM C311 is not a suitable indicator for pozzolanic activity [82]. For this reason, a constant w/b for the control and metakaolin mortars as EN DIN 196-1 should be chosen for CSI.

3.3 Factors affecting the pozzolanic activity of metakaolin

3.3.1 Mineralogical compositions of kaolin

The pozzolanic activity of metakaolin is mainly affected by its amorphous phase content. Quality and quantity of amorphous phase depend on not only the thermal treatment process but also on the mineralogical composition of raw material. A higher kaolinite content of kaolin results normally in a higher amorphous phase content of metakaolin. Calcinated kaolin that contains less amorphous phase possesses a lower pozzolanic activity [75]. It has been shown that the strength activity of mortars depends significantly on amorphous phase content as well as the degree of de-hydroxylation of calcinated kaolin [74]. The compressive strength of mortars containing calcinated kaolin, which has a higher kaolinite mineral content, is higher than of that having a lower kaolinite mineral content [83, 84, 85]. There has also been a tendency of the strength

activity to increase with the content of amorphous phase, until the content of amorphous phase of about 85 Wt.-% is achieved [51].

It is noted that, the quality of a poorer crystallization state (not well-ordered kaolinite) results in a higher lime activity for metakaolin [75, 66]. So, a quality comparison of different kaolins that is only based on its mineral content is not accurate. As such, it also needs to take into account the kind of pozzolanic activity (strength activity or free lime reaction) and other properties influencing pozzolanic activity such as BET surface. For example, there has been close correlation between strength activity of mortars and particle size distribution of de-hydroxylated clays [86].

Normally kaolin contains not only kaolinite but also other minerals. Their presences as impurities certainly lead to a lower pozzolanic activity of calcinated kaolin. Montmorillonite and illite contents in calcinated kaolin lead to its lower strength activity, and muscovite has very little effect on strength activity of calcinated kaolin [87]. Montmorillonite as OMMT (organo-modified montmorillonite) can also improve the strengths of cement mortars [88]. Despite this, illite and quartz (< 30 Wt.-%) do not prevent the geo-polymerization reaction [89].

3.3.2 BET surface of kaolin and metakaolin

The fineness (<500 µm) of kaolin is no matter what kaolin is transformed in to metakaolin, while BET surafce of metakaolin profoundly influences its strength activity in the early stages. With the residue at 500 µm of 0 – 71.8 Wt.-%, the particle size of kaolin does not affect the thermal conversion of kaolin to metakaolin as well as the strength activity of metakaolin [90]. BET surface of metakaolin has also been shown to influence the early hydration behaviour of cement hydration, i.e. higher BET surface metakaolin (25.4 BET m^2/g) produces a greater rate of heat evolution, a higher cumulative hydration heat, and the greater intensities during early hydration of cement pastes than lower BET surface metakaolin (11.1 BET m^2/g) [91]. The strength of mortar, made of different metakaolins with similar chemical compositions but different BET surfaces in the range of 13 - 20 BET m^2/g, is investigated in [70]. The results show that a higher BET surface of metakaolin gives a faster development of mortar strength on day 7 and 28 of the hydration process. Dealuminated kaolin (90.5 m^2/g) exhibits a much higher lime activity than silica fume (18.6 m^2/g), especially during early hydration [92]. Hence, it can be concluded that BET surface of metakaolin is an important factor for the pozzolanic activity up to 28 days. In addition, metakaolin with the finer PSD has better lime activity as shown in [93].

BET surface of metakaolin influences the absorption capability of cation during pozzolanic reactions. As commonly known, specific surface areas influence the reaction rate of solids in a solution [94]. A higher BET surface leads to a decreased pozzolanic reaction rate per one area ratio, but to an increased pozzolanic reaction amount, i.e. a higher lime consumption for metakaolin. Studies of the effectiveness of BET surfaces on strength show that, a lower BET metakaolin surface gives a lower strength [95, 70, 96]. However, after day 90 the deviation is limited [70].

3.3.3 Calcinations of kaolin

The calcination of kaolin is a thermal treatment process to remove its water. The water removal can be influenced by alkali contents of kaolin [97]. Metakaolin can be manufactured by three different processes. The first process is the conventional calcination-process which takes minutes [57] or several hours [98, 99]. The second process is the rapid calcination-process where the fine kaolin is treated by a flash – calciner for a matter of a few seconds [65]. Finally, metakaolin can be produced by a thermal treatment at a low heating temperature over several days within a highly pressured environment [100]. Generally, metakaolin is produced by the conventional calcination-process. In the following paragraphs, the effects of the conventional calcination-process will be reviewed.

The process of removing the water from kaolin is assessed by a de-hydroxylation degree (D_{TG}), which is calculated according to the Equations 3.5+6 [74, 52, 101] and illustrated in Figure 3.6. Depending on the value of D_{TG}, three regions of phase transformation can clearly be distinguished as follows [101]: the de-hydroxylation region (D_{TG} <0.9), the metakaolinite region (0.9< D_{TG} <1) and the "mullite/spinel" region (D_{TG} =1).

$$D_{TG} = 1 - (M/M_{max}) \qquad \text{Equation 3.5}$$

$$\text{Or } D_{TG} = (SK\text{-}SMK)/SK \qquad \text{Equation 3.6}$$

Where:

$D_{TG:}$ the dehydroxylation degree (in TG analysis)

M and M_{max} are the residual and maximum mass loss,

SK: area of the endothermic peak corresponding to the de-hydroxylation of kaolinite

SMK: area of the residual peak of remaining kaolinite in metakaolin.

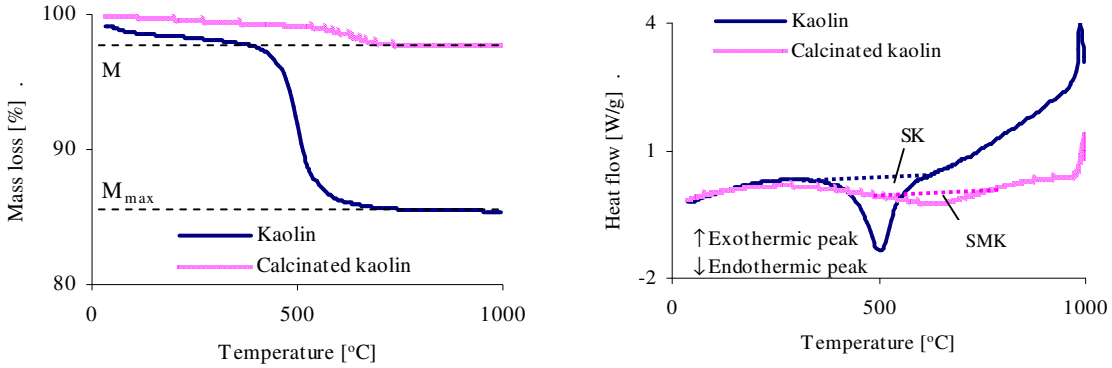

(a) illustration for Equation 3.5 (b) illustration for Equation 3.6

Figure 3.6 Illustration for the calculation of Equations 3.5+6

In some respects the amorphous phase content can also assess the quality of metakaolin, and both D_{TG} and the amorphous phase content are influenced by the thermal treatment process.

During the calcination, the amorphous phase content increases strongly when the temperature reaches the de-hydroxylation temperature. However beyond this temperature, amorphous phase content seems to remain constant. In addition, evidence of a correlation between the pozzolanic activity and D_{TG} of metakaolin could not be obtained [65, 52]. However, with a D_{TG} of more than 0.95 the highest strength activity is achieved [52]. The D_{TG} and the strength activity (tested by the lime activity method, see Table 3.1) of kaolin in dependence of calcination temperature are shown in Table 3.2.

Table 3.2 D_{TG} and strength activity of kaolin v.s calcination temperature [65, 74, 52]

	Temperature of the calcination [°C]					
	20-400	550	600	700	800	950
De-hydroxylation, α [-]	< 0.18	0.68-1	0.89-1	0.95-1	0.97-1	-
Strength activity [MPa]	-	7.8-12.5	9.8-12.5	10.8-11.5	10.2-11.9	#0

#0 it is not solidified

A change in coordination sites for $Al^{3+[VI]}$ to $Al^{3+[V]}$ and $Al^{3+[IV]}$ [36, 21] takes place during the calcination. It has been assumed that the maximum activity for metakaolin is obtained by producing a maximum concentration of $Al^{3+[IV]}$ and $Al^{3+[V]}$ and a minimum concentration of $Al^{3+[VI]}$ [102].

The calcination duration and energy consumption during calcination are influenced by the heating rate and calcination pressure. The rise of the heating rate increases the temperature of occurrences of de-hydroxylation endothermic-peaks [103, 39] and re-crystallization exothermic-peaks [104]. An increase in pressure ($P_{H2O} < P_{total}$) results in a reduction in the de-hydroxylation peak width [105]. It can be seen that, fast heating rates as well as a rise in the pressure allows the de-hydroxylation process (calcination) to come to completion more rapidly. Depending on the calculation of thermochemical constants [106, 107], the rise in heating temperature in addition to fast heating rates is also accompanied by the absorption of a smaller amount of energy [103].

The calcination time and amount of heating energy required is influenced by the grinding process of kaolin. The endothermic DTA effects (associated with de-hydroxylation) shift to lower temperatures and decrease in intensity as grinding time increases [108, 109]. The effect of grinding for kaolin causes its increase in the amount of absorbed/coordinated water [109]. As such, the calcination duration and amount of heat energy is reduced with increased grinding time.

3.3.4 Activators of metakaolin

There are three methods for accelerating pozzolanic activity of metakaolin; the mechanical method, the thermal method and the chemical method.

The mechanical method involves a process of prolonged grinding [109, 110, 108, 111] to decrease the particle size and increase the disorder degree in amorphous phase content of metakaolinite. The disorder degree of amorphous phase content of metakaolinite increases with its grinding time, although metakaolinite is never entirely amorphous and has a degree of disorder (which varies with the conditions of preparation) [111]. Mechanical activator (increased surface) shows an acceleration of the pozzolanic reaction that occurs during the first 3 days, and the finer natural pozzolan (291 – 554 Blain m^2/g) produces a higher strength development of lime–pozzolan cements [112].

The thermal method is an elevated temperature cure over a room temperature (20 - 25 ^oC). The increase in temperature (up to 40 - 60 ^oC) promotes a rapid occurrence of pozzolanic reactions, which lead to the early formation of hydration products in the system of cement and lime pastes. This will be analysed in detail in the next section 3.4.1+3.4.2.

The chemical method is the use of chemical additions such as KOH, NaOH, Na_2SO_4, $CaCl_2$, and so on to promote of pozzolanic reactions from metakaolin [113, 114, 115, 116, 117, 118, 119,

120, 121, 122, 123]. Depending on the [Si]/[Ca] mol ratio in the mixture, the dosage of chemical activators and their kind are chosen to increase the pozzolanic reaction rate of metakaolin and strength development of metakaolin products.

Compared to the mechanical and thermal methods with respect to the cost per unit strength development, chemical activation is the most efficient and feasible method for the activation of natural pozzolans [112, 124].

Additionally, the alkali content (Na_2O_{eq}) of cement influences the pozzolanic activity of metakaolin. It is well-known that alkalis content affects the stability of ettringite and the hydration process of C_3A and C_3S as well as the microstructure of cement during the hydration process. This in turn affects CH amount present in aqueous phase [125], which activates metakaolin. This indicates that a higher alkali content of cement, more and quicker CH is created in aqueous phase. As such, the pozzolanic reaction of metakaolin takes place quicker.

3.4 Influence of metakaolin on the properties of normally cementitious materials

The presence of metakaolin in normal products of mortar and concrete affects the hydration process. The formation of various hydration products from pozzolanic reaction occurs and leads to positive changes in the microstructure. This in turn modifies mechanical and chemical properties such as strength and durability.

3.4.1 Hydration products in composite cement

The main hydration products of cement pastes containing metakaolin are C-S-H phases, stratlingite (C_2ASH_8) and C_4AH_x (e.g. x = 13, 6) [48, 49]. Depending on the w/b ratio, the temperature and duration of cures as well as the used levels of metakaolin, hydration products are formed at different times in various quantity.

Stratlingite C_2ASH_8 is first formed by a reaction between CH (from cement) and metakaolin in suspensions at an ordinary temperature. After that, depending on the components and cure conditions, C-S-H phases, hydrogarnet (C_3AH_6), and C_4AH_x will be yielded [48]. With w/b ratios between 0.28 - 0.34, cure in water at 20 °C, C_4AH_{13} is not detected before 180 days, except C_2ASH_8 [49]. At increased w/b ratio up to 0.55 and the cure condition of 100% RH, hydration products are formed between day 3 - 7 for C_2ASH_8 and by days 180 – 360 for C_4AH_{13} [126]. However, when the cure temperature is 60 °C and the cure is under water for 123 days, no evidence of the formation of C_4AH_{13} and C_3AH_6 (traces) is found, and C_2ASH_8 does not appear

as a crystalline phase [127]. The speed rate of ettringite formation from Al_2O_3 of metakaolin is faster than that from C_3A and C_4AF of cement clinker at the temperature of 20 ^oC [128].

The increased formation of hydration products raises the lime consumption. Thoroughly by the use of microwave treatment, the complete lime-consumption is achieved for levels of 15 Wt.-% metakaolin [129]. This concludes that, a rapid generation of heat inside the cement paste accelerates not only the pozzolanic reaction but also the lime consumption capability of metakaolin.

In the system of cement, the content of SO_4^{2-} and $Al(OH)_4^-$ influences the formation of ettringite and mono-sulfate. It is known that mono-sulfate is created when less SO_4^{2-} content is present in solution, whereas more SO_4^{2-} content in solution is a favor of ettringite formation instead of mono-sulfate [130]. Metakaolin could influence the formation of ettringite and mono-sulfate in the system of cement - metakaolin. In that, the high content of Al^{3+} in metakaolin can lead to decrease the mol ratio of sulfate to aluminum, which creats a favor of mono-sulfate formation.

3.4.2 Hydration products in lime system

The formation of hydration products at the metakaolin to lime ratios of 1:0.4-6 was investigated in [131, 132, 126, 133, 127, 73, 134]. Results showed that, an increase in temperature quickly promotes the occurrence of pozzolanic reactions and the formation of hydration products as follows:

- at 20 °C: C-S-H phases (after 2 days), C_2ASH_8 and C_4AH_{13} (after 9 days), C_3AH_6 (after 360 days), and CH traces depended on the metakaolin lime ratios.

- at 55 °C: C_2ASH_8, C_3AH_6, C_4AH_{13}, and traces of C-S-H phases.

- at 60 °C: C-S-H phases (after 6 hours), C_2ASH_8 and C_4AH_{13} (after 12 hours), C_3AH_6 (after 21 hours). The coexistence of metastable and stable phases is up to 60 months.

3.4.3 Microstructure in metakaolin-cement pastes

The structure of concrete includes a frame structure of coarse particles (aggregates and sands) and a micro-structural development of cement paste which always contains pores. They are capillary pores and gel pores (also called the interlayer space or collapsible interlayer structure in

C-S-H) in hydrated cement paste [48]). During the mixing process, air pores (from tens μm to mm in size [135, 130, 136]) and compacting pores (radii>1mm, [130]) are added into the structure. During hydration , shrinkage-pores (also called the extremely fine pores, 10 nm in size, [130, 136]) and hollow shell pores (also called hadley grains, 3 - 15 μm [137, 136]) are formed in the microstructure. The volume of hollow shell pores and total pores are decreased, but the volume of gel pores increases during hydration process.

When a certain percentage of cement is replaced by metakaolin, a continuous reduction in total pore volume with age takes place. The proportion of pores with radii smaller than 10-20nm increases, whilst the proportion of large pores (radii bigger than 0.02 mm) in the paste decreases [138, 72]. This is called a feature refining microstructure or filler effect. In comparison with silica fume used in UHPC, the microstructural refining feature of metakaolin is better [139]. The ultrafine metakaolin (20 Wt.-%, 8600 m^2/kg) substantially enhances the pore structure of the concretes and reduces the content of more harmful large pores [140].

3.4.4 Strength of metakaolin products from mortar and concrete

Metakaolin improves the compressive strength of mortar and concrete. This is due to the removal of portlandite by pozzolanic reactions, especially around 14 day mark [141, 142]. To obtain the greatest strength, the optimum replacement level of cement by metakaolin in mortar at the w/b of 0.40 - 0.50 is 10 - 15 Wt.-% [141, 143], while the optimum replacement level in concrete at the w/b of 0.25 - 0.5 is about 10 - 20 Wt.-% [142, 70, 144, 145, 146, 147, 148, 149].

3.4.5 Durability of metakaolin products from mortar and concrete

A significant problem in concrete durability is ASR caused by a reaction between a highly alkaline cement paste and reactive aggregates [150]. There are three conditions required for ASR to occur: (1) a sufficiently high alkali content of the cement (or alkali from other sources), (2) reactive aggregates, and (3) water (to allow cement to be reacted, creating CH). If all the three conditions are present, alkali-silica gel will be formed in four steps as follows [151, 152]:

1. The reaction between the hydroxyl ions (OH^-) in the pore solution and reactive silica in the aggregate to form a silica gel ($Si_2O \cdot OH^-$) ;

2. The alkalis contribute initially to the high concentration of hydroxyl ions in solution and later to the formation of an alkali-silica gel from the silica gel ((Na_2K_2) $\cdot Si_2O \cdot nH_2O$);

3. Calcium ions from cement then react with the alkali-silica gel to convert it to hard expansive calcium silicate hydrate ($(CaNa_2K_2) \cdot Si_2O \cdot nH_2O$).

4. The expansive pressure generated by these above reactions induces the cracking of the aggregate and surrounding concrete, which causes the deterioration of concrete.

Increased metakaolin content reduces the CH content, absorbs alkali ions and refines the pore structure due to pozzolanic reactions. These three factors are considered to be the principal factors affecting improvement in alkali silica reaction (ASR). The investigation of ASR was mainly performed by a high-activity metakaolin (as defined in section 3.1.1), which showed that expansion of mortar bars and concrete prisms is reduced with increasing levels of the high-activity metakaolin [31, 153, 154].

Another problem with durability of concrete is sulfate attack (external and/or internal attacks, sulfuric acid attack). This is due to the penetration of sulfates in solution or a source of sulfate incorporated into concrete. As a result, hydration products with volume expansion (mono-sulfate, delayed ettringite formation, gypsum) and destroying C-S-H phases (thaumasite) are formed [48, 155, 156]. Ettringite and gypsun cause an expansion that leads to a loss of concrete strength. The softening phenomenon on concrete is often caused by formation of thaumasite, which its appearance is considered as a deterioration product destroying C-S-H phases [156]. Sulfate attack is controlled by the concentration of SO_4^{2-}, alkali (in solution outside the concrete or pore solution inside the concrete), and the mount of C_3A and C_3S in cement. In the aggressive chemical environment of a Na_2SO_4 solution, at low metakaolin contents (0 - 10 Wt.-%), the expansion of the mortar bars is controlled by the amount of C_3A available to react to form an expansive product [157]. At a high metakaolin content (15-25 Wt.-%) CH availability becomes restricted, and the expansion is very much smaller [157]. Other aggressive chemical environments in tests simulating sulfate and acid attacks on metakaolin are investigated for sodium sulfate (Na_2SO_4), sulfuric acid (H_2SO_4), a mixture of sodium sulfate (Na_2SO_4) and magnesium sulfate ($MgSO_4$), and magnesium sulfate ($MgSO_4$). The results show an increase of the chemical resistance in the mortar and concrete products containing metakaolin in comparison with products contaning pure cement [145, 158, 159, 160, 161]. Furthermore it is observed that, the increase in the w/b (0.4-0.6) results in a lower sulfate resistance at a normal temperature cure (20 – 23 ^{o}C) [159] and at a low temperature cure (5 ^{o}C) [158]. This could be due to the formation on thaumasite, which is believed to form partly under low temperature conditions [162, 163, 164].

3.4.6 Workability of metakaolin-cement paste and metakaolin concrete

The workability of a mixture depends on its setting time and flow properties. A good workability is needed to provide a good comfort for the building industry (enough time for performance – setting time, and easy performance in applications – flow properties). Studies have shown that BET surface of metakaolin plays a significant role in setting time. The initial and final setting times are reduced with the increase of BET surface in metakaolin (11.1 - 25.4 m^2/g) [95, 165]. Metakaolin tends to increase the water demand of composite cement containing it, as such it decreases workability of mortars when compared to Portland cement mortars. The necessary superplasticizer dosage to achieve the target slump in concrete increases with the increase of BET surface of metakaolin, indicating that concrete workability reduces with increasing BET surface [95]. This is a disadvantage property of metakaolin due to its high BET surface that also leads to the increase in water demand content [166].

The flow properties of concrete are controlled by the particle size distribution (PSD) and the particle packing of metakaolin and cement. The finer PSD shows the higher deformation coefficient derived by the spread-flow [167, 168].

3.4.7 Other effects on metakaolin products of mortar and concrete

An increased metakaolin content refines the pore structure and reduces the CH content in mortar and concrete products. These two factors, refined pore structure and reduced CH, are considered to be the principal factors improving the resistance to chloride permeability [169, 31, 170, 147, 148, 171, 172]. An increase in chloride binding capacity has been observed for metakaolin-blended cement paste samples [173]. Other advantaged roles of metakaolin are the resistance to freezing and thawing cycles [148]; factors increasing microhardness of the interfacial transition zones in concrete [174, 170] and improving corrosion performance for embedded steel (at 15 Wt.-% metakaolin used) [143]. When a part of cement is replaced by metakaolin, it mitigates autogenous volume changes [175, 176, 177].

Mortars containing metakaolin result in a slight heat increase of the hydration process when compared to a 100% Portland cement mortar. This is due to the high pozzolanic activity of metakaolin [178]. Metakaolin initially (< 1 hour) diminished hydration heat of cement hydration [179, 93]. However, at extended periods (up to 120 hours) mortars and binary blends containing metakaolin produced a slight heat increase when referred to a 100% Portland cement [178, 179].

3.5 The use of metakaolin in other special fields

3.5.1 Metakaolin in HPC and UHPC

In recent years, a great deal of research and development into the methods of producing HPC and UHPC is carried out [180]. The addition of metakaolin as SCM that is repalced for silica fume or rice husk ash in HPC and UHPC is possible [149, 139, 161]. It is noted that, silica fume is essentially a cheap waste material. However, the high cost of silica fume is caused by its a greater demand as well as due to high transportation costs (high voulme of powder). As compared to silica fume, metakaolin is not too expensive and its available deposite as well as its most common advantage of high whiteness. Additionally, as compared to rice husk ash, the industrial implementations of metakaolin is more possible than that of rice husk ash due to its concentration in deposite and its production in combination with the production of clinker. For these reasons, the use of metakaolin for the application in HPC and UHPC is currently highly desirable.

The usage of high quality metakaolin is suitable for producing UHPC and HPC due to its very good filling capacity and its excellent property of pozzolanic activity. A good or normal quality metakaolin is suitable to be used as SCM in HPC and normal concrete due to its usage in high volume with low cost.

In order to gain an optimal strength for UHPC, silica fume is often used as SCM because of its filler effect and good pozzolanic activity. In comparison with silica fume, the pozzolanic activity (as lime consumption tested by TGA) of metakaolin is similar to that of silica fume [70, 139], but its physical filler effect (due to its very small particle size of 5 - 50nm, i.e. 100 times smaller than Portland cement) is better than metakaolin's (4 – 10 μm) [168, 50, 181, 182]. However, previous results confirmed that metakaolin constitutes a promising material as a substitute for silica fume because it is more cost than metakaolin [148].

Previous studies have made comparisons between silica fume and metakaolin in their application in mortar and concrete products. After 90 days, the compressive strength of metakaolin concretes (10 Wt.-% metakaolin) reaches 134 MPa, which is higher than that of silica fume concrete (10 Wt.-% silica fume, 120 MPa) [144, 147]. A similar compressive strength after 180 days in metakaolin mortars and silica fume mortars has also been examined [70]. Split tensile strength and flexural strength of metakaolin concrete increases with curing ages [148]. In UHPC containing metakaolin, the compressive strength can be as high as 192 MPa (without cure) and 243 MPa (at 150 ^{o}C cure), and the flexural strength can obtain 30 MPa and 42 MPa, respectively

[149]. Dealuminated kaolin (produced by the ferric aluminum sulfate industry) gains strength more rapidly (blended pastes) than silica fume due to the high rate of pozzolanic reaction [183]. As such, it can be shown that concrete using metakaolin in compositions can achieve, at least, a similar strength to that of concrete containing silica fume.

3.5.2 Metakaolin in geopolymer

Metakaolin is usually used within mortar and concrete products. However, a geo-polymer binder is also synthesized by the alkali activation of metakaolin. A number of studies have been carried out, indicating that in the future use of geo-polymer products made by metakaolin will be within the building construction industry [89, 114, 184, 185, 186, 187].

4. Methods

4.1 Chemical and mineral characterisation

4.1.1 Inductively coupled plasma optical emission spectrometry (ICP-OES)

All oxide compositions of dry powder materials and ion concentrations of solutions are determined by ICP-OES analysis (argon-plasma from the spectrometer of Perkin-Elmer, Optima 3000). The pH value is measured by a glass electrode.

4.1.2 X-ray powder diffraction (XRD)

Samples for XRD were finely ground by hand with a mortar and pestle of corundum until all particles are passed the 63 μm sieve. For cement paste samples at early ages (a few hours - 2 days of the hydration process), before grinding, the coarse sample (≈< 5 mm) was rinsed with isopropanol and acetone to stop the hydration process. The coarse sample was dried at 35 ^{o}C for at least 2 hours. For cement paste samples at later ages, in order to stop the hydration process, samples were quickly ground by hand with a mortar and pestle of corundum after samples were taken out of their curing place.

Approximate 1 g of the ground sample was placed in a polyethylene sample holder for determining phases. The X-ray diffractometer (Siemens, D-5000) operates with Cu–Kα radiation. Diffractograms are recorded from 4 to 70° 2θ (0.03^{o} step size, 4s counting time).

In order to quantify X-ray amorphous phases, ZnO (20 Wt.-%, 0.4 g) was added in samples (80 Wt.-%, 1.6 g) as an internal standard. This blended powder is ground by a Mcrone-Micronising mill (Frequency 50 Hz) for two minutes before placed in a polyethylene sample holder. The quantitative phase analysis was calculated with the Rietveld software package TOPAS 4.2 (XRD-Rietveld).

4.2 Physical characterisation

4.2.1 BET surface, PSD and density

Before analysed, samples were dried in an oven at 105 ± 2 ^{o}C up to constant mass and then cooled down to the room temperature in an exsiccator. The SSA-BET surface was determined by the single point BET method via nitrogen adsorption/desorption at 20 ^{o}C. This method, when compared to the Blaine test, gives a better indication of the true surface area of the material.

Moreover, it is especially valuable for revealing the large internal pore structure of some pozzolans [188]. The specific surface area can be computed by using the calculation from particle size distribution (PSD). This surface called a PSD surface, in that the calculation assumes a sphere shape of particle.

PSD was performed by particle-size-analyse laser diffraction particle size analyzer (COULTER LS 230 with PIDS), 80 % ultrasound, in water for kaolin and calcinated kaolin and in isopropanol for cement.

The density of metakaolin was measured by pycnometer (Micromeritics Accupyc 1330).

4.2.2 Differential Scanning Calorimetry / ThermoGravimetric (DSC/TG)

In order to investigate the conversion of kaolinite into metakaolinite, Differential Scanning Calorimetry/ Thermo Gravimetric Analysis analysis (DSC/TG) investigations were carried out by using a Universal V4.5ATA instrument at a heating rate of 10 ^{o}C / min. The samples (~ 20 mg, < 63 μm) were heated from ambient temperature to 1000^{o}C in N_2 air flow of 100 ml/min. The amount of residual water, as the peak of dissipation mass analysed by DSC/DTA, was determined by the intensity height of peak (%.^{o}C^{-1}).

4.2.3 Scanning Electron Microscop (SEM)

The microstructure was observed by a scanning electron microscope (SEM) including secondary electrons (SE) (Nova NanoSEM 230, FEI, Netherlands and Philips, XL 30 SEM-FEG). Operating conditions were set to 1–25 kV and 1–10 Torr. Before SEM analysis, the samples were obtained from lime paste, cement paste, and mortar bars by creating a freshly fractured sample with hammer and chisel and without any further preparation. The advantage of SEM is that it allows the investigation of samples without any coating (ESEM). The identification of the development of hydration was detected by energy dispersive X-ray spectroscopy (EDX) in the SEM.

4.2.4 Other methods

Setting time of blended paste was tested in accordance with EN DIN 196-1. Spread flowability and compressive strength of mortar were examined according to EN DIN 196-1 for German materials and TCVN 3121:2003 for Vietnamese materials. The porosity of mortar was investigated by mercury intrusion porosimetry (MIP).

4.3 Strength development of mortar

4.3.1 Strength development in dependence of replacement levels of metakaolin

The mixture ratio of the blend:sand:water was 1:3:0.6. In the blend, cement was replaced by metakaolin with 20 – 40 Wt.-%. The samples were moulded in prism forms (40×40×160 mm^3). After demoulding, three sample groups were cured separately in water at 8 ^oC, 20 ^oC and 40 ^oC. The compressive strengths of samples were measured after day 2, 7 and 28.

4.3.2 Strength development in dependence of the calcite addition

The impact of adding calcite was investigated and based on strength activity (CSI). The ratio of blend (cement, metakaolin and calcite):sand:water was 1:3:0.6. The samples were moulded in prism forms (40×40×160 mm^3). After demoulding, samples were cured in water at 20 ^oC. The compressive strength of samples was measured after days 2, 7 and 28.

4.3.3 High performance mortar

Control high performance mortar has the ratio of cement / binder : sand : water was 1/1:2:0.3. The cement mass of 20 Wt.-% was replaced by metakaolin for high performance metakaolin mortars. Polycarboxylate superplasticizer was used to obtain almost the equivalent spread flowability of mortars (19.5 - 21.5 cm). When CEM I 52.5 N was used in the control mortar, Starkenberg sand was used. The curing regime and strength test of mortars were examined after days 7, 28 and 360 in accordance with EN DIN 196-1. Furthermore, when VPC 40 was used in the control mortar, Loriver sand was used. The curing regime and strength test (after days 7 and 28) of mortars were conducted in accordance with TCVN 3121:2003. The porosity of mortars was measured by MIP after 28 days of the hydration process.

4.4 Pozzolanic activity of metakaolin

4.4.1 The compressive strength index method (CSI)

CSI describes strength activity of metakaolin whereby strength test of mortar prisms (40×40×160mm^3) is performed by a combination between ASTM C331 and EN 450. In accordance with ASTM C331, a pozzolana replacement of 20 Wt.-% metakaolin for cement was used. Binder to sand ratio (1:3), w/b ratio (0.5) and curing regime (in water, 20 ^oC) was carried

out in accordance with EN 450. The compressive strengths (according to EN DIN 196-1) of samples were measured on day 28 of the hydration process. The pozzolanic activity was calculated as described in Equation 4.1:

$$CSI = 100CS_{MK}/CS_{PC} \quad \text{Equation 4.1}$$

Where

CSI: compressive strength index [%]

CS_{MK}/CS_{PC}: compressive strength of metakaolin mortar (80 Wt.-% cement and 20 Wt.-% metakaolin) / control mortar (100 Wt.-% cement) [N/mm^2]

4.4.2 The saturated lime method

This test was done according to Vietnam standard TCVN 3735:1982 [63]. At room temperature (25 ± 2 °C), 1g of metakaolin was mixed with 100 ml of saturated lime solution (the free lime content of 2β) to create the solution of S_1. After 48 hours of the hydration process, 50 ml of this solution (S_1) was taken out to check the free lime content (a_1). A new 50 ml of saturate lime solution (the free lime content of β) was supplemented in to the residual from S_1 to form the solution of S_2, which had the current free lime content of a_1+β. After further 48 hours, the free lime content of S_2 was checked with the same procedures as for S_1. Then the missing solution was refilled with saturated lime solution, and a solution S_3 was created like S_2. This process was performed 15 times over the course of 30 days ($S_1 \rightarrow S_{15}$). The free lime consumption was calculated by the summation of results from 15 testing times as described in Equation 4.2.

$$FLC_{SL} = (\beta - a_1) + \left(\sum_{i=1}^{14} \frac{a_i + \beta}{2} - a_{i+1}\right) \quad \text{Equation 4.2}$$

Where

FLC_{SL}: free lime consumption in relation to the mass of metakaolin [mg/g]

β: free lime content in 50ml of saturated lime solution, CaO [mg]

a_1: free lime content in 50ml of solution S_1 after 48 hours, CaO [mg]

a_i: free lime content in 50ml of solution S_i after 48i hours, CaO [mg]

4.4.3 Free lime consumption calculated using thermo gravimetric analysis (TGA-CaO method)

The lime consumption of the blended pastes with a w/b ratio of 0.38 - 0.5 was investigated. The blended pastes were stored in air-sealed plastic boxes (250 ml) at 20 ^{o}C in 100 % RH. After various cure times, the free lime content and free lime consumption were calculated from H_2O peak (characteristic peak of portlandite) determined by TG analysis as described in Equations 4.3-5 (see Appendix 13.2).

$$FL_{PC} = \frac{56M_o x}{1800(M_{1000} + M_{CO_2})} \quad \text{Equation 4.3}$$

$$FL_{BP} = \frac{56M_o x(1 - \frac{\alpha.y}{100})}{1800(M_{1000} + M_{CO_2})} \quad \text{Equation 4.4}$$

$$[FLC_{TGA}] = [mg/g] = [(FL_{PC} - FL_{BP})/\alpha] \quad \text{Equation 4.5}$$

Where

FL_{PC}/FL_{BP}: free lime content (CaO) in the cement paste/blended pastes [mg/g]

FLC_{TGA}: free lime consumption in relation to the mass of metakaolin [mg/g]

M_o/M_{1000}: mass of samples at a beginning temperature/1000^{o}C during TG analysis [mg]/[g]

M_{CO2}: mass loss of CO_2 content from $CaCO_3$ [g]. $M_{CO2} = 0.01M_o x^*$. Where x^* is mass loss of CO_2 [Wt.-%], x^* was determined like x factor.

x: mass loss of water content from $Ca(OH)_2$ [Wt.-%]. This x was determined by the method of [189] and [190].

y: the mass loss of metakaolin at 1000 ^{o}C during TG analysis [Wt.-%]

α: the mass rate of metakaolin replaced for cement. In this study, $\alpha = 0$ (cement) and 0.1-0.4 (blended paste).

4.4.4 The modified Chapelle test (mCh)

Metakaolin (1 g) was mixed with 1 g $Ca(OH)_2$ and 200 ml of water in a 600 ml glass beaker stirred by a magnet bar for 5 minutes. This beaker then was sealed and put at 40 ^{o}C. The pozzolanic activity of metakaolin was determined by the amount of lime consumed after various

curing periods. The lime consumption amount was calculated from the remaining $Ca(OH)_2$, which was dissolved by adding sugar to form a calcium saccharate complex [191]. Solutions then were vacuum filtered through a 0.45 μm pore size filter paper. The filtrate was analysed for Ca^{2+} by ICP-OES.

4.5 Durability tests of mortar

4.5.1 Expansion change by ASR

The expansion changes were evaluated by mortar prism tests according to the alternative method provided in the German Alkali-Guidelines (2007). The cement (CEM I 32.5 R) was replaced by 10 - 20 Wt.-% of metakaolin to get the powder blend (450g). Sodium hydroxide (6.97 g) and potassium sulfate (3.83 g), which their content are calculated in order to get the content of Na_2O_{eq} 2.50 Wt.-% in blend composition, were added to the mixing water (225 g) in order to be dissolved completely before adding cement and metakaolin. At the end of the process, reactive quartz sand (0.2 - 2mm, 1350g) was added. After moulding in the prisms of 40×40×160 mm^3, the mortar prisms were cured at 20 ^oC in 100 % RH for 24 hours. Thereafter mortar prisms were demoulded, and the mortar prisms were cured at 70 ^oC in 100 % RH. After curing on days 14, 21, and 28 the expansion changes of the mortar prisms were measured. Each mixture contained three prisms, and the final expansion result was the mean value measured on three prisms.

4.5.2 Ion binding in ASR and sulfate attack

The tests of ion binding for ASR were done with the metakaolin lime pastes (metakaolin:CH:NaOH/KOH = 1:1:0.04 with w/b 0.75 - 654 mmol Na^+ /l, and 467 mmol K^+ /l) and metakaolin cement pastes (metakaolin:CEM I 32.5 R = 0.25:1 with w/b 0.35), and for sulfate attack the tests were done with the lime pastes of metakaolin: Na_2SO_4: $Ca(OH)_2$ rate of 1:0.1:1 with the w/b of 0.75.

Metakaolin and CH / cement was blended by hand until a uniform colour for the powder was achieved. NaOH / KOH / Na_2SO_4 was mixed with water until a completely dissolution was obtained. The lime / cement pastes were mixed with the ion solution / water for 4 minutes to get a homogeneous blended lime / cement paste through a mixer. The resulting pastes were stored in air-sealed plastic boxes (250 ml, ϕ30) at 20 ^oC in 100 % RH. After various hydration times, the blended paste with the volume ca. 250 ml was demoulded and put into the squeezing device (ϕ40) to separate aqueous phase. Maximum load was 240 kN for the hydrated lime paste and 320

kN for the hydrated cement paste. The aqueous phase (the extracted solution) was collected by a syringe with an attached needle (filter 0.45 µm) and sealed airtight in plastic vials. Immediately the extracted solution is got, it is diluted with acid HNO_3 (1%) before calculating from the atoms measured by ICP-OES. The pH value was measured by a glass electrode.

The residual water in solid phase (after the squeezing device has been performed) was calculated by the mass loss of samples (~ 1 g, particles smaller than 5 mm) after calcination of 1000 ^oC in 3 hours. Depending on this residual water, the ion concentration in the extracted solution and the input parameters (mixture rates), the ion concentration such as sodium and potassium per 1kg metakaolin from the hydrated lime pastes was calculated as described in Equations 4.6-8. This aims to observe clearly the ion binding of metakaolin in dependence of its BET surface.

$$M_p = M_{sa} + 0.01(xM_{mk}^{1000} + yM_{ch}^{1000}) - M^{1000} \qquad \text{Equation 4.6}$$

$$d_p = \sum_{i=1}^{5} 10^{-3} M_i C_{es}^i + (1000 - \sum_{i=1}^{5} 10^{-3} M_i C_{es}^i . d_i^{-1}) \qquad \text{Equation 4.7}$$

$$C^i_{p.mk} = 10^3 [M_p d_p^{-1} C^i_{es}] x^{-1} \qquad \text{Equation 4.8}$$

Where

M_p: mass of the pore solution from the hydrated paste [Wt.-%]

M_{sa}: water mass in the composition of blended paste. 42.86 Wt.-%

x: mass percentage of metakaolin in the composition of blended paste [Wt.-%]

M_{mk}^{1000}: mass loss of the metakaolin after the calcinations [Wt.-%].

y: mass percentage of $Ca(OH)_2$ in the the blended paste [Wt.-%]

M_{ch}^{1000}: mass loss of the $Ca(OH)_2$ part from the solid part after the calcination [Wt.-%].

M^{1000}: mass loss of the solid part (chemical water, xM_{mk}^{1000}, yM_{ch}^{1000}) of blended paste after squeezing device and the calcinations of 1000 ^oC in 3 hours [Wt.-%]

d_p: density of the pore solution [g/l]

M_i: the standard atomic mass. i_1(K), i_2(Na), i_3(Ca), i_4(Al) and i_5(Si) [g/mol]

C^i_{es}: the concentration of the ion in the extracted solution [mmol/l]

d_i: density of atomics [g/cm^3]. (H_2O density of 1 g/cm^3)

$C^i_{p.mk}$: the total ion amount of the pore solution per 1kg metakaolin from the hydrated-blended lime paste [mmol/kg]

For blended cement paste, y is the mass percentage of cement (100 and 80 Wt.-%), and M_{cem}^{1000} (2.21 Wt.-%, mass loss of cement after the calcination) is replaced for M_{ch}^{1000} in the Equation 4.6. The total ion amount of the pore solution per 1kg hydrated-blended cement paste ($C^i_{p.cp}$, mmol/kg) is described in Equation 4.9 as follows:

$$C^i_{p.cp} = 10[M_p d_p^{-1} C^i_{es}] \qquad \text{Equation 4.9}$$

4.5.3 Expansion change by external sulfate attack

Mortar bars (10×10×60 mm^3) were prepared from the mixtures of a binder:sand:water = 1:3:0.6. The binder contained 0, 10, and 20 Wt.-% metakaolin in combination with 100, 90, and 80 Wt.-% cement VPC 40. Sand was used according to EN DIN 196-1.

After mixing the fresh mortar was moulded in the form 10×40×60 mm^3 and the mortar bars were cured at 20 ^oC in 100 % RH for 24 hours. Afterwards, mortar bars were demoulded and cured at 20 ^oC in water in 14 days. Then, the mortar bars were exposed to the corrosive solution of Na_2SO_4 (3000mg SO_4^{2-}/l). This solution was replaced with new solution every month for 12 months. However, for the remaining months the solution was not renewed. The temperature during the testing period was 20 °C.

The length of the specimens were recorded every 2 months up until the 6 month mark, and after 18 - 22 months of cure. The results given were the average of bars (5 – 7 bars). As soon as the samples (at least 50% of bars) were fractured due to the external sulfate attack, SEM/EDX is used to determine the expansion hydration products of samples on micro-cracks and fractured areas. This SEM/EDX investigation was performed again when all bar samples were fractured.

4.5.4 Strength change by acid sulfuric attack

The strength change of mortar prisms (40×40×160 mm^3) was conducted. The cement mass (CEMI 52.5 N) of 10, 20 and 30 M.-% was replaced by metakaolin, and the ratio of binder:sand:water is 1:3:0.6.

After mixed and moulded in the prisms of 40×40×160 mm^3, mortar prisms were cured at 20 ^oC in 100 % relative humidity for 24 hours. Thereafter mortar prisms were demoulded and cured at 20 ^oC in water for 14 days. After that, the mortar prisms were exposed to the corrosive solution

H_2SO_4 1.M-%. Three prisms were put in a plastic box containing ca. 1.5 l of the corrosive solution.

After 19 months of curing, the compressive strength of samples was tested according to EN DIN 196-1. The final result are the mean value of three prisms. SEM/EDX is used to determine the expansion hydration products of samples on micro-cracks and fractured areas.

5. Materials

5.1 Kaolin

The kaolins used in this study were two samples of Vietnamese kaolin named HTK and DQK. They were taken from the Lam Dong area. An overview of extraction for kaolin from raw material is shown in Appendix 13.3.

The extracted kaolins (HTK & DQK), which have a physical status of pressed pieces with a maximum dimension of 10 cm and the maximum humidity of 3 Wt.-%, were packed in 10 kg bags and transported to Germany. Here, they were dried in an oven at 100 ± 5 ^{o}C up to constant mass, then ground up to 10 mm by a crusher, and ground up to a residue of 0 – 5 Wt.-% content at 500 µm dry-sieve (No.35) by a rolling ball mill. HTK and DQK were then used for the following investigations. The chemical compositions of HTK and DQK were analysed using ICP-OES, and their mineralogical compositions were analysed by XRD- Rietveld. The measurement results are shown in Table 5.1. As seen, HTK and DQK possess a low value of whiteness that indicates their low quality for producing high quality ceramics.

Table 5.1 Chemical and mineralogical composition of Vietnamese kaolin

	HTK [Wt.-%]	DQK [Wt.-%]			HTK [Wt.-%]	DQK [Wt.-%]
SiO_2	46.40	46.50	Kaolinite	$Al_2Si_2O_5(OH)_4$	93.1	92.1
Al_2O_3	36.10	35.60	Quartz	SiO_2	2.4	2.4
Fe_2O_3	1.40	1.50	White mica^{+}	$KAl_2[AlSi_3O_{10}.(OH)_2]$	2.4	4.5
TiO_2	0.30	0.03	Orthoclase	$K[AlSi_3O_8]$	1.4	1.0
CaO	0.10	-	Rutile	TiO_2	0.5	0.1
MgO	0.10	0.10				
K_2O	0.47	1.06	Whiteness, Hunter Lab - L		65.6	60.3
Na_2O	0.02	0.03	$[SiO_2]/[Al_2O_3]$, mol rate		2.19	2.22
P_2O_5	0.03	0.08	[Si]/[Al], mol rate		1.10	1.11
LOI_{1000}	13.40	12.70	Available alkalis, Na_2O_{eq} (equivalent)		0.33	0.73

+ Muscovite is one of white micas [192, 193]

The specific surface area measured by the BET method was 25.3 m^2/g for HTK, and 19.5 m^2/g for DQK. Their particle size distributions analysed by particle-size-analyse instrument are shown in Figure 5.1, and their density are 2.602 g/cm^3 for HTK and 2.604 g/cm^3 for DQK.

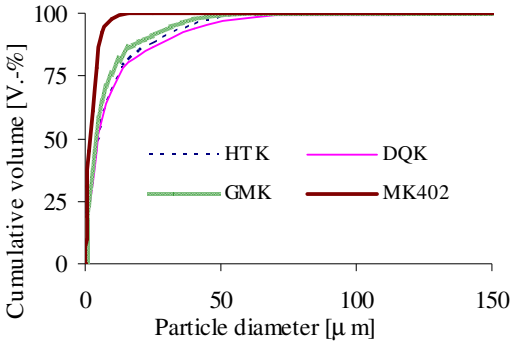

Figure 5.1 The particle size distribution.

5.2 Commercial metakaolin

In this study, two commercial metakaolins (from Germany) were used as a comparative metakaolin. The first metakaolin was MK402, and other was GMK of Centrilit NC powder of MC-Bauchemie Müller GmbH & Co.KG Chemische Fabriken. Their chemical (analysed by ICP-OES) and mineralogical (analysed by XRD/XRD- Rietveld) compositions are presented in Table 5.2, and their particle size distribution (D_{50} of GMK and MK402: 3.8 and 4.7 µm) is shown in Figure 5.1. The BET surface of GMK and MK402 are 10.1 and 12.1 m^2/g, and their densities are 2.57 and 2.58 g/cm^3 respectively.

Table 5.2 Chemical and mineralogical compositions of commercial metakaolin

	SiO_2	Al_2O_3	Fe_2O_3	SO_3	TiO_2	CaO	MgO	K_2O	Na_2O	LOI^+_{1000}
GMK [Wt.-%]	53.70	42.90	0.50	-	0.02	-	0.10	0.41	0.09	1.20
MK402 [Wt.-%]	56.2	37.2	0.8	-	0.03	-	0.2	3.36	0.19	0.9

	Amorphous phase	Quartz	Muscovite	Orthoclase
GMK [Wt.-%]	92.1	4.2	2.7	-
MK402 [Wt.-%]	73.4	4.9	7.8	13.9

5.3 Cement

In this investigation, four ordinary different German Portland cements were used. In addition, a ordinary Vietnamese Portland cement (VPC 40) was used. Their chemical (analysed by ICP-OES) compositions and physical properties (tested by EN DIN 196-1 for German cement, TCVN 6016:1995 and TCVN 6017:1995 for Vietnamese cement) are presented in Tables 5.3+4. CEM I 52.5 R is a low alkali cement (Na_2O_{eq} = 0.47), whereas CEM I 32.5 R is a high alkali cement (Na_2O_{eq} = 0.94). The alkali content of other cements is normal as seen in Table 5.3.

Table 5.3 Chemical composition of cement

	SiO_2	Al_2O_3	Fe_2O_3	SO_3	TiO_2	CaO	MgO	K_2O	Na_2O	Na_2O_{eq}	LOI_{1000}
CEM I 52.5 N [Wt.-%]	20.6	4.5	2.5	3.4	0.2	62.8	1.3	0.9	0.2	0.79	2.6
CEM I 52.5 R [Wt.-%]	19.4	5.3	2.5	3.2	0.3	61.2	1.2	0.61	0.07	0.47	4.9
CEM I 42.5 N [Wt.-%]	21.1	3.8	2.4	2.9	0.2	64.6	1.4	0.8	0.2	0.73	3.0
CEM I 32.5 R [Wt.-%]	20.9	5.4	3.1	3.0	0.32	60.9	3.8	1.19	0.16	0.94	1.8
VPC 40 [Wt.-%]	20.0	5.5	2.8	2.3	0.3	63.1	2.1	0.9	0.2	0.79	1.8

Table 5.4 Properties of cement

	Density [g/cm³]	Blaine surface [cm²/g]	Setting time [h:min]		Water demand [Wt.-%]	Compressive strength [N/mm²]			
			Initial	Final		2d	3d	7d	28d
CEM I 52.5 N	3.12	5310	2:20	3:40	30.0	36.6	-	49.0	60.8
CEM I 52.5 R	3.09	5950	2:20	3:50	31.0	36.2	-	56.6	65.4
CEM I 42.5 N	3.13	3550	2:10	3:10	27.0	26.5	-	43.4	56.3
CEM I 32.5 R	3.16	3450	4:20	5:35	28.5	23.6	-	36.4	50.1
VPC 40	3.10	3546⁺	2:25⁺	3:40⁺	27.3⁺	-	24.2⁺	-	46.4⁺

⁺ tested by Butson Cement Company

It is noted that Vietnamese cement VPC 40 (compressive strength after 28 days have to be higher than 40 N/mm²) can be considered to have a similar strength to CEM I 42.5 N in Germany. For

this reason, in the following investigations in the strength development of metakaolin mortars, CEM I 42.5 N is used instead of VPC 40.

5.4 Aggregates

The standard sands selected for CSI test method come from the standards of EN DIN 196-1 and TCVN 1770 [194]. Starkenberg sand (in mortars, combination with CEM I 52.5 N) and Loriver sand (in mortars, combination with VPC 40) have been used to manufacture high performance mortar.

5.5 Superplasticizer

Polycarboxylate superplasticizer, used in this study, was a commercial product of Sika ViscoCrete-2600. Its density is 1.08 g/cm^3 and pH is 4.5 [195]. Superplasticizer was used in the mixtures of high performance mortar.

6. The optimal thermal conversion of Vietnamese kaolin into metakaolin

6.1 Induction

The object of this study was to produce a good quality metakaolin made from low quality Vietnamese kaolin. As such, in this part of the study Vietnamese kaolins (HTK and DQK) were calcinated to find the optimal conversion rate of kaolin into metakaolin. The optimal thermal conversion is the thermal treatment process of kaolin, whereby calcinated kaolin (metakaolin) produces the highest pozzolanic activity in comparison with other calcinated samples using other thermal treatment processes and the same preparation conditions. The optimal thermal conversion rate was determined by using experimental technologies (e.g, XRD) as well as the pozzolanic activity of calcinated samples. DSC/TGA and XRD techniques were used to characterise calcinated kaolins. The change of mass, density and fineness was determined to monitor calcinated kaolins. Furthermore, pozzolanic activity of metakaolin was assessed by strength activity (CSI) due to its reference characterisation as analysed in section 3.2.

6.2 Calcinated kaolin characterisation

6.2.1 Calcination of kaolin and preparation of samples

HTK and DQK were dried in an oven at 100 ± 5 ^{o}C up to constant mass and then calcinated in an electric kiln Universal TC 805 instrument at various temperatures (500 - 800 ^{o}C) over 1 - 5 hours. A mass of approximate 135 g kaolin was calcinated through heating from room temperature up to the required heating treatment using a heating rate of 10 ^{o}C/min. After the calcinations, the samples were cooled down to the room temperature again in an exsiccator.

BET, PSD and density of calcinated kaolin are analysed as described in section 4.2.1. The mass loss of calcinated samples was then calculated as described in Equation 6.1.

$$ML = 100(M_{bc}-M_{ac})/M_{bc} \qquad \text{Equation 6.1}$$

Where

ML: mass loss of calcinated kaolin after the calcinations [Wt.-%]

M_{bc}: mass of sample before the calcinations [g]

M_{ac}: mass of sample after the calcinations [g]

M_{bc} and M_{ac} were assessed by a experimental scale with the accuracy of 0.01g.

6.2.2 Thermal and gravimetric changes of kaolin

In order to evaluate thermal and gravimetric changes, DSC/TG was used. During the thermal treatment investigations utilising DSC, a defined endothermic peak related to the de-hydroxylation in the range of 400 - 600 °C was observed for both HTK and DQK (see Figure 6.1.a). This strong endothermic peak is typical of kaolinite minerals [37, 38, 39, 40, 41, 196, 197]. The maximum endothermic peak occurred at 503 °C for HTK and at 501 °C for DQK. Another defined exothermic peak, indicating the creation of crystalline phases such as spinel and mullite, occurred at 950 - 1000 °C. The maximum exothermic peak was at 986 °C for HTK and at 993 °C for DQK. Despite the transformation of kaolin into metakaolin taking place at temperatures between 400 - 600 °C, a strong transformation occurred at approximately 500 °C (see Figure 6.1.a). As a result, the thermal treatment process between temperatures of 500 - 800 °C was chosen to calcinate HTK and DQK kaolin.

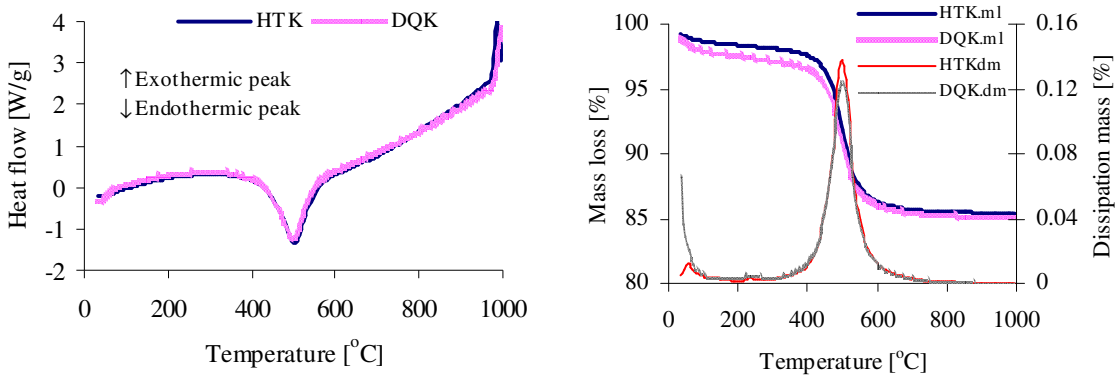

(a) (b)

Figure 6.1 DSC/TG thermogram. (a) Heat flow. (b) Mass loss (ml), dissipation mass (dm).

Figure 6.1.b presents the mass loss of kaolin during the thermal treatment by DSC/TG. A clear-cut mass loss and a strong-intensity peak of dissipation mass took place between 400 - 600 °C. The mass loss between temperatures of 400 - 600 °C was 11.3 Wt.-% for HTK and 10.5 Wt.-% for DQK. The mass loss at a temperature of 1000 °C was 13.76 for HTK and 14.22 Wt.-% for DQK. The intensity height of dissipation mass peak, corresponding to the mass loss of H_2O/OH^- content from kaolinite, was 0.14 %.°C^{-1} for HTK and 0.12 %.°C^{-1} for DQK.

The analysis of DSC/TG showed defined thermal peaks, which suggest that HTK and DQK are well pure kaolin. Mineralogical analysis showed a high content of kaolinite (≈ 90 Wt.-%) in HTK and DQK (see Table 5.1), and this further confirmed the results analysed by DSC/TG.

6.2.3 Mass loss of calcinated kaolin

The thermal treatment of kaolin is a process of mass loss due to the removal of OH^- groups. After calcinations, the mass loss of samples was calculated as described in Equation 6.1. Figure 6.2 showed the mass loss of calcinated kaolin during the calcinations at temperatures of 500 - 800 ^oC, which lasted between 1 - 5 hours. The results obtained revealed that, at the calcination temperature of 500 ^oC the mass loss increased strongly between 1 - 3 hours for HTK (see Figure 6.2.a) and between 1 - 2 hours for DQK (see Figure 6.2.b). A longer heating process did not cause further significant mass losses. This indicates that the transformation of kaolin into metakaolin can be completed by the thermal treatment at 500 °C for a period of 4 hours for HTK and of 3 hours for DQK.

During the calcinations at temperatures between 600 – 800 ^oC (HTK600-800, DQK600-800) for 1 - 5 hours, there was only a slight increase in mass loss. This suggests that a complete conversion of kaolin into metakaolin occurred before a temperature of 600 ^oC was reached. These results agree with DSC/TG analysis, indicating that the factor of mass loss (calculated as described in Equation 6.1) can be used as a basic principle for determining the complete conversion of kaolin into metakaolin.

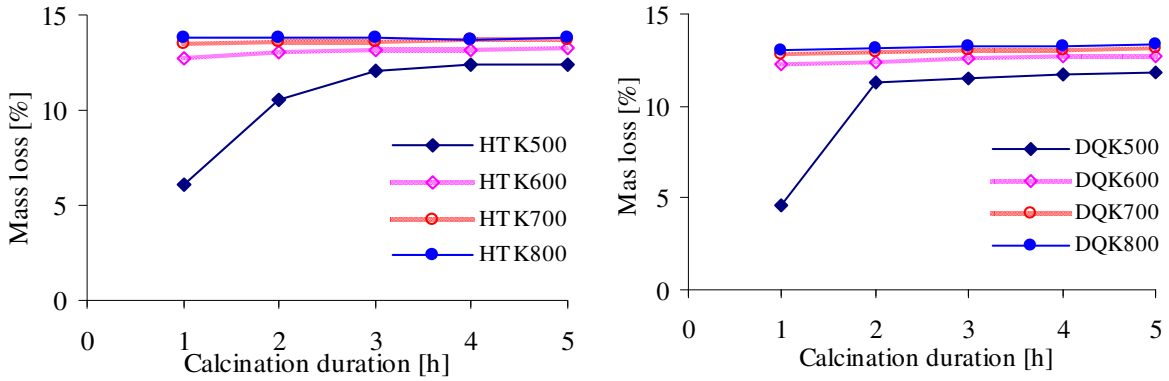

Figure 6.2 Mass loss in dependence of temperature and duration in the calcinations

6.2.4 The mineralogical transformation of calcinated kaolin

XRD background in the region of 18.5-23.5° 2θ is suitable to estimate the degree of disorder in kaolinite samples [198, 199]. This indicates the crystallization state of kaolinite. It is well-known that a less crystallization state results in a higher lime activity of calcinated kaolin [75, 66]. XRD analysis of used kaolin in Figure 6.3 shows that the crystallization state of HTK was poorer than that of DQK as seen by the XRD background (calculated as HI index [200]) in the region of 18.5-23.5° 2θ. This indicates that calcinated samples of HTK provide a higher lime activity than that of DQK. However, the effect of crystallization state on strength activity has as yet not been determined.

The XRD patterns (see Figure 6.3) of calcinated kaolin show that, at 500 °C the intensity of characteristic peaks from kaolinite gradually reduced and disappeared when heating duration is increased. The characteristic peaks of kaolinite disappeared after the thermal treatment at 500 °C lasting for 4 hours for HTK and for 3 hours for DQK. A formation of crystalline phases (spinel / mullite) in samples, which are calcinated up to 800 °C for 4 - 5 hours, could not be observed. This result correlates well to results of DSC/TG analysis (see Figure 6.1).

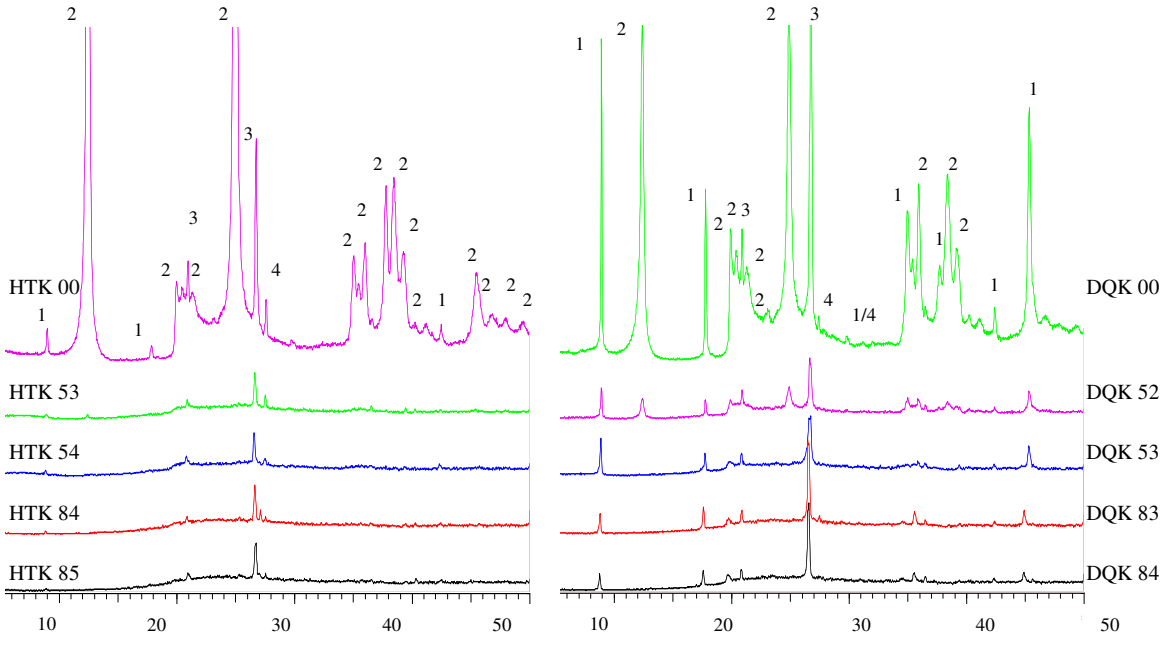

Figure 6.3 XRD patterns of untreated kaolin (HTK and DQK) and calcinated kaolin (Kxy, samples are calcinated at 100x °C temperature in y hours) with peaks of 1 (muscovite), 2 (kaolinite), 3 (quartz) and 4 (orthoclase). (a) HTK, (b) DQK.

The impurities in the kaolin HTK and DQK are muscovite, quartz and orthoclase. During the calcination up to 800 ^{o}C, a transformation took place for the mineral muscovite, but this was not the case for quartz and orthoclase. A starting transition of quartz into cristobalite or tridymite occurs at 1100 °C [201, 202]. As such, quartz does not influence the quality of metakaolin during the calcination up to 800 ^{o}C. Despite this, the phase transition of muscovite is a de-hydroxylation process with a major phase transition occurring at about 700 - 800^{o}C [203, 204]. This leads to change in the fold coordination of Al atoms, from $Al^{3+[VI]}$ to $Al^{3+[V]}$; The c-axis of muscovite at high temperatures is longer than the c-axis of the original muscovite phase [205, 204]. It also results in the easy release of potassium from muscovite, which has a negative influence in mitigating ASR [206, 204, 207]. The size and organisation degree of the muscovite network is closely related to E-modulus in ceramic and silicone materials [208, 209]. When kaolin is calcinated up to 800 ^{o}C, muscovite can influence the quality of metakaolin. If orthoclase is present, migmatites can be created from muscovite as a metamorphic event at over 650 ^{o}C under a high pressure [210]. The breakdown of muscovite + quartz at 757 ^{o}C can be influenced by H_2O [211]. As such, the transition of impurity such as muscovite, quartz and orthoclase hardly occurs. However, the quantity of these impure minerals is insignificant (see Table 5.1). Thus, the mini change in mass of impurities and their effect on the transformation of kaolinite into metakaolin during calcination were not investigated in this study

The results of quantitative phase analysis by XRD-Rietveld of kaolin and calcinated kaolin at various temperatures and periods is shown in Table 6.1. Mullite was never observed in the applied calcinated conditions, and the amorphous phase content of calcinated kaolin increases during the calcinations. Amorphous phase content of calcinated HTK/DQK during the calcination at 500 ^{o}C increased from 26/9 Wt.-% for 1 hour to 89.7/85.8 Wt.-% for 4 hours. At 500 °C in 4 hours for HTK and in 3 hours for DQK, the increase in amorphous phase content was almost constant. Calcination at 800 °C did not bring further significant increase of amorphous phase content. Muscovite quantity increased during the calcination up to 500 ^{o}C due to the conversion of kaolinite to muscovite/illite at temperatures ranging from 250 - 307 °C [212]. Also, at 500 ^{o}C of calcination, the small increase in mass of muscovite content for HTK54/DQK53 could be mainly due to the total mass loss of kaolin. However, probably the limited potassium content of kaolin, which is a necessary condition for the conversion of kaolinite to muscovite/illite [212], prevented the further formation of muscovite/illite from kaolinite during the calcination at 800 ^{o}C. The conversion of other minerals which transformed in smaller amounts is out of the scope of this study.

Table 6.1 Mineralogical phase in calcinated samples calculated by XRD-Rietveld analysis

	Amorphous phase	Quartz	Muscovite / Illite	Orthoclase	Sanidine Na0.16	Kaolinite
HTK 00	-	2.4	2.4	1.4	-	93.1
HTK51	26.0	3.0	2.2	2.9	-	65.9
HTK54	89.7	3.6	4.0	2.8	-	-
HTK84	92.5	3.3	2.7	-	1.5	-
DQK00	-	2.4	4.5	1.0	-	92.1
DQK51	9.0	4.8	5.8	2.4	-	78.1
DQK53	85.5	5.3	7.7	1.5	-	-
DQK83	86.2	5.7	6.3	-	1.4	-

Kxy: kaolin that is calcinated at 100*x temperature of the calcination in y hours.
- : minerals are not found or have a very small amount

6.2.5 Density, BET surface and PSD of calcinated kaolin

Figure 6.4 represents the measured density of calcinated kaolin at different temperature and duration of the calcinations. In generally, density of calcinated kaolin was smaller than that of kaolin (2.60 g/cm^3 for HTK and DQK), except calcinated kaolin at 800 ^{o}C (2.61 g/cm^3 for HTK84 and 2.60 g/cm^3 DQK83). During the calcination from 500 – 800 ^{o}C lasting 1 – 5 hours, the changes of density were observed as follows: At the calcination temperature of 500 ^{o}C lasting from 1 - 3 hours, the density of calcinated sample was reduced, which is explained by the partly mass loss from H_2O^-/ H_2O^+/ OH^- groups as analysed in section 3.1.2. However, no further reduction was observed when samples were prolongly heated at 500 ^{o}C. A tendency for an increased in density was observed at the calcination temperatures of 600 - 800 ^{o}C lasting for 1 - 3 hours. Achieved results demonstrate that, the pre-dehydration was completed after the calcinations at 500 ^{o}C which lasted for 3 hours. This is further confirmed by the analysis of DSC/TG, XRD and mass loss above.

The change of density can correspond with the collapse of kaolinite layers (as analysed in section 3.1.2) which leads to the gradual reduction of BET surface in calcinated kaolin as seen in Figure 6.5. A strong reduction in BET surface was observed over the total samples calcinated at 500 ^{o}C within 1 hour down to samples calcinated at 800 ^{o}C within 5 hours (2.1 for HTK and 3.4 m^2/g for DQK).

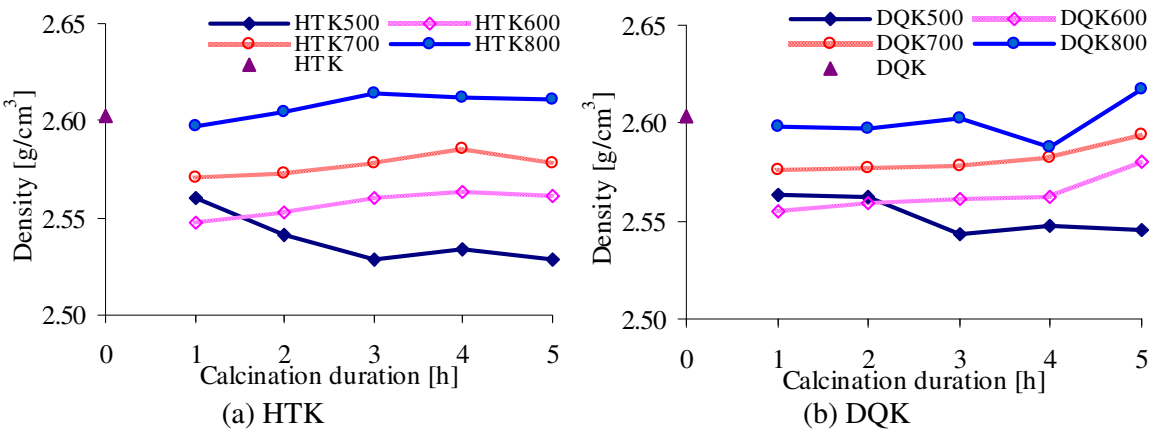

Figure 6.4 Density in dependence of temperature and duration in the calcinations

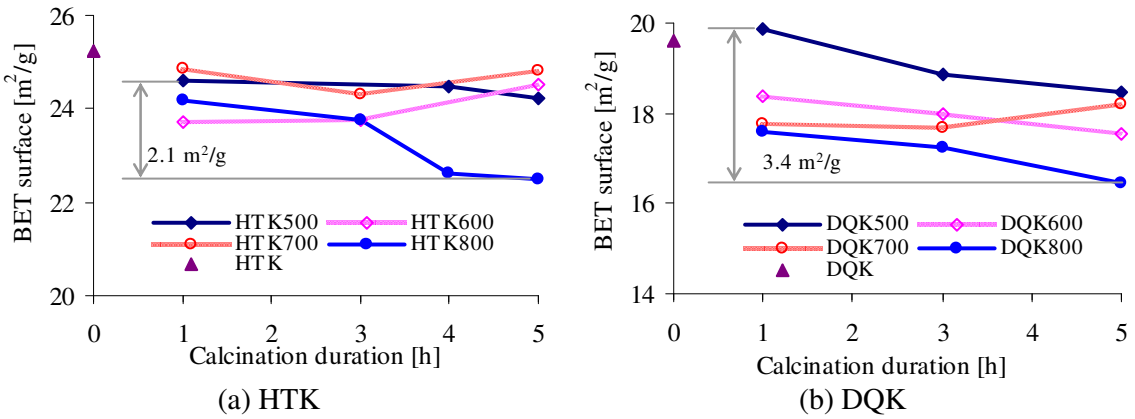

Figure 6.5 BET surfaces in dependence of temperature and duration in the calcinations

The results of PSD from HTK kaolin and calcinated HTK are shown in Figure 6.6. The agglomeration phenomenon takes place during the calcination. In generally, calcinated kaolin showed the increase in volume of particles bigger than ca. 4µm as compared to that of kaolin. This behaviour is especially easily seen at the level of particle size bigger than ca.20µm. An agglomeration among particles into coarser particles (> ca.100 µm) was observed for calcinated kaolin during calcinations, while such coarser particles are not present in kaolin as seen in Figure 6.6 (details in Appendix 13.4). Calcinated kaolin also showed the reduction of volume in particles smaller than ca. 4µm as compared to that of kaolin. Taken together, achieved results confirm the the collapse of kaolinite layers (see section 3.1.2) which leads to the agglomeration phenomenon among particles (Figure 6.6), causing the reduction of BET surface in calcinated kaolin as seen in Figure 6.5. The same behaviour was observed on calcinated DQK during the calcinations (see Appendix 13.4)

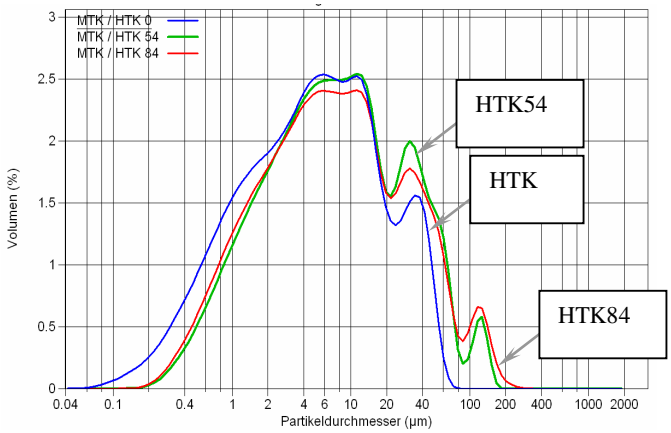

Figure 6.6 Particle size distribution of kaolin and calcinated kaolin.

6.2.6 Residual water in calcinated kaolin

Analysed by XRD (see Figure 6.3), calcinated kaolin at 500 °C (HTK54, DQK53) showed no more characteristic peaks of kaolinite. However, the mass loss analysis (see Figure 6.2) indicated that, there was still residual water in calcinated kaolin at 500 °C. In order to prove the presence of residual water, DSC/TG analysis was carried out again for certain samples such as HTK54 / HTK84 and DQK53 / DQK83 as shown in Figure 6.7.

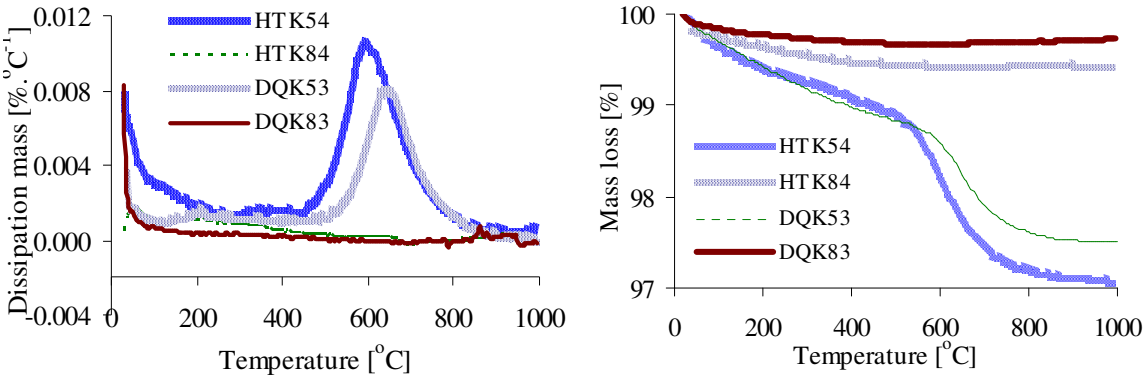

(a) Dissipation mass (b) Mass loss

Figure 6.7 DSC/TG thermogram of calcinated kaolin.

The results as shown in Figure 6.7.a reveal that, HTK84 and DQK83 do not contain any peaks of dissipation mass regarding residual OH^- groups, whereas HTK54 and DQK53 contain. This can be seen also by the mass loss shown in Figure 6.7.b. The residual water can be shown to have definitely come from kaolinite/metakaolinite due to of the following reasons:

(1) According to the XRD- Rietveld in Table 6.1, the residual H_2O^+/OH^- in all samples can only come from kaolinite/metakaolinite and muscovite. Their masses are reduced due to the de-hydroxylation during the calcination.

(2) The mass loss of muscovite at 980 ^oC due to the removal of hydroxyls is 4.7 Wt.-% [204]. The presence of a small amount of muscovite in samples (see Table 6.1), such as HTK54 (4.0 Wt.-%) and DQK53 (7.7 Wt.-%), can lead to their mass loss up to 0.31 Wt.-%. However, the mass loss of HTK54 and DQK53 was more than 2 Wt.-% (see Figure 6.2 and Figure 6.7.b). For this reason, the peak of dissipation mass must also be due to the mass loss of kaolinite/metakaolinite.

(3) The removal of H_2O^+/OH^- groups can occur between temperatures of 400 – 1000 ^oC [213]. If the residual water coming from muscovite is assumed, the peak of dissipation mass should occur between temperatures of 800 – 900 ^oC [204]. Besides that, the mass loss of residual water coming from kaolinite/metakaolinite mainly occurred at about 450 °C [42]. However, as seen in this study, the peak of dissipation mass took place between temperatures of 450 – 800 ^oC (see Figure 6.7.a). Taken together, these results suggest that the peak of dissipation mass is not due to the mass loss of muscovite.

It can be inferred therefore from these three reasons, that the peaks of dissipation mass (shown in Figure 6.7.a) are characteristic peaks from the residual water in kaolinite/metakaolinite. The question of whether this residual water can influence the pozzolanic reaction capability as well as ion binding at varying cure temperatures should be answered, as this information is very useful for the application field of metakaolin with respect to durability.

6.2.7 Residual water in relation to BET surface for calcinated kaolin

It can be shown from Figure 6.2, Figure 6.5 and Figure 6.7 that the basic principle in the calcination process for kaolin is the loss of water (H_2O^- / H_2O^+ / OH^-) causing the reduction in BET surface. Therefore, BET surface reduction is considered as the factor that indicates the transformation from metakaolin with residual water to total de-hydroxylation metakaolin (without residual water). A higher BET surface is determined in metakaolin containing the residual water (see Figure 6.8). Their presence indicated that the collapse of kaolinite layers (from 7.15 A^o down to 6.3 A^o [43]) had not completely occurred. Thus, freer layer surfaces could be available, and therefore BET surface was higher. Additional results from this study contribute

to further explain the reduction in BET surface during the calcination that has previously been observed [37, 50, 51, 52, 53, 54, 55].

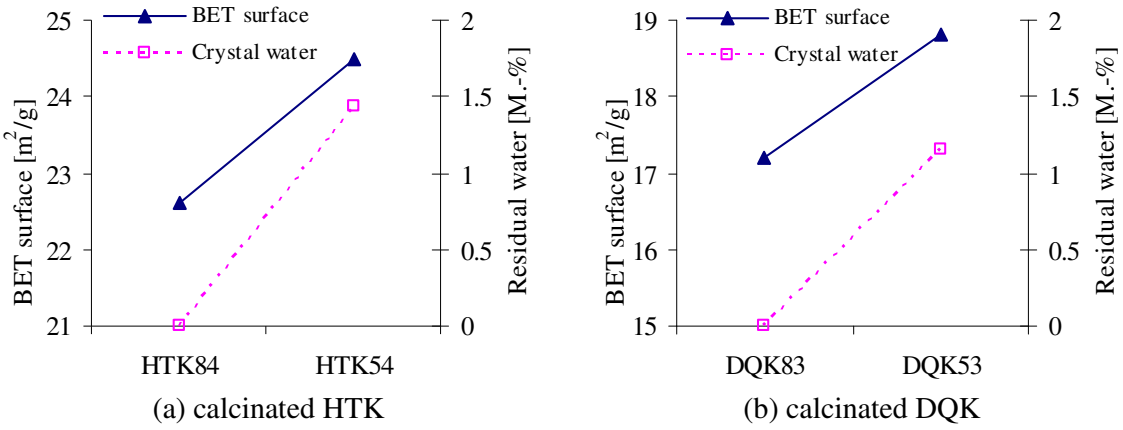

Figure 6.8 The relation between BET surface and residual water content during calcination

6.3 The pozzolanic activity of calcinated kaolin based on CSI

Strength activity, tested by CSI as described in Equation 4.1 for HTK and DQK, is represented in Figure 6.9. HTK and DQK metakaolin showed a higher strength activity than the control sample (CEM I 52.5 N), except HTK that was calcinated at 500 °C within 1 hour.

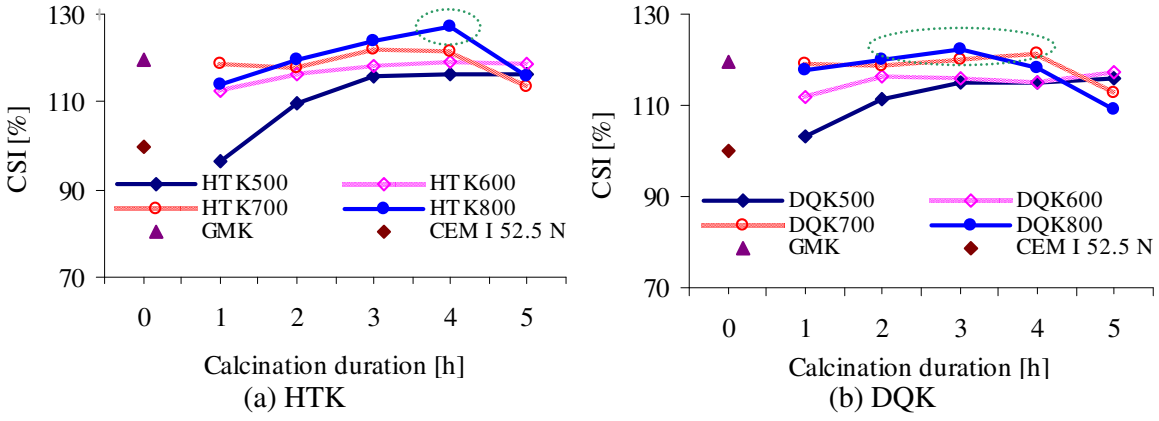

Figure 6.9 Strength activity by CSI

At the calcination temperature of 500 °C, the strength activity value increased strongly between 1 - 3 hours for HTK (see Figure 6.9.a) and between 1 - 2 hours for DQK (see Figure 6.9.b). A longer heating process did not cause further significant increase in strength activity. This is in a

good agreement with the complete transformation of kaolin into metakaolin, which was revealed by XRD analysis (see Figure 6.3) and mass loss (see Figure 6.2).

HTK54 and DQK53 showed a significantly lower activity of strength than the commercial product GMK. A similar pozzolanic activity like GMK was observed in HTK74, DQK73 and DQK82. The maximum strength activity was achieved at the calcination temperature of 800 ^{o}C lasting for 4 hours for HTK (HTK84) and for 3 hours for DQK (DQK83) respectively. This indicates that either the increasing content of amorphous phase (see Table 6.1) as proved in [74, 75], or the conversion of phases and the increase of density (see Figures 6.3+4) in calcinated kaolin could be a further benefit for CSI.

6.4 Representative samples for next investigations

In order to study the potential utilisation of Vietnamese metakaolin in future, two metakaolin groups calcinated at 500 and 800 ^{o}C were chosen as representative samples. HTK84 and DQK83 were chosen as representative samples calcinated at 800 ^{o}C due to their highest CSI and structure without residual water. HTK54 and DQK53 have been chosen due to their structure with the presence of residual water.

Table 6.2 Properties of Vietnamese metakaolin

	HTK54	HTK84	DQK53	DQK83
Mass loss [Wt.-%]	12.4	13.7	11.5	13.2
Amorphous content [Wt.-%]	89.7±1.0	92.5±1.4	85.5±1.4	86.2±1.5
Density [g/cm^3]	2.53	2.61	2.54	2.60
BET surface [m^2/g]	24.5	22.6	18.8	17.2
D_{50} [µm]	7.3	7.0	6.3	5.7
CSI [MPa.-%]	116	127	115	122
Presence of residual water	Yes	No	yes	No
Residual water mass$^+$ [Wt.-%]	1.43	0	1.15	0

+ determined by DSC/TGA, refering to the peak of dissipation mass and calculating as [189] and [190].

In addition to this, two commercial products, GMK and MK402, were used to compare with Vietnamese metakaolin. GMK and MK402 have no residual water in their structure, and their properties are described in section 5.2.

6.5 Discussion

It is concluded from Figure 6.3 that calcinated kaolin is called metakaolin when its peak of kaolinite is absent in XRD partten. It is inferred from Table 6.2 that a high content of amorphous phase is not the only requirement for the highest value of CSI, but the absence of residual water is needed.

Depending on strength activity in this study (see Figure 6.9), a thermal treatment table for Vietnamese metakaolin was selected and recommended (see Table 6.3). For good quality metakaolins, the strength activity of HTK and DQK (calcinated at 700 - 800 ^{o}C for 3 - 4 hours) is higher or similar to that of the commercial metakaolin product GMK. Other samples in the table of thermal treatment process are normal quality metakaolin that their strength activity are higher or similar to that of the control sample CEM I 52.5 N. In practical manufacture conditions, one to two hours of calcination at 500 ^{o}C is not long enough for a large amount of kaolin. At least 4 hours of calcination for HTK and 3 hours of calcination for DQK should be carried out for the pilot manufacturing. However, not longer than 4 hours due to the economical factor of energy consumption. Depending on the features of each technology calcinating metakaolin, each thermal treatment process from the Table 6.3 could be used. For example, to turn the waste heat emission from the manufacturing process of cement or ceramic into advantage, the thermal treatment process at 500 ^{o}C within 4 hours for HTK and 3 hours for DQK could be used for producing metakaolin. This is convenient for energy save.

Table 6.3 Thermal treatment process of HTK and DQK

	Good quality Metakaolin		Normal quality Metakaolin			
Heating temperature [^{o}C]	700	800	500	600	700	800
HTK, calcination duration [h]	3-4	3-4	4	2-4	1-2	1-2
DQK, calcination duration [h]	4	3	3	2-3	1-3	1-2

6.6 Concluding remarks

HTK and DQK were calcinated between temperatures of 500 - 800 ^{o}C over a period of 1 - 5 hours. Their chemical- physical-mechanical properties before and after the calcinations were determined. The gained results provided the basic principle for determining the optimal thermal conversion rate of kaokin in to metakaolin. The following conclusions can be drawn:

(1) Kaolin is transformed into metakaolin at the thermal treatment of 500 ^{o}C over a 4 hour period for HTK and for 3 hours for DQK. The optimal thermal treatment for HTK and DQK is at 800 °C for 4 and 3 hours, respectively. With these thermal treatments, the produced metakaolin (HTK84 and DQK83) exhibits the highest CSI.

(2) The thermal treatment of kaolin is a process of mass loss due to the removal of the H_2O^-/ H_2O^+/OH^- groups. Thus, the factor of mass loss (determined by Equation 6.1) can be used for determining the complete conversion of kaolin in to metakaolin.

(3) During the calcination, because of the removal of the H_2O^+/OH^- groups and the collapse of kaolinite layer structure, the mass and BET surface of calcinated kaolin tends to decrease, while its density tends to increase. It can be concluded that the presence of residual water as well as the not fully collapsed layer structure in calcinated kaolin causes an increased BET surface during the calcinations.

(4) The peak of dissipation mass in TGA analysis can be used for determining the characteristic peaks from the residual water in kaolinite/metakaolinite.

(5) A save indicator for complete conversion of kaolinite into metakaolinite is the absence of kaolinite peaks in XRD patterns.

7. Estimation of pozzolanic activity for metakaolin by means of lime consumption

7.1 Induction

The meaning of pozzolanic activity is needed for assessing an optimal thermal treatment process for producing metakaolin. The optimal conversion rate from kaolin to metakaolin often depends on the pozzolanic activity such as the strength activity (indirect testing method) or lime consumption (direct testing method) [214, 215, 52, 38, 74, 76]. Strength activity is a direct measurement of concrete performance. Thus, strength activity is often used as a reference method for determining the pozzolanic activity of calcinated kaolin. The lime consumption value of metakaolin provides no clear information about the performance of concrete products. In addition the lime consumption value of metakaolin is influenced by the pozzolanic reaction that takes place both though cation absorption (on the surface of metakaolin) and adsorption (on the surface of hydration products), and cation exchange (between amorphous phase of metakaolin and free lime CaO). The cation adsorption can take place continuously, as long as the cation is free and the surface of metakaolin is available. The cation exchange continues unless one of conditions as amorphous phase content (metakaolinite), free cation (e.g, Ca^{2+}) and a connective condition between them (pore solution) is absent.

An open question that has to be answered is, whether or not the pozzolanic activity assessed by means of lime consumption can be used for assessing metakaolin quality as the reference method CSI. Thus, in this part of the study the direct testing methods (the saturated lime method, TGA-CaO method and mCh) were compared to the indirect test (CSI). Due to the fact that testing durations for the hydration of the direct tests TGA-CaO method and mCh are non-standard methods, their testing durations need to be determined. The testing duration ensures that achieved value of lime consumption after a certain hydration time reaches a stability-threshold value (almost constant). Testing duration for the saturated lime method is fixed at 30 days according to the Vietnamese standard [63], and time periods for mCH can fluctuate between 8 and 15 days as EN DIN 196-5 [216].

In order to find out the optimal direct testing method, a commercial metakaolin product (GMK) was included to serve as a reference for the Vietnamese metakaolin: HTK (HTK54, HTK84), DQK (DQK53, DQK84). It should be noted that HTK54 / HTK84 and DQK53 / DQK83 were made from the same kaolin HTK / DQK but calcinated by different thermal treatment processes. Therefore, HTK54 / DQK53 (at 500 ^{o}C calcination) possesses the similar chemical compositions

and amorphous phase contents to HTK84/DQK83 (at 800 °C calcination). However, they are different for BET surface and PSD as shown in section 6 (see Table 6.2). Since section 3.3.2 showed the influence of BET surface and PSD on the pozzolanic activity of metakaolin, their influence will also be considered in the following. As such, the experiment setup will not only be a comparison of different testing methods for evaluating of lime consumption v.s CSI, but also a monitor of the role of BET surface and PSD on these will be investigated. The obtained results are important for the optimisation of thermal treatment process as well as the classification of metakaolin.

7.2 The saturated lime method

Table 7.1 presents the pozzolanic activity tested by the saturated lime method (see section 4.4.2). Of all tested samples, GMK with the lowest D_{50} surface had the greatest value of lime consumption. This reflects the role of PSD when samples are submerged in solution. However, no correlation was found between BET surface factor and lime consumption value. The value of lime consumption decreased as follows: GMK > HTK54 ≈ HTK84 ≈ DQK53 ≈ DQK83. This does not agree with the results from the reference test CSI (HTK84 ≥ DQK83 ≥ GMK > HTK54 ≥ DQK53).

Table 7.1 Lime consumption tested by the saturated lime method
(1g metakaolin, 850 ml saturated lime solution, 30d, room temperature)

	HTK54	HTK84	DQK53	DQK83	GMK
Consumed CaO at 30 days [mg/g]	192-196	180-197	188-193	185-195	231-239
BET surface [m^2/g]	24.5	22.6	18.8	17.2	10.1
D_{50} [μm]	7.3	7.0	6.3	5.7	3.8

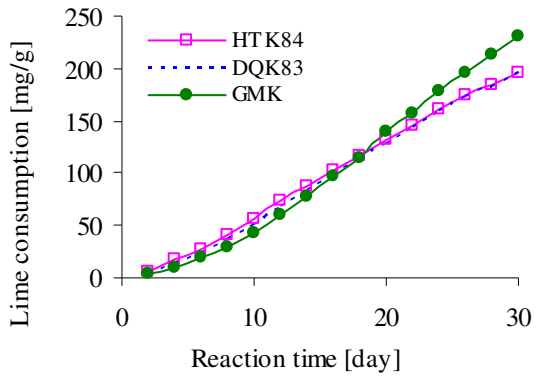

Figure 7.1 Lime consumption tested by the saturated lime method for samples (1g metakaolin, 850 ml saturated lime solution, 30d, room temperature).

The cause for the lack of correlation in results between the saturated lime method and CSI could be that selected hydration period on the days 30 is too short. As shown in Figure 7.1, the lime consumption cumulatively increases up to 30 days of reaction process. The slope of the curves, i.e. the rate of lime consumption, was not reached a threshold value. Thus, it may occur that observed trends vary significantly at a longer hydration period. Therefore, the results of the saturated lime method are not considered to be reliable.

7.3 TGA-CaO method

Unlike the saturated lime method, the determination of CaO consumption by TGA analysis in TGA-CaO method (see section 4.4.3) is still not considered as a standard test method. Up to now, no reaction period is assigned to which test has to be followed up. For this reason, the lime consumption (calculated as described in Equation 4.5) was determined at various time as shown in Figure 7.2. The results show that after 7 days of the hydration process the increase in lime consumption value is limited up to 28 days. Thus, a period of 28 days was chosen to compare lime consumption values by TGA-CaO method.

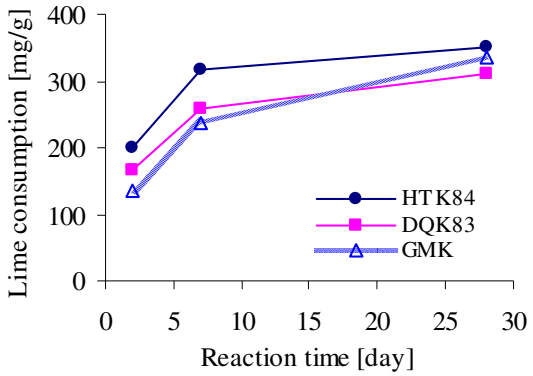

Figure 7.2 Lime consumption tested by TGA-CaO method for samples (CEM I 52.5 N: metakaolin = 80:20 Wt.-% at the w/b of 0.5, 20 °C and 100%RH).

Table 7.2 Lime consumption tested by TGA-CaO method
(CEM I 52.5 N: metakaolin = 80:20 Wt.-% at the w/b of 0.5, 20 °C and 100%RH)

	HTK54	HTK84	DQK53	DQK83	GMK
Consumed CaO at 28 days [mg/g]	387	352	361	310	336
BET surface [m^2/g]	24.5	22.6	18.8	17.2	10.1
D_{50} [µm]	7.3	7.0	6.3	5.7	3.8

Table 7.2 shows that cement pastes containing metakaolin with a higher BET surface possess a higher value of lime consumption. The impact of D_{50} is absent in the values of lime consumption. The lime consumption value decreased as follows: HTK54 > DQK53 > HTK84 ≥ GMK ≥ DQK83. For both TGA-CaO method and CSI, the value of pozzolanic activity reduces as follows:

The first group with the presence of residual water: HTK54 > DQK53

The second group without the presence of residual water: HTK84 ≥ GMK ≥ DQK83

The reason for the disconnection between TGA-CaO method and CSI in all tested groups (with and without residual water) is due to the influence of metakaolin surface. BET surface of HTK54 - DQK53 group is higher than that of HTK84 - DQK83 - GMK group. As such, the lime consumption value of HTK54 - DQK53 group is higher than that of HTK84 - DQK83 - GMK group as analysed in section 3.3.2 and 6.2.7. However, the difference in BET surface between these two groups (< 3 BET m^2/g) is too few and such is not considered to be relevantly high enough (7 – 70 BET m^2/g) for impacting on CSI significantly as showed before by [70, 92].

In order to see the clear influence of BET surface on the value of lime consumption at a limit water condition (at low w/b ratio), the w/b of 0.38 was investigated in this respect.

Table 7.3 Lime consumption tested by TGA-CaO method
(CEM I 52.5 N: metakaolin = 80:20 Wt.-% at the w/b of 0.38, 20 ^oC and 100%RH)

	HTK54	HTK84	DQK53	DQK83	GMK
Consumed CaO at 28 days [mg/g]	351	296	313	248	273
BET surface [m^2/g]	24.5	22.6	18.8	17.2	10.1
D_{50} [μm]	7.3	7.0	6.3	5.7	3.8
Amorphous content [Wt.-%]	89.7	92.5	85.5	86.2	92.1

Table 7.3 shows the lime consumption value of metakaolin from mixtures with w/b 0.38. The same influence of BET surface as Table 7.2 was observed on the gained results of lime consumption. Due to the fact that HTK54 and DQK53 have a higher BET surface than HTK84 and DQK83 respectively. Also their amorphous phase content is almost similar to that of HTK54 and DQK53 respectively. This indicates that lime consumption of metakaolin correlates well with its BET surface.

7.4 mCh

As mCh (see section 4.4.4) does not declare a standard curing time, a sample HTK84 was prepared and investigated after various periods to determine the reaction time for all samples. The aim was to find the hydration period when the rate of lime consumption is limited as shown in Figure 7.3. The gained results show that, the development of lime consumption was stable and almost constant after 9 days. Therefore, the reaction time of 9 days was chosen for following experiments from mCh.

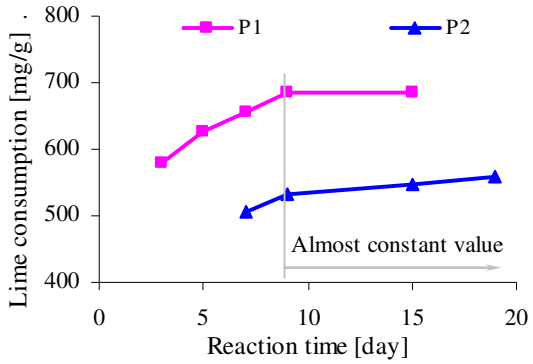

Figure 7.3 Lime consumption of HTK84 with reaction time. P_1: Sample with utrasound 80% in 4min. P_2: sample with the preparation as section 4.4.4.

Table 7.4 presents the lime consumption results tested by mCh. It shows that, metakaolin with a lower D_{50} had a higher value of lime consumption. However the results from mCh did not correlated with BET surface. The value of lime consumption decreases as follows: GMK > HTK84 ≈ DQK83 > HTK54 ≈ DQK53. In this order, only GMK does not agree with the results from the reference test CSI (HTK84 ≥ DQK83 ≥ GMK **>** HTK54 ≥ DQK53). The reason for the disagree of GMK is unclear, but it may be due to the production process of this commercial metakaolin GMK (e.g, usage of polymers for grinding process).

Table 7.4 Lime consumption tested by mCh (1g metakaolin, 1g CH, 200ml H, 9d, 40°C)

	HTK54	HTK84	DQK53	DQK83	GMK
Consumed CaO at 28 days, [mg/g]	487	533	480	526	625
BET surface [m^2/g]	24.5	22.6	18.8	17.2	10.1
D_{50} [µm]	7.3	7.0	6.3	5.7	3.8

The reason why D_{50} shows its more dominant effect on the value of lime can be explained as follows. The test condition is performed at a high temperature (40 ^{o}C) with the use of excess water (200ml) as well as a long hydration time (9 days), which leads to reactions across the complete surface of the metakaolin (gained high value of lime consumption, Table 7.4). As a result, the impact of BET surface was obscured.

7.5 Discussion

7.5.1 Estimation of pozzolanic testing methods by means of lime consumption

Figure 7.4 presents the lime consumption of metakaolin tested by the saturated lime method, TGA-CaO method and mCh. The given values in the saturated lime method were the average value calculated from Table 7.1, and the given values for TGA-CaO method and mCh came from Table 7.2 and Table 7.4. As can be seen, the different values of lime consumption were given by different testing methods.

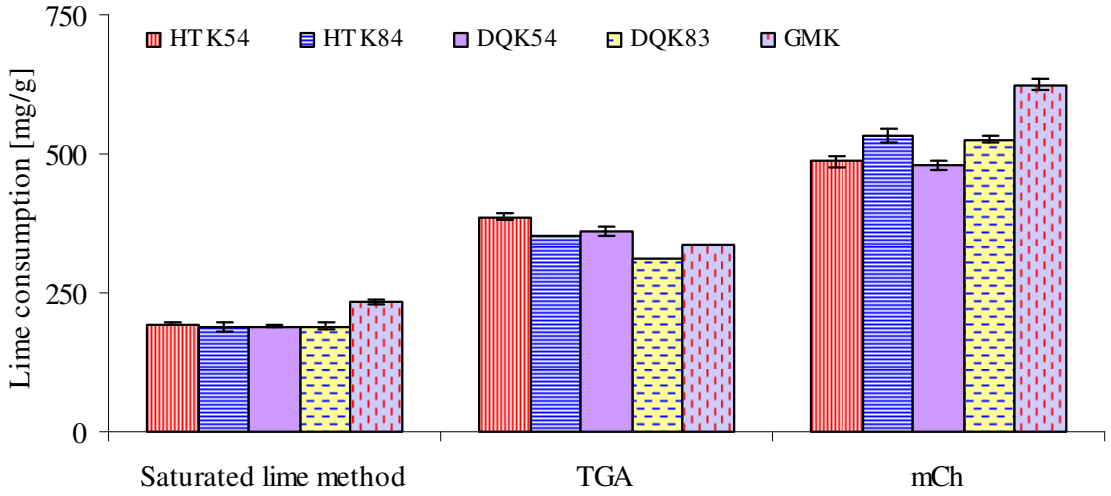

Figure 7.4 The lime consumption of metakaolin measured by different testing methods.

The mCh method showed the highest lime consumption from the samples tested, whilst the saturated lime method showed the smallest value; with the TGA-CaO method resulting in a medium rate of consumption. A higher reaction temperature of 40 ^{o}C and a direct connection between CH and metakaolin could be the reason why mCh showed the highest value of lime consumption. Therefore, these consumption rates can be considered as the maximum lime consumption valuations that metakaolin can achieve. On the contrary, reaction temperature of

20°C and the concentration of Ca^{2+} ions of the saturated lime method were lower. In addition the testing age is 30 days, although the development of lime consumption vs. reaction time did not reach a stop value or threshold value (see Figure 7.1). For these reasons, the saturated lime method delivered the smallest value of lime consumption. This also shows that, the low concentration of Ca^{2+} ion in the saturated lime method does not suit to assess the high pozzolanic activity of metakaolin. The saturated lime method therefore would better suit for evaluating a low pozzolanic activity material such as fly ash and slag. In TGA-CaO method, metakaolin contacts directly with Ca^{2+} coming from the hydration process of cement in the condition of limited water content (w/b of 0.38 - 0.5). Moreover, a large amount of heat is released during the hydration of cement, which results in an increase in temperature up to 45 °C in the early age of the hydration process [217]. Thus, pozzolanic reaction of metakaolin is promoted and the lime consumption values are between that of the saturated lime and mCh methods. In addition, the hydration process required for a test to be carried out is at the 28 day mark. Thus, the increase in lime consumption vs. reaction time is already low (see Figure 7.2). As such, the lime consumption evaluation by TGA-CaO method is a good reflection on the actual behaviour of metakaolin in concrete. Due to this, TGA-CaO method can be seen to be the most suitable method to characterise the pozzolanic activity of metakaolin. Furthermore, it is referred from section 7.3 that, with respect to a certain content of residual water in metakaolin structure, TGA-CaO method can reach a good balance between metakaolin and cement performance. These findings also match the results presented in [218].

7.5.2 Direct tests in relation to indirect test

It can be inferred from Tables 7.1+2+4 and direct test CSI (see section 6.3) that, there is no linear correlation between results investigated by the direct test and CSI. The reason for this lack of correlation is due to the following:

A linear correlation between CSI (strength activity, indirect test) and lime consumption (lime reaction, direct test) is impossible. The lack of correlation between them is generally explained by the difference of measurement conditions as well as the type of pozzolan and cement [219, 69]. However, the problem in mismatch between results from different testing methods for pozzolanic activity of metakaolin is due to two reasons.

The first reason is the different unit measuring pozzolanic activity. The measurement unit used for the direct test depends on the amount of lime consumption, and this contains two similar ratios. One is the amount of the lime consumption in relation to the mass of metakaolin (mg/g

ratio), and the other is the amount of the lime consumption in relation to the amorphous phase content in metakaolin (mg/g AP ratio). These two current ratios are not always compatable with the current ratio of the indirect test, which is the relative compressive strength (% ratio). This makes the comparison and correlation of direct and indirect tests impossible.

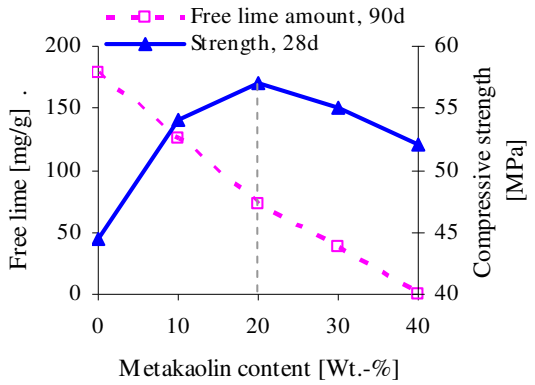

Figure 7.5 Free lime of lime pastes and compressive strength of mortars v.s metakaolin content (CEM I 52.5 N: metakaolin = 100:0 / 90:10 / 80:20 / 70:30 / 60:40 Wt.-%)

The second reason is a non-linear relationship between lime consumption and compressive strength v.s metakaolin content as described in Figure 7.5. The increase in metakaolin amount or in the amorphous phase content does not always lead to an increase in relative compressive strength but always leads to a reduction in free lime content (the increase in lime consumption). It is logical that a certain amount of cement clinker is needed to obtain a sufficient compressive strength of mortar, which is high at a certain amount of metakaolin used. Normally, maximum compressive strength is achieved when 10 - 20 Wt.-% of cement is replaced by metakaolin in mortars and concretes [141, 143, 142, 70, 144, 145, 146, 147, 148, 149]. If more than 20 Wt.-% metakaolin is used, the compressive strength decreases [142, 148]. However, after 90 days the lime content drops down to zero when 40 Wt.-% cement has been replaced by metakaolin. Taken together, it is concluded that the comparison and correlation of direct and indirect tests cannot be carried out.

As analysed, the correlation between different tests is impossible. However, in order to have an overall assessment of metakaolin quality, two factors of CSI and lime consumption need to be assessed. CSI is used as an overall assessment in the reliability (mechanical strength and

chemical) of concrete products, while the lime consumption factor is used to predict their durability such as ASR and sulfate attack.

7.6 Concluding remarks

The following results were obtained.

(1) The lime consumption tested by the saturated lime method, TGA-CaO method, and mCh does not agree with the reference test CSI, although TGA-CaO method can be seen to be the most suitable method to characterise the pozzolanic activity of metakaolin and to provide the best agreement between metakaolin and the performance of cement and concrete products.

(2) BET surface has a significant impact on lime consumption evaluation tested by TGA-CaO method, whilst D_{50} shows its more dominant effect on the value of lime consumption tested by mCh.

(3) The mCh method shows the highest lime consumption from the samples tested, whilst the saturated lime method shows the smallest value; with the TGA-CaO method resulting in a medium rate of consumption.

8. Influence of metakaolin on mechanical and physical properties of cement and concrete

8.1 Induction

Before 1990, the compressive strength of reinforced concrete in Vietnamese constructions reached mainly 20 MPa and seldom 30 - 40 MPa. Nowadays, the compressive strength of reinforced concretes is mainly 30 MPa for normal building constructions and up to 60 MPa for special constructions. Very high compressive strength concrete (more than 100 MPa) has rarely been studied and applied for building constructions like bridge structures in Vietnam. Recently, the potential of manufacturing high performance concrete (60 – 80 MPa) in Vietnam has been addressed. Preliminary results confirmed that available materials in Vietnam can be successfully used for producing HPC [220]. Imported silica fume (from Elkem Silicon Material in Kingdom of Norway) and superplasticizer (Sika in Switzerland and MBT in Australia) facilitates the production of HPC and UHPC in Vietnam [221]. Recent studies have shown that Vietnamese rice husk ash can be applied to produce HPC and UHPC [222, 223]. However, the potential to use Vietnamese metakaolin for producing HPC has not been the subject of investigation. Therefore, in the present study, strength development was investigated not only for normal metakaolin mortars but also for high performance mortars with ca. 100 MPa. More recently within Vietman, there is the strong change of hydro-meteorologic for temperature from 7.3 to 42.2 ^{o}C [224, 225]. As such, different temperature treatments (8 – 20 - 40 ^{0}C) have been used to prepare mortars. In order to effectively employ metakaolin in composite cement as well as to reduce the amount of Portland cement clinker to 55 Wt.-%, metakaolin is used in combination with calcite in different levels for the remaining 45 Wt.-%. This aim was to find an optimal combination of composite cement containing metakaolin and calcite, whereby the highest strength of mortar can be obtained. In addition to this, the properties of workability and porosity from selected mixtures were tested as shown in the following section.

8.2 Setting time and spread-flowability

The effect of various levels of metakaolin on setting times and water demand of metakaolin pastes is shown in Table 8.1. The initial setting time of composite cements containing 20 – 40 Wt.-% metakaolin was less than that of the control, except the usage of 30 – 40 Wt.-% HTK54 or HTK84. The final setting time of composite cements with 20 – 40 Wt.-% metakaolin exceeded that of the control (CEM I 42.5 N, 190min), except DQK53.

In order to obtain a normal water demand less than 35 Wt.-%, the maximum use level of metakaolin is 20 Wt.-% for HTK54 and HTK84 in composite cements. The 30 – 40 Wt.-% levels for HTK54 and HTK84, which have the water demand of 40 – 45 Wt.-%, can be combined with CEM I 42.5 N only when: (1) a dry superplasticizer (powder) is added to cement powder; or (2) a kind of superplasticizer is added in to the solution during the mix process of concrete. Nevertheless, DQK53 and DQK83 can be used up to 40 Wt.-% to make composite cement (water demand ≤ 35 Wt.-%).

Table 8.1 Effect of metakaolin levels on setting time (CEM I 42.5 N: 27Wt.-%, 130min/190min)

	20 Wt.-%			30 Wt.-%			40 Wt.-%		
	Water demand	Setting time [min]		Water demand	Setting time [min]		Water demand	Setting time [min]	
	[Wt.-%]	Initial	Final	[Wt.-%]	Initial	Final	[Wt.-%]	Initial	Final
HTK54	35	130	220	40	135	225	44	140	235
HTK84	35	120	190	40	140	220	45	155	230
DQK53	30	115	170	32	120	175	34	125	180
DQK83	31	120	210	33	120	215	35	130	215

Table 8.2 Effect of metakaolin surfaces on setting time

CEM I 52.5 N [Wt.-%]	Metakaolin			Water demand [Wt.-%]	Setting time [min]	
	Content, type [Wt.-%, type]	BET surface [m^2/g]	D_{50} [μm]		Initial	Final
100	0			30	140	220
80	20, HTK54	24.6	7.3	39	160	220
80	20, HTK84	22.6	7.0	39	165	205
80	20, DQK53	18.0	6.3	34	140	210
80	20, DQK83	17.2	5.7	36	150	200
80	20, GMK	10.1	3.8	38	135	195

The combination between Portland cement with a high water demand (CEM I 52.5 N, water demand 30 Wt.-%) and metakaolin is even more choosing as shown in Table 8.2. Only 20 Wt.-% metakaolin used in composite cement led to a rise of water demand up to 34 – 39 Wt.-%. The BET surface and D_{50} have an important effect on this behaviour. HTK54/HTK84 (24.6/22.6 m^2/g) and GMK (D_{50} of 3.8 μm) induced a strong increase in water demand up to 38 – 39 Wt.-%. As a result, it is recommended that a composite cement using a high metakaolin level should be combined with a low water demand of Portland cement.

Table 8.3 shows the spread-flowability of cement pastes with respect to BET surface and PSD. An increase of BET surface as well as a reduction of D_{50} in metakaolin reduced the spread-flowability of blended paste. The same reduction of spread-flowability in blended pastes (26.5 cm of the control down to 18.0-18.5 cm of HTK54/HTK84/GMK blended pastes) was seen for the sample having the high BET surface (HTK54/HTK84) and another sample having the smallest D_{50} (GMK). This result confirmed the similarities in water demand between HTK54/HTK84 and GMK blended pastes in Table 8.2. However, in order to get a similar spread-flowability, the high performance mortar of HTK84 (high BET surface) has to use more superplasticizer than that of GMK (low D_{50}) as shown in Table 8.4.

Table 8.3 Effect of metakaolin on spread-flowability of cement pastes (the w/c and w/b of 0.5).

CEM I 52.5 N [Wt.-%]	Metakaolin			Spread-flowability [cm]
	[Wt.-%, type]	BET surface [m^2/g]	D_{50} [µm]	
100	0			26.5±0.5
80	20, HTK54	24.6	7.3	18.0±0.5
80	20, HTK84	22.6	7.0	18.5±0.5
80	20, DQK53	18.0	6.3	21.5±0.5
80	20, DQK83	17.2	5.7	21.5±0.5
80	20, GMK	10.1	3.8	18.5±0.5

Table 8.4 Effect of metakaolin on spread-flowability of high performance mortar (the cement / binder:sand:water ratio of 1/1:2:0.3) with respect to superplasticizer

	Superplasticizer [Wt.-%]	Spread-flowability [cm]
100 Wt.-% CEM I 52.5 N	1.8	21.0±1.0
80 Wt.-% CEM I 52.5 N + 20 Wt.-% HTK 84	2.5	19.5±0.5
80 Wt.-% CEM I 52.5 N + 20 Wt.-% DQK 83	2.0	20.5±0.5
80 Wt.-% CEM I 52.5 N + 20 Wt.-% GMK	2.0	21.5±0.5
100 Wt.-% VPC 40	0.8	24.0±1.0
80 Wt.-% VPC 40 + 20 Wt.-% HTK 84	1.2	20.5±0.5
80 Wt.-% VPC 40 + 20 Wt.-%DQK 83	1.0	21.5±0.5
80 Wt.-% VPC 40 + 20 Wt.-%GMK	1.0	22.5±0.5

8.3 Strength

8.3.1 Strength of mortars in dependence of different replacement level of metakaolin

Figure 8.1 shows the strength of mortars containing metakaolin at the cure temperature of 8 °C. The compressive strength of mortars containing HTK54 was found to be lower than that of the control mortar CEM I 42.5 N during the early stages of the hydration process (days 2 and 7). Whilst mortars of HTK84 achieved a similar compressive strength to that of the control pure cement. After day 28, mortars with the 20 – 30 Wt.-% HTK54/HTK84 (shown as HTK54.20, HTK54.30, HTK84.20, HTK84.30 in Figure 8.1) showed a higher compressive strength than the control mortar. Metakaolin mortar with 40 Wt.-% HTK54 (HTK54.40 in Figure 8.1) showed a lower compressive strength than the control mortar, whereas metakaolin mortar with 40 Wt.-% HTK84 (shown as HTK84.40 in Figure 8.1) gained a higher compressive strength than that of the control mortar. It should also be noted that, strength for mortars containing HTK54 is always lower than those containing HTK84 with replacement levels from 20 – 40 Wt.-% of metakaolin.

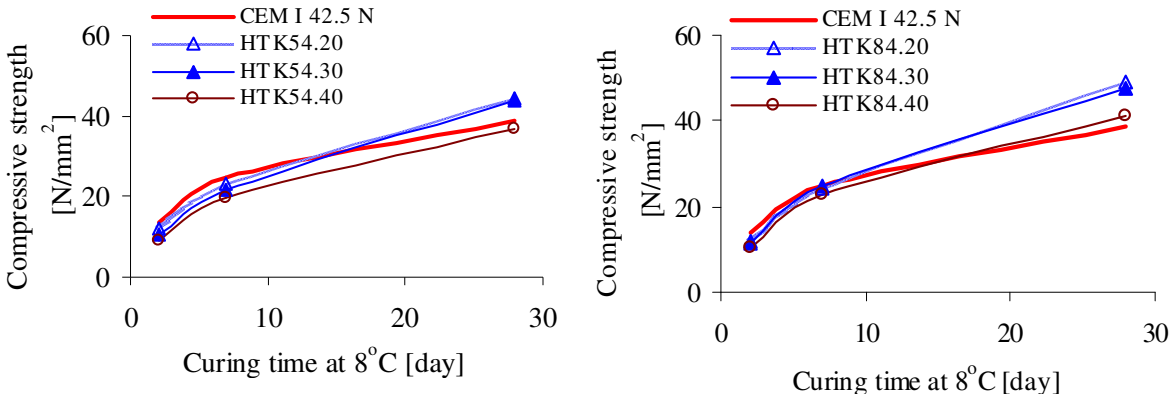

(a) HTK54 (b) HTK84

Figure 8.1 Strength development of mortars (form 40×40×160mm^3, CEM I 42.5 N:metakaolin = 100:0 / 80:20 / 70:30 / 60:40 Wt.-%, binder:sand = 1:3, w/b of 0.6, in water at 8 °C)

At curing temperature of 20 °C the compressive strength of mortars containing HTK54 and HTK84 was lower than that of the control mortar CEM I 42.5 N after 2 days of the hydration process as shown in Figure 8.2. However after days 7 and 28, mortars containing HTK54 had a similar strength to the control mortar, whereas the strength of HTK84 mortars was higher than that of the control mortar.

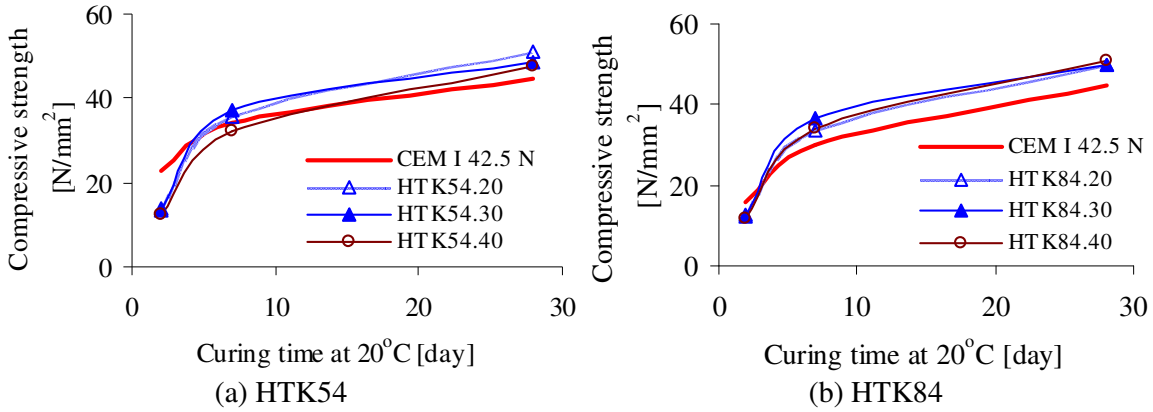

Figure 8.2 Strength development of mortars (form 40×40×160mm^3, CEM I 42.5 N:metakaolin = 100:0 / 80:20 / 70:30 / 60:40 Wt.-%, binder:sand = 1:3, w/b of 0.6, in water at 20 °C)

At the cure temperature of 40 °C and after 2 days of the hydration process, the compressive strength of metakaolin mortars for HTK54 and HTK84 was always higher than that of the control mortar CEM I 42.5 N as seen in Figure 8.3. There was not much difference in the compressive strength of mortar containing HTK54 for the different replacement levels (different percentages) of metakaolin, whereas the increase in content of HTK84 led to the increase in compressive strength of mortars containing 20 – 30Wt.-% metakaolin.

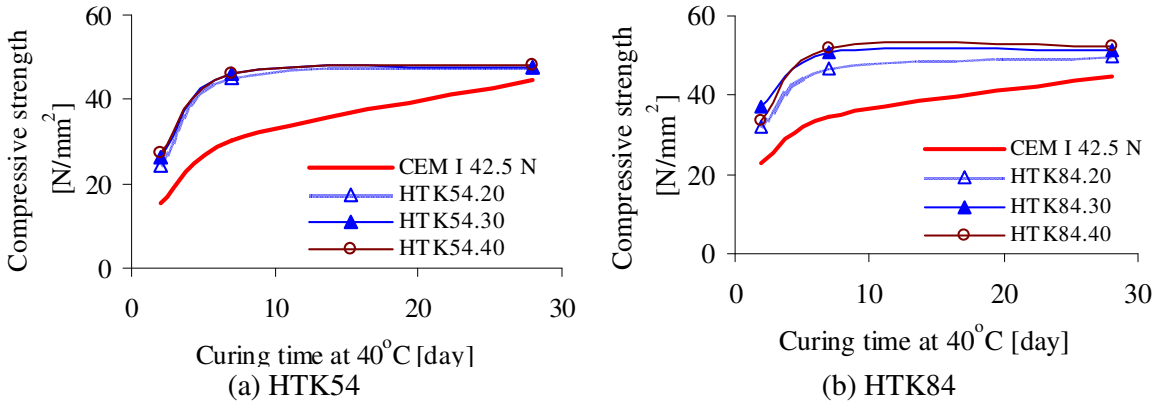

Figure 8.3 Strength development of mortars (form 40×40×160mm^3, CEM I 42.5 N:metakaolin = 100:0 / 80:20 / 70:30 / 60:40 Wt.-%, binder:sand = 1:3, w/b of 0.6, in water at 40 °C)

The same trends for compressive strength of mortar containing DQK53 / DQK83 and GMK were also observed in Figure 8.4 (DQK53 / DQK83) and Appendix 13.5 (GMK).

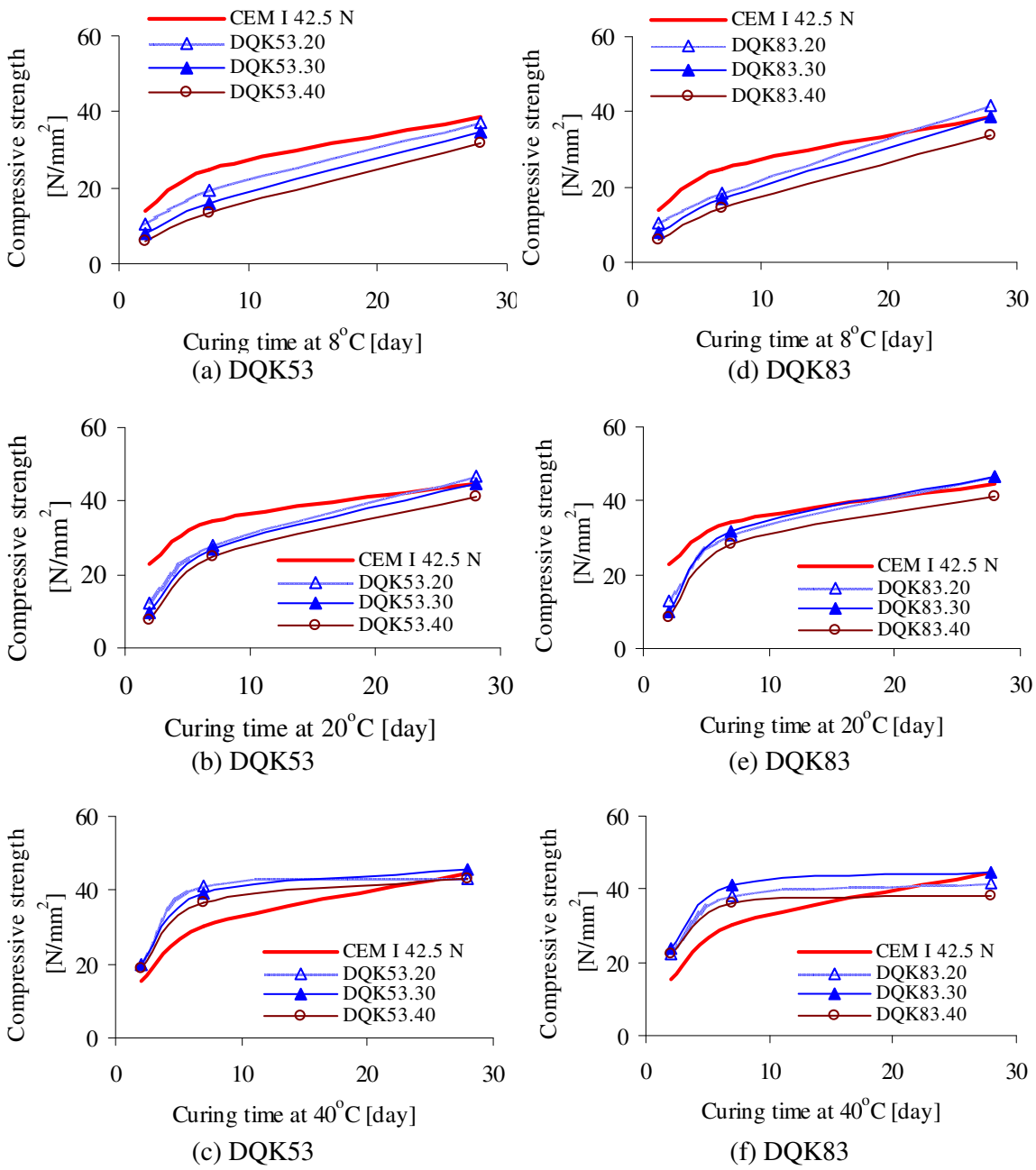

Figure 8.4 Strength development of mortars (form 40×40×160mm^3, CEM I 42.5 N:metakaolin = 100:0 / 80:20 / 70:30 / 60:40 Wt.-%, binder:sand = 1:3, w/b of 0.6, in water at 8-40 °C)

8.3.2 Strength of metakaolin mortars in dependence of calcite addition

One of the aims in producing composite cement is the reduction in clinker amount. In order to produce composite cement, calcite is often used because of its known advantages. Namely that it is easy to mix, convenient to transport, its favorable deposit locations, and its low cost. Calcite, normally used as a filler addition up to 5 Wt.-%, is known to react to cement as an active participant in the hydration process [226]. Calcite and metakaolin can be combined and used as

additions in composite cement. Due to their favorite together packing and the active factor of aluminum in metakaolin to calcite, a higher level of calcite (> 5 Wt.-%) can be used in composite cement [227]. For this reason, a strength investigation into metakaolin mortar (0 – 40 Wt.-% HTK84) with the presence of calcite (5 - 45 Wt.-%) was carried out as shown in Table 8.5.

Table 8.5 The composition rate of blend powder in mortars

	CEM I 42.5 N [Wt.-%]	Metakaolin [Wt.-%]	Calcite [Wt.-%]
CEM I 42.5	100	-	-
45C.0HTK84	55		45
25C.20HTK84	55	20	25
15C.30HTK84	55	30	15
5C.40HTK84	55	40	5

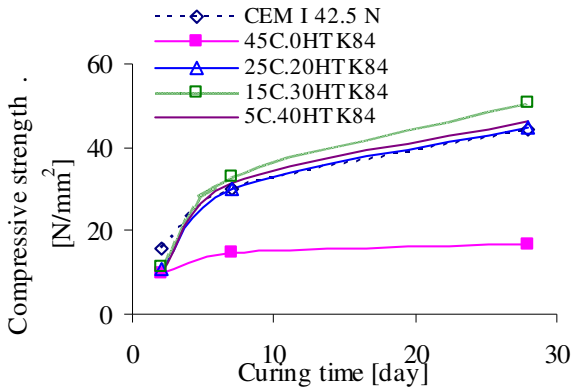

Figure 8.5 The strength development of mortars (form 40×40×160 mm^3, CEM I 42.5 N:calcite and metakaolin = 55:45, calcite:metakaolin = 45:0/25:20/15:30/5:40 Wt.-%, the binder:sand rate of 1:3, w/b of 0.6, in water at 20 °C, the control CEM I 42.5 N)

The results in Figure 8.5 show that, the combination of 30 Wt.-% metakaolin and 15 Wt.-% calcite gave the highest strength of mortar. A similar strength was observed for the control mortar CEM I 42.5 N and mortar mixtures containing 20 Wt.-% metakaolin/25 Wt.-% calcite; 40 Wt.-% metakaolin / 5 Wt.-% calcite. This indicates that the combination of metakaolin and calcite for composite cement is favorable, and that the optimal combination is 30 Wt.-% metakaolin and 15 Wt.-% calcite for the type of cement in this investigation. In combination with metakaolin, a high content of calcite (15 Wt.-%) in composite cement leads to an increase in strength. The reason for this behaviour could be due to: (1) the high content of aluminum in metakaolin could act as an activator for calcite, forming new hydration products, resulting in a density structure; (2) the favourable compaction of calcite causes a density structure of mortar.

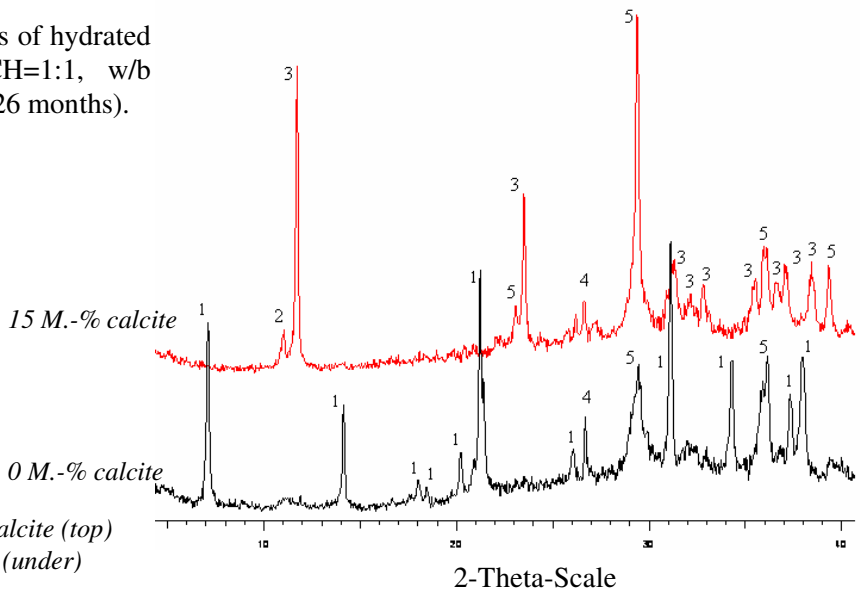

Figure 8.6 XRD analysis of hydrated lime paste (HTK84:CH=1:1, w/b 0.75, 20 °C, 100 %RH, 26 months).

1- Stratlingite
2- Mono-carbonate
3- Hemi-carbonate
4- Quartz
5- Calcite.

Lime paste with 15M.-% calcite (top)
Lime paste without calcite (under)

A XRD investigation for lime paste was conducted as shown in Figure 8.6. The results gained show the formation of hydration products such as hemi/mono-carbonate, which confirms surely that calcite is activated by the aluminum within the metakaolin.

The strength development of other Vietnamese metakaolins was investigated at the found optimum combination incase calcite (26 670 Blaine cm^2/g - 8.32 BET m^2/g, 2.71 g/cm^3) was replaced by quartz powder (1 890 Blaine cm^2/g, 2.66 g/cm^3), see Figure 8.7. Gained results show that mortar of calcite provided a higher compressive strength than that of quartz powder, which confirms surely again that the high strength of mortars containing calcite is due to its favourable compaction. As such, the potential of calcite use with a high level in combination with metakaolin for composite cement is possible.

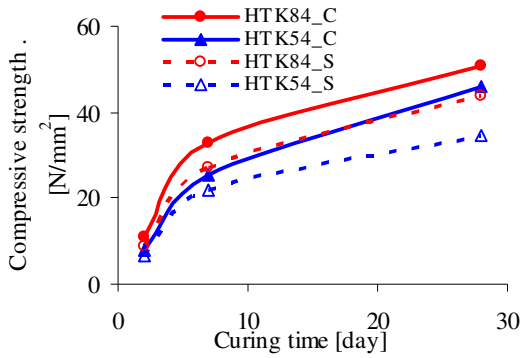

Figure 8.7 Strength development of mortars for HTK54/ HTK84 (form 40×40×160 mm^3, CEM I 42.5 N:metakaolin: calcite (C)/quartz powder (S) = 55:30:15/15 Wt.-%, the binder:sand rate of 1:3, w/b of 0.6, in water at 20 °C)

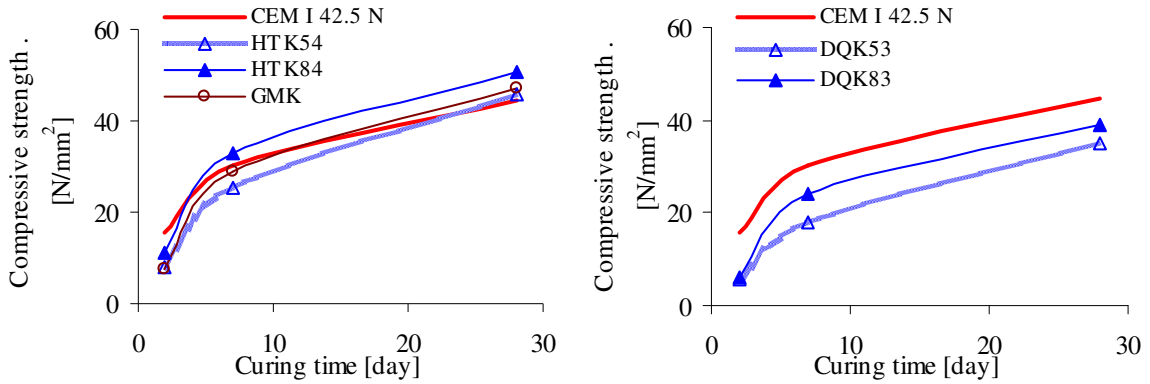

(a) Mortars for HTK54/84 and GMK (b) Mortars for DQK53/83

Figure 8.8 Strength development of mortars (form 40×40×160 mm^3, CEM I 42.5 N:metakaolin:calcite = 55:30:15 Wt.-%, the binder:sand rate of 1:3, w/b of 0.6, in water at 20 ^oC)

The strength development of other Vietnamese metakaolins and GMK was also investigated at the found optimum combination (CEM I 42.5 N:metakaolin:calcite=55:30:15 Wt.-%), see Figure 8.8. As shown, both HTK84 and HTK54 induced a similar strength of mortars at 28 days to the control CEM I 42.5 N (see Figure 8.8.a). However, for both DQK83 and DQK53, a lower strength of their mortars was determined as compared to the control CEM I 42.5 N (see Figure 8.8.b). The commercial product GMK showed a lower strength of mortar as compared to that of HTK84 (see Figure 8.8.a).

8.3.3 High performance mortar

Figure 8.9 shows the compressive strength of HPM for CEM I 52.5 N (see Figure 8.9.a) and VPC 40 (see Figure 8.9.b).

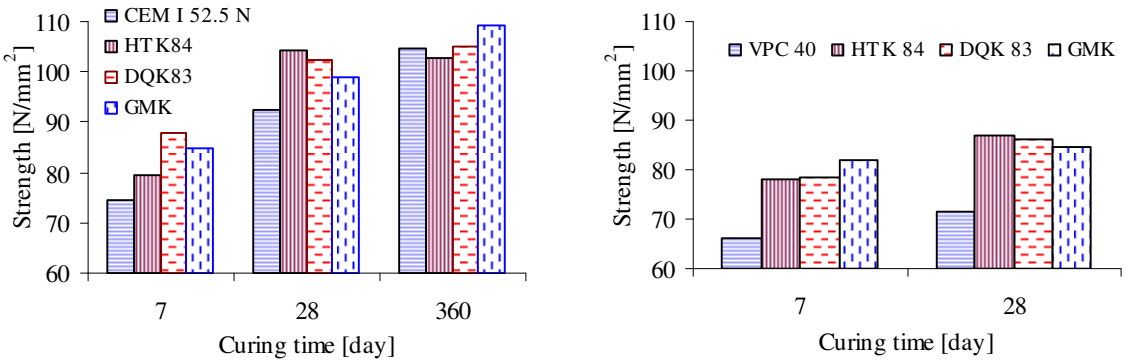

(a) CEM I 52.2 N (b) VPC 40

Figure 8.8 Compressive strenght of HPM (the cement / binder:sand:water ratio of 1/1:2:0.3) containing 20 Wt.-% metakaolin, in water at 20 ^oC.

On days 7 and 28 of the hydration process, samples with metakaolin had a higher compressive strength in comparison with the control CEM I 52.5 N and VPC 40. After 360 days of the hydration process, the compressive strength of samples containing metakaolin (HTK84, DQK83) was similar to that of the control (CEM I 52.5 N). Vietnamese metakaolins (HTK84, DQK83) achieved the same compressive strength as commercial metakaolin GMK on early days of the hydration process, whereas GMK showed a higher strength than HTK84 and DQK83 on the later days of the hydration process.

8.3.4 Porosity of high performance mortar

This investigation was conducted with intact samples of HPM prisms (see section 8.3.3) by MIP (see section 4.2.4) as shown in Figure 8.10. For the durability of high performance concrete, the most destructive size of pores is larger than 50 nm which critically affect the permeability parameter [135]. Thus, the porosity of high performance mortar is determined and classified by a median pore diameter of 50nm. In comparison with the control sample CEM I 52.5 N, mortars containing metakaolin showed a smaller volume of pores larger than 50 nm. The volume of destructive pores (larger than 50 nm) was almost the same for GMK, HTK84 and DQK83 mortars.

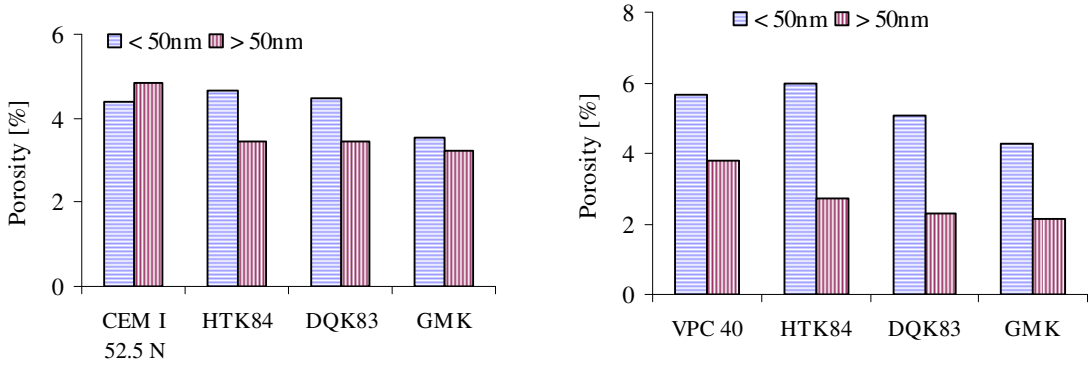

(a) CEM I 52.5 N (b) VPC 40

Figure 8.10 Prosity of HPM (the cement / binder:sand:water ratio of 1/1:2:0.3) containing 20 Wt.-% of metakaolin, in water at 20 ^{o}C for 28 days.

8.4 Discussion

It is inferred from Tables 8.1-2 that, an increase in BET surface of metakaolin increased the initial setting time of cement pastes, but this influence of BET surface is absent in final setting time. Depending on the results of water demand (normally smaller than 35 Wt.-%), 20-40 Wt.-%

DQK53/DQK83 can be used for making composite cement, while a solution to reduce the water demand is needed for producing composite cement containing more than 20 Wt.-% HTK54/HTK84.

Also it is inferred from Tables 8.3-4 that, the correlation between BET surface of metakaolin and spread-flowability of cement pastes and HPM is not always obvious, especially in the case of GMK, the commercial metakaolin.

The results of compressive strength on mortars in Figures 8.1-3 infer that, on early days of the hydration process (days 2 and 7) cure temperature strongly influences the compressive strength of metakaolin mortar. The lower curing temperature (8 ^{o}C) of mortar prisms, the lower of their compressive strength on early days. Thus, it is assumed that, at a higher curing temperatures (40 ^{o}C), the pozzolanic reaction of metakaolin promotes the higher compressive strength of its mortar. The compressive strength of mortar cured at 8 to 40 ^{o}C for 2 days increased from 9 to 24 N/mm^2 for HTK54, and from 12 to 33 N/mm^2 for HTK84. Over 28 days of curing, the temperature only slightly influenced the compressive strength of metakaolin mortar. The increase in compressive strength of mortar cured at 8 to 40 ^{o}C for 28 days was 11 N/mm^2 for both HTK54 and HTK84. In general, the compressive strength of metakaolin mortars is higher or similar to that of the control Portland cement mortar after 28 days at all temperatures (8 – 20 – 40 ^{o}C). The compressive strength of metakaolin mortars is decreased in order of HTK84 ≥ DQK83 ≥ HTK54 ≥ DQK53 after 28 days of the hydration process.

It can be inferred from Figures 8.5-7 that, calcite is not only a filler addition but also an active one in composite cement using metakaolin. As seen in Figure 8.8, with the addition of 30 Wt.-% HTK54 or HTK84 and 15 Wt.-% calcite, 45 Wt.-% of Portland cement clinker was reduced in composite cement without its reduction in strength as compared to the control (100 Wt.-% cement). However, the addition of DQK53 or DQK83 induced a lower strength of mortar as compared to the control. This indicates that the use of DQK53 and DQK83 for composite cement is not successful with respect to strength.

In summary, depending on the intended aim of composite cement and weather conditions of cure, each Vietnamese metakaolin (HTK54, HTK84, DQK53, DQK83) can be used as follows: (1) A composite cement with a low water demand should be combined with DQK53 or DQK83; (2) A high strength of composite cement is gained by using HTK84. However, in the case of high cure temperature (40 ^{o}C) HTK54, DQK53 and DQK83 achieved a similar strength to HTK84; (3) For

reducing CO_2 emissions, a composite cement containing metakaolin and calcite is proposed that by application of HTK54 or HTK84, it allows a reduction in 45 Wt.-% Portland cement clinker.

8.5 Concluding remarks

The following conclusions were drawn:

(1) The presence of metakaolin creates an increase in water demand and mainly affects the initial setting time although the final setting time is slightly influenced. An increase in BET surface of metakaolin increased the initial setting time of cement pastes, but this influence of BET surface is absent in final setting time.

(2) Depending on the results of water demand (normally smaller than 35 Wt.-%), 20 - 40 Wt.-% DQK53/DQK83 can be used for producing composite cement, while a solution to reduce the water demand is needed for producing composite cement containing more than 20 Wt.-% HTK54/HTK84.

(3) The temperature strongly influences the compressive strength of metakaolin mortar on the early days of the hydration process, while in later days of the hydration process this influence is only limited. The lower / higher curing temperature (8 / 40 ^{o}C) of mortar prisms, the lower / higher of their compressive strength on early days.

(4) Both HTK84 and DQK83 contribute to the increase in strength of HPM. The porosity of HPM seemed not to be significantly influenced by different metakaolins in comparison between Vietnamese metakaolins HTK84 and DQK83 and the commercial product GMK.

(5) The main purpose of this study is to determine the possibility of producing Vietnamese metakaolin as a replacement for other additives in the manufacture of composite cement. Depending on the intended use of composite cement and weather conditions of cure, each Vietnamese metakaolin (HTK54, HTK84, DQK53, DQK83) can be used appropriately as follows:

- A composite cement with a low water demand should be combined with DQK53 or DQK83;
- A high strength of composite cement is gained by using HTK84. However, in the case of high cure temperature (40 ^{o}C) HTK54, DQK53 and DQK83 achieved a similar strength to HTK84;

- A composite cement that aims to reduce CO_2 emissions and to improve economics of cement prodcuts should added metakaolin and calcite. It is proposed that by adding HTK54 or HTK84, it allows a reduction in 45 Wt.-% Portland cement clinker without the strength reduction.

9. Influence of metakaolin in mitigating ASR

9.1 Induction

There are already quite a number of testing methods for ASR. For example, in concrete prism testing method there are the standards ASTM C1293 [228] and CAN/CSA A23.2 – 14A [229] as well as the FIB cyclic climate storage [230]. Within these tests, reactive aggregates and high-alkali cement are added into the mixture. The ASR risk can also evaluated by measuring the expansion of mortar bars that are soaked in NaOH solution [231, 232] and / or contain reactive quartz sands [233]. Additionally tests to determine the OH^- concentration in aqueous phase of cement pastes are used to assess the threshold of sustaining ASR as well as maintaining steel passivation [234, 235, 236, 237]. In this study, the expansion limit of mortar prisms containing reactive quartz sand according to the German Alkali-Guideline (2007) alternative method for ASR [233] was chosen because it is an accelerated test. This test has been described in greater detail in section 4.5.1.

The results in sections 6 and 7 showed that, the presence of residual water within the metakaolin structure correlated with a high BET surface. Metakaolin due to its high BET surface is known to have a higher lime consumption. Metakaolin with its pozzolanic feature could provide an alkali binding potential. Thus, it is assumed that metakaolin could mitigate ASR behaviour of concrete. The mitigation degree of ASR may vary in dependence of metakaolin types, i.e. with or without residual water. Therefore, the influence of two different kinds of metakaolin on the resistance of ASR was studied as follows.

The first type of metakaolins (HTK84, DQK83) contains no residual water, while the second type of metakaolins (HTK54, DQK53) does and show a larger BET surface. In addition, commercial products (GMK, MK402), which have no residual water and possess a finer particle size and the smallest BET surface, were tested in comparison with Vietnamese metakaolin. The properties for those metakaolins have already been specified in section 5.2 and section 6.4.

9.2 The expansion change of mortar prisms

Figure 9.1 shows the expansion change of mortar prisms v.s curing time. Limit I (1.5mm/m) is the maximum expansion demand for the sufficiently non-reactive resistance in ASR, and limit II (2mm/m) is the maximum expansion demand for the potentially reactive resistance in ASR [238]. A mixture can be considered critical with respect to its ASR potential when the expansion

exceeds Limit II, whereas it can be considered uncritical when the expansion is smaller than Limit I. The expansion of mortar prisms containing metakaolin were very low and did not indicate any deleterious reaction like ASR. According to the German Alkali-Guideline (2007), an amount of 10 Wt.-% metakaolin seems to have the potential to mitigate ASR.

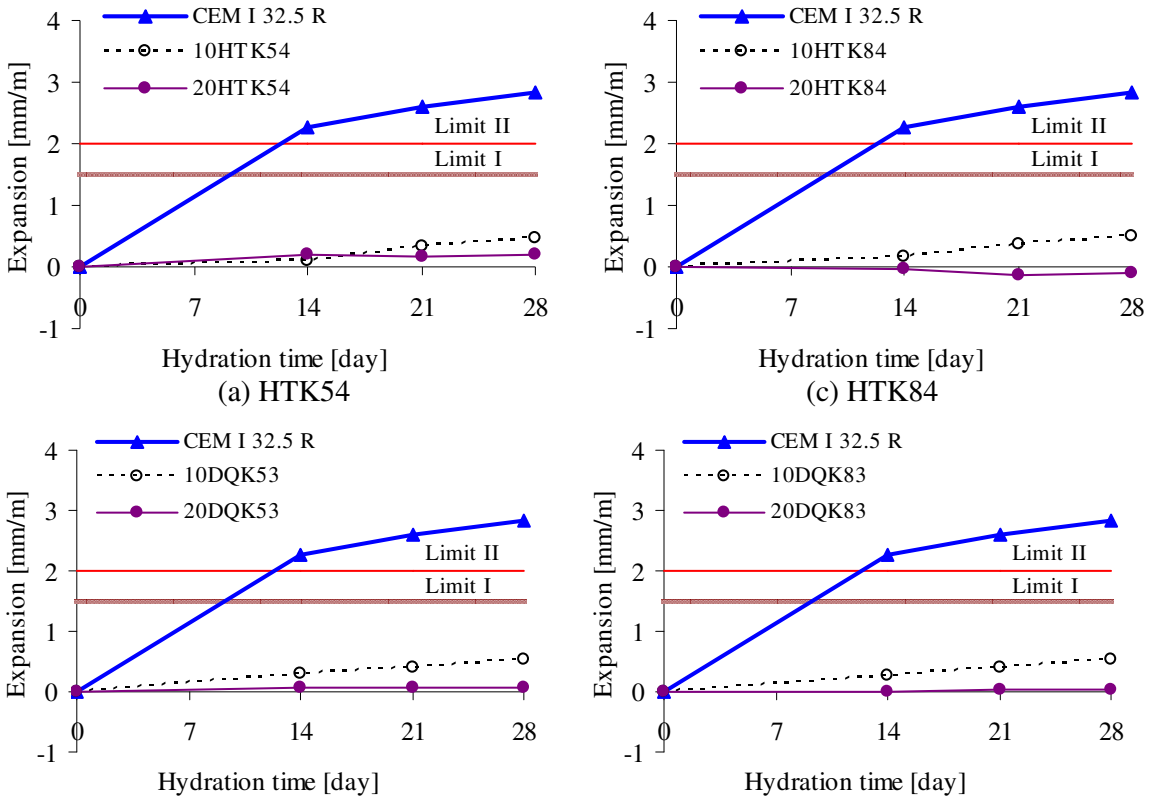

Figure 9.1 The expansion of mortar prisms (CEM I 32.5 R:metakaolin=100:0/90:10/80:20Wt.-%, Binder:reactive quartz:solution=1:3:0.5, Water:NaOH:K_2SO_4=1:0.031:0.017, 100%RH, 70°C)

There was no significant difference in expansion change between metakaolin samples with residual water (HTK54 and DQK53) and without residual water (HTK84 and DQK83). This means that, the effect of residual water of metakaolin with regards to ASR could not be verified within this test. However, it is noted that, the use of 20 Wt.-% metakaolin showed a lower expansion change than that of 10 Wt.-% metakaolin. As more metakaolin was replaced by cement, a greater resistance to ASR was observed.

The same behaviour of expansion change was also observed for GMK and MK402 (see Appendix 13.6). However, MK402 containing 7.8 Wt.-% of muscovite showed a higher

expansion than other metakaolins. This could be due to the release of K^+ from muscovite $KAl_2[AlSi_3O_{10}.(OH)_2]$ as shown before by [206, 207].

9.3 Ion binding of cement pastes in dependence of metakaolin

In order to understand why metakaolin can mitigate ASR, a test for ion binding was performed as already described in section 4.5.2.

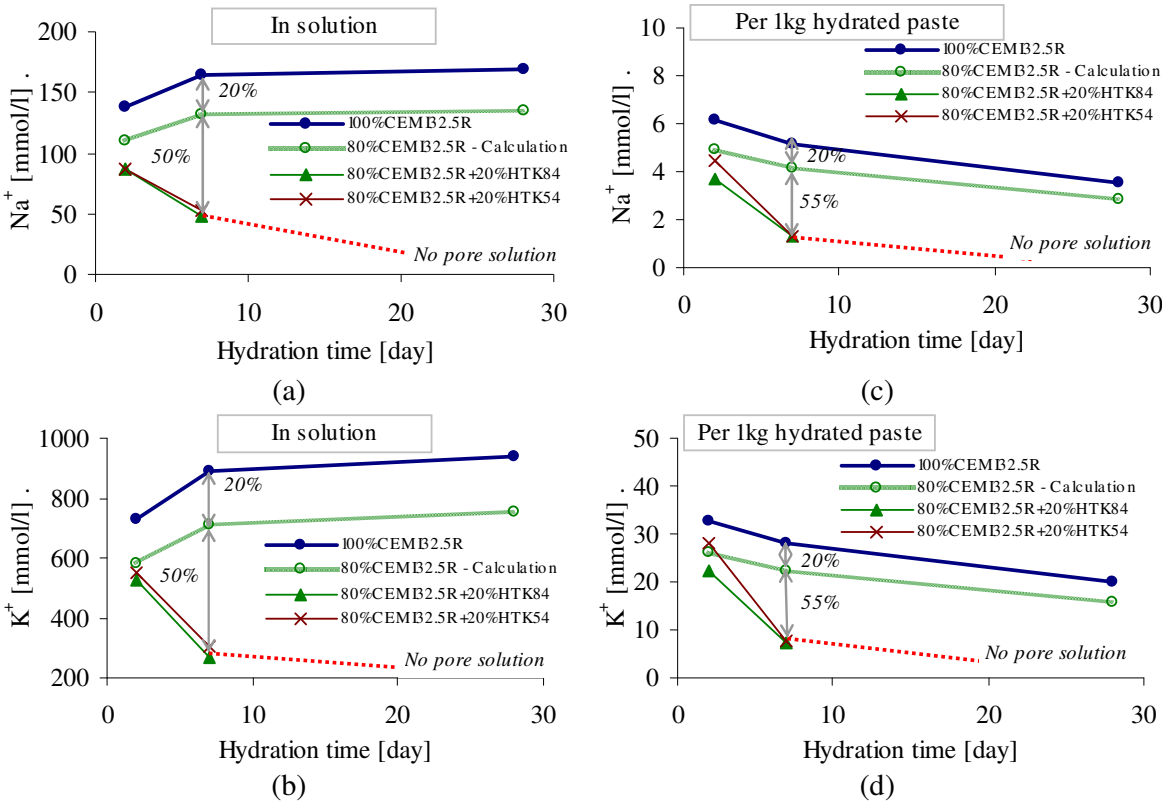

Figure 9.2 Ion concentration. (a, b) in the extracted solution, (c, d) per 1kg hydrated cement pastes (CEM I 32.5 R:metakaolin=100:0/80:20Wt.-%, w/b0.35, 100% RH, 20 °C).

In cement pastes, the ion binding from two samples HTK54 and HTK84 in combination with a high alkali cement (CEM I 32.5 R, N_2O_{eq} = 0.94) was investigated. The results are depicted in Figure 9.2. After two days of the hydration process, the alkali ion concentration of metakaolin pastes (80% CEM I 32.5 R, 20 Wt.-% metakaolin) was similar to that of the calculated diluted paste, and was smaller than that of 100 Wt.-% control sample. This means that, the reduction of ion concentration in metakaolin samples was caused by the dilution effect of cement. However after seven days of the hydration process, a strong reduction in alkali ion concentration was found for metakaolin samples (ca. 75% reduction). This indicates that after 7 days due to

pozzolanic activity of metakaolin a significant amount of alkali can be bound to metakaolin by hydration phases. This should result in a reduction of the ASR risk in concretes.

After 28 days, the amount of aqueous phase of metakaolin pastes was so low that no aqueous phase could be extracted. Thus, no results of alkali ion concentration are available.

9.4 Microstructure of metakaolin during cement hydration

After the first day of the hydration process in cement pastes, no pozzolanic reaction for high alkali cement pastes containing 20 Wt.-% metakaolin was observed by SEM (Nova NanoSEM 230, FEI, Netherlands) as shown in Figure 9.3. The dissolution structure of metakaolin on its surface and edges was also not confirmed. However, the following day some dissolution structure points were seen in Figure 9.4.

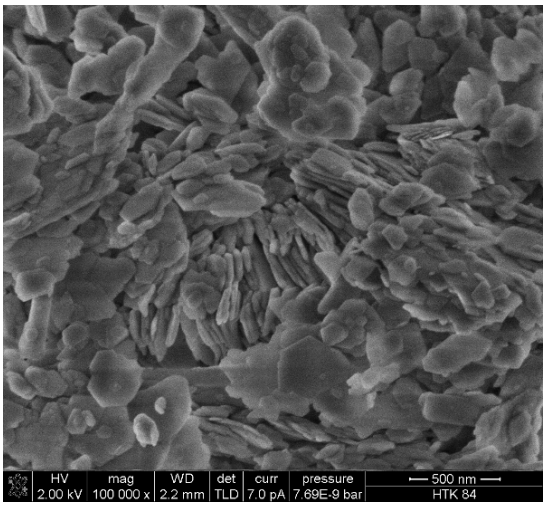

(a) HTK84

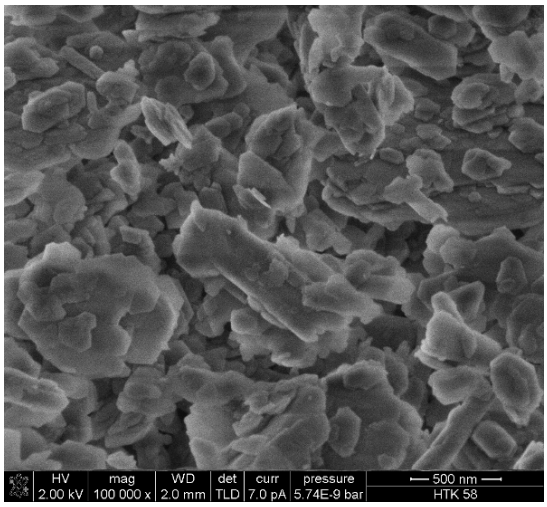

(c) HTK54

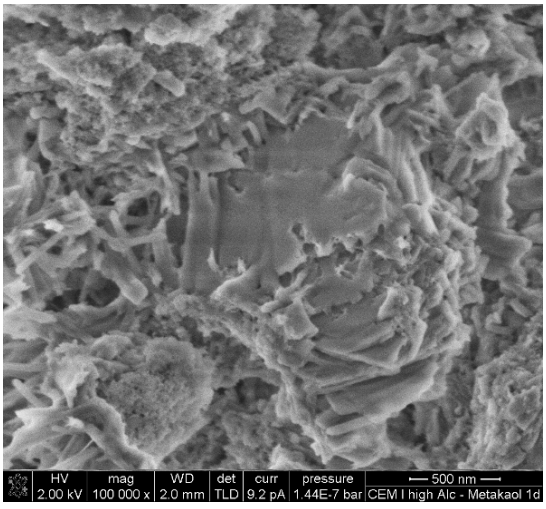

(b) HTK84 after 1 day of hydration

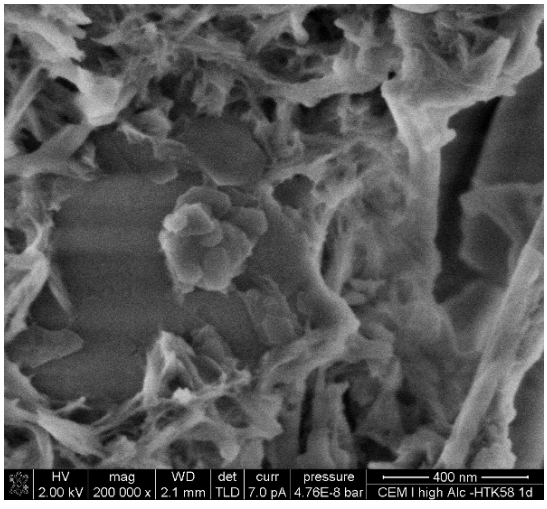

(d) HTK54 after 1 day of hydration

Figure 9.3 SEM-SE imaging technique of metakaolin and cement pastes (CEM I 32.5 R (Na_2O_{eq} 0.94):metakaolin = 80:20 Wt.-%, w/b = 0.38, 100% RH, 20 °C).

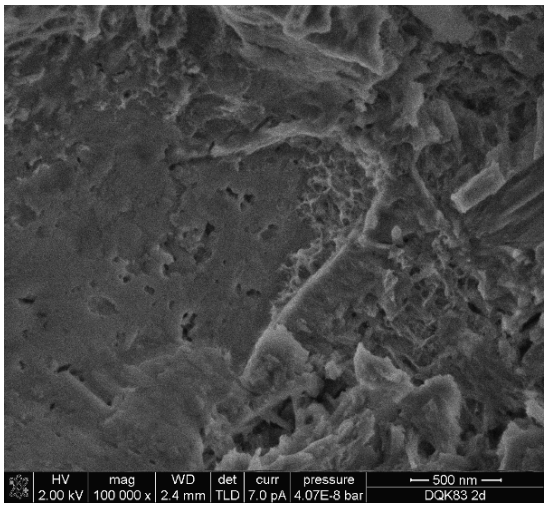

(a) DQK83 after 2 day of hydration

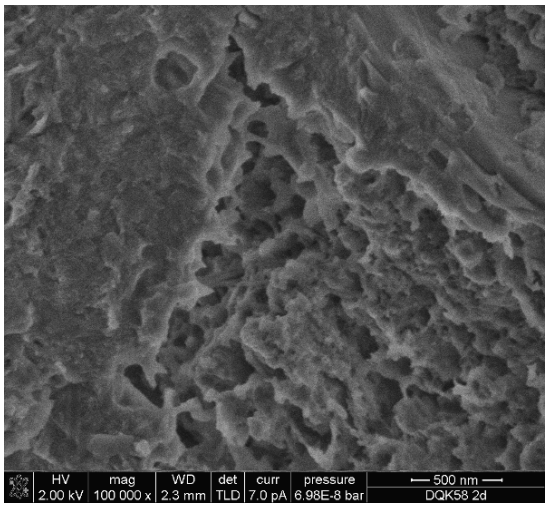

(b) DQK53 after 2 day of hydration

Figure 9.4 SEM-SE imaging technique of cement pastes (CEM I 32.5 R (Na_2O_{eq} 0.94):metakaolin = 80:20 Wt.-%, w/b = 0.38, 100% RH, 20 °C).

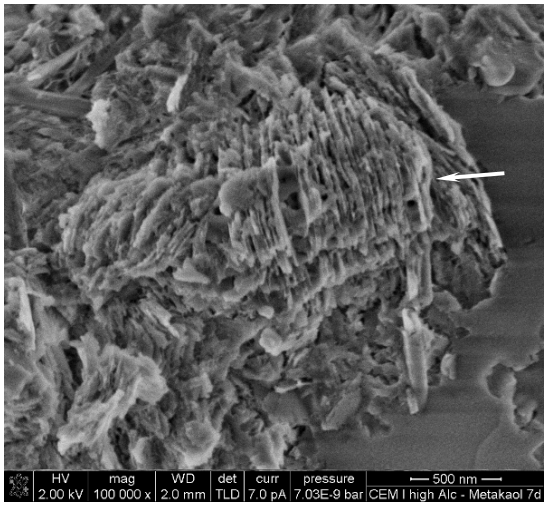

(a) HTK84 - Dissolution from edges

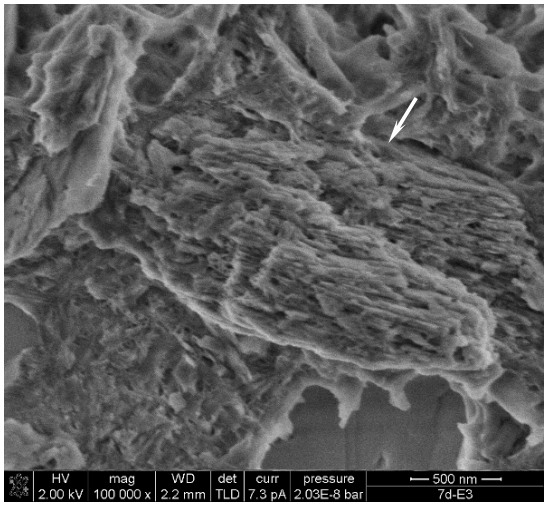

(c) HTK54 - Dissolution from edges

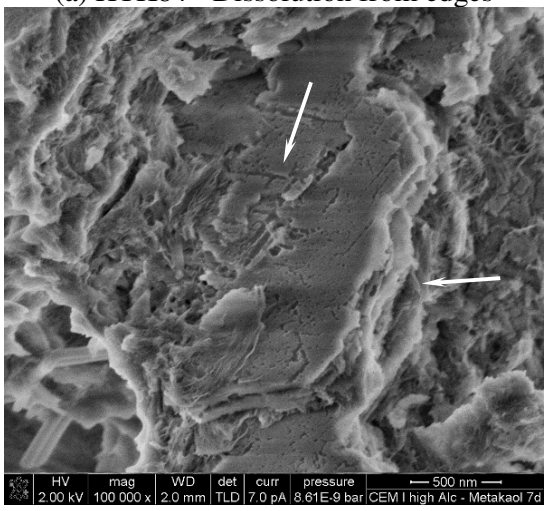

(b) HTK84 - Dissolution on the surface+edges

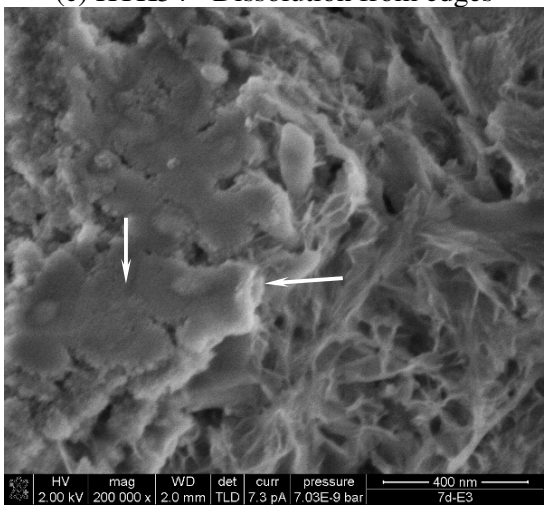

(d) HTK54 - Dissolution on the surface + edges

Figure 9.5 SEM-SE imaging technique of cement pastes (CEM I 32.5 R (Na_2O_{eq} 0.94):metakaolin = 80:20 Wt.-%, w/b = 0.38, 100% RH, 20 °C) at 7 hydration days.

After 7 days of the hydration process, a strong pozzolanic reaction occurred on both the surface and edge of the metakaolin HTK84 / HTK54 (see Figure 9.5). The hydration products (e.g, C-S-H, CASH phases) were formed in the space between two adjacent layers (see Figure 9.5.a+c) and on the surface structure of the layers (e.g, Figure 9.5.b+d).

It is a well-known fact that the presence of alkali ion as chemical activator strongly promotes the occurrence of pozzolanic reactions. Thus, in combination with a lower alkali content cement CEM I 52.5 R (Na_2O_{eq} = 0.47), less dissolution structure on the surface and fewer amount of hydration products between two adjacent layers of metakaolin was seen (see Figure 9.6).

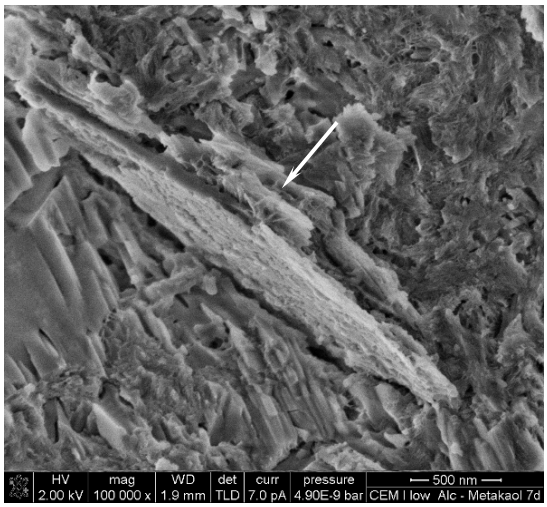

(a) HTK84-Hydration products between layers

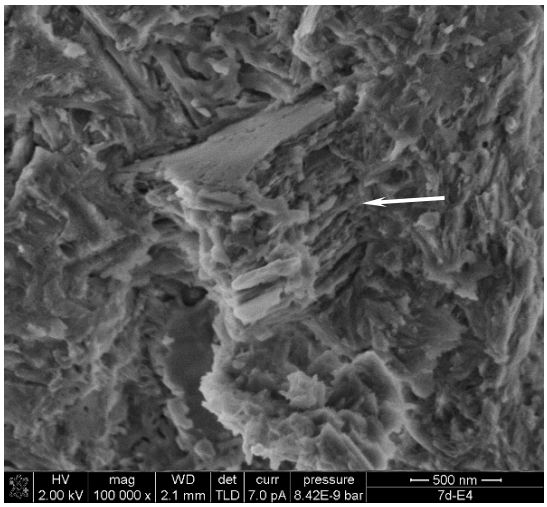

(c) HTK54 - Dissolution from edges

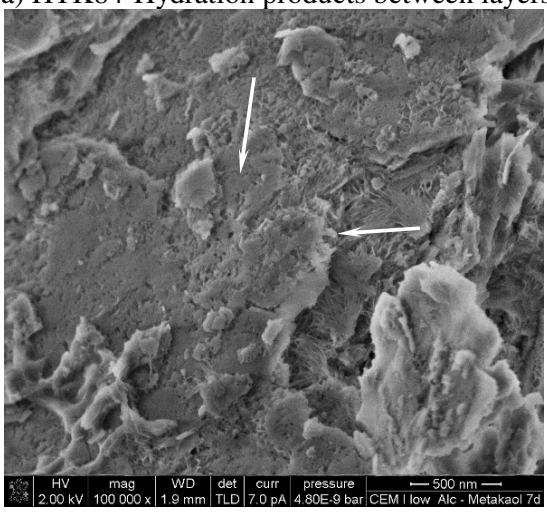

b) HTK84 - Dissolution on the surface+edges

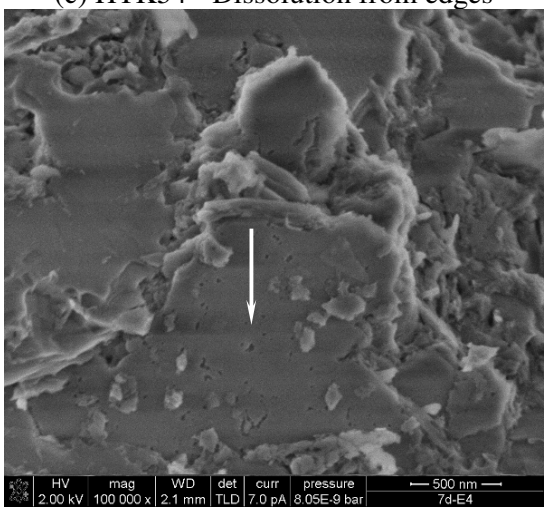

(d) HTK54 – Dissolution on the surface

Figure 9.6 SEM-SE imaging technique of cement pastes (CEM I 52.5 R (Na_2O_{eq} 0.47):metakaolin = 80:20 Wt.-%, w/b = 0.38, 100% RH, 20 °C) at 7 hydration days.

In comparison to HTK54 (with residual water), the dissolution of metakaolin surface was obvious for HTK84 (without residual water) as seen in Figures 9.5.b, 9.6.b and Figures 9.5.d, 9.6.d. It should be noted that, a tendency of pozzolanic reaction occurred at first at the edge of

particles for HTK54 (see Figure 9.6.c+d). While for HTK84 the tendency only occurred on the surface of metakaolin (see Figure 9.6.a+b). This behaviour can be explained as follows: HTK54, with the presence of residual water which causes a higher BET surface, shows a better ion adsorption capability (in the space between two adjacent layers) than ion exchange (on the surface). Thus, a high value of lime absorption (see Tables 7.2+3) and a reduced dissolution on the surface (see Figure 9.6) are the pozzolanic activity parameters of HTK54. In contrast, HTK84, without residual water which results in a lower BET surface, showed a greater ion exchange capability than compared to ion absorption capability. Therefore, a low value of lime adsorption (see Tables 7.2+3) and a better dissolution on the surface (see Figure 9.6) are the pozzolanic activity parameters of HTK84. The same behaviour of lime adsorption and structure dissolution was observed for DQK83 and DQK53 (see Tables 7.2+3 and Figure 9.7).

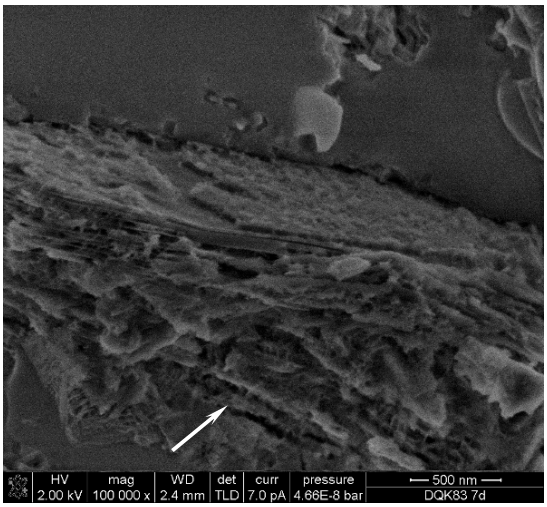

(a) DQK83-Hydration products between layers

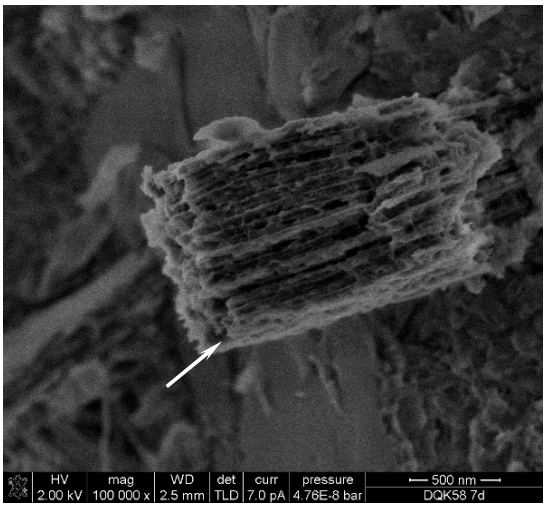

(c) DQK53 - Dissolution from edges+ Hydration products

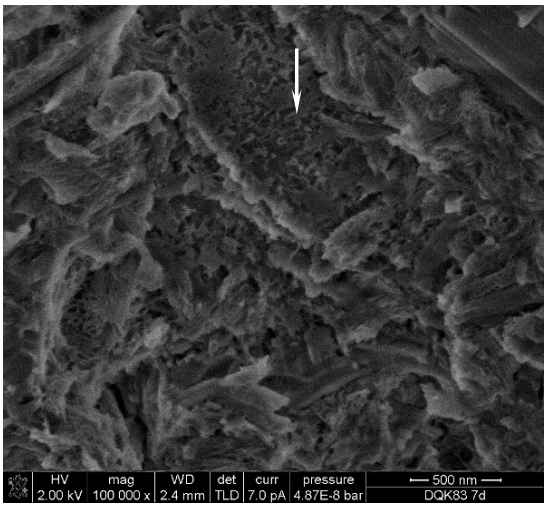

(b) DQK83 - Dissolution on the surface

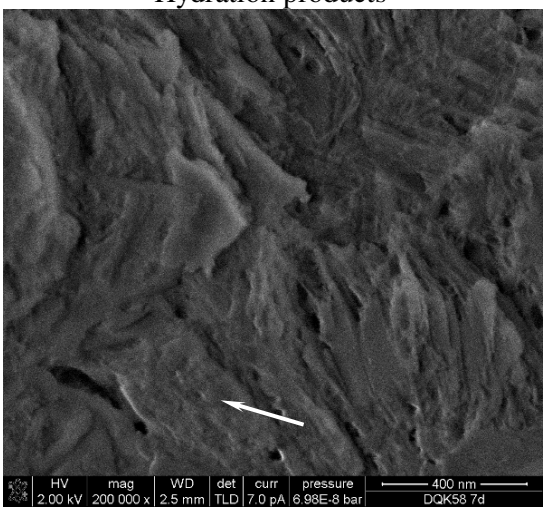

(d) DQK53 – Dissolution on the surface+ Hydration products

Figure 9.7 SEM-SE imaging technique of cement pastes (CEM I 32.5 R (Na_2O_{eq} 0.94):metakaolin = 80:20 Wt.-%, w/b = 0.38, 100% RH, 20 °C) at 7 hydration days.

9.5 Discussion

Section 7 shows the consumption capability of free lime for metakaolin. Results in Figure 9.2 in this section also show a high capability of alkali binding for metakaolin. These both factors indicate the mitigation capability of metakaolin with respect to ASR (see Figure 9.1). Depending on these achieved results, the behaviour of ion binding for pozzolanic reaction of metakaolin can be explained by 3 activity parts as follows.

- *First activity part*: This involves ion adsorption on the surface of hydrated metakaolin, whereby cations (e.g, Na^+/K^+ as seen Figure 9.2) from cement hydration process are adsorbed, or precipitated, or both adsorbed and precipitated into new hydration phases that are created from metakaolin [239, 240, 241].

- *Second activity part*: This involves the dissolution of metakaolin structure, whereby Al^{3+}/Si^{4+} are released from metakaolin to the aqueous phase (e.g, see Figure 9.6.b+d).

- *Third activity part*: This involves ion absorption on the surface of metakaolin, whereby cations (e.g, Ca^{2+}) from cement hydration process are consumed and bound on the surface of metakaolin to form hydration products (e.g, see Figure 9.7.a).

As analysed above, the pozzolanic activity of metakaolin can be considered as a consequence of surface energy. For example, as compared to HTK84, a higher BET surface of HTK54 showed a higher absorption value of cations (as in the first and the third activity parts, e.g Figure 9.8) but less dissolution structure (second activity part, e.g, Figure 9.6).

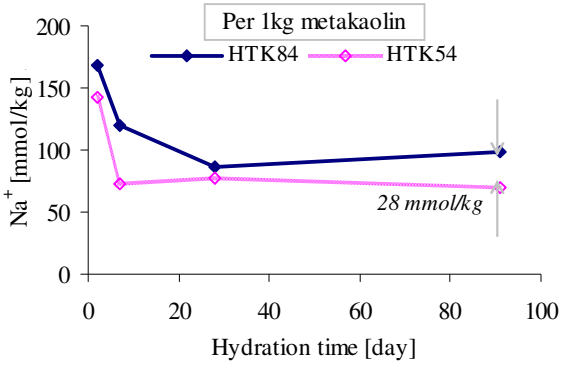

(a) Lime paste added NaOH
Metakaolin:CH:NaOH=1:1:0.04, w/b 0.75, 100%RH, 20°C

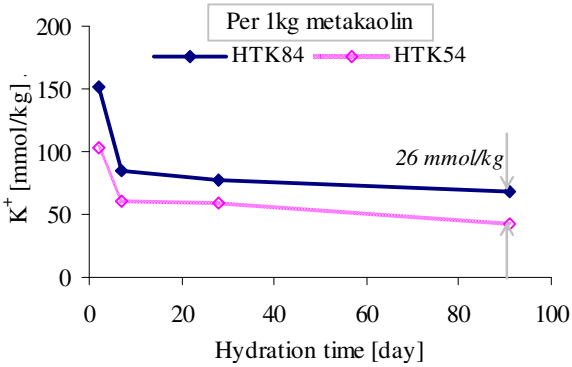

(b) Lime paste added KOH
Metakaolin:CH:KOH=1:1:0.04, w/b 0.75, 100%RH, 20°C

Figure 9.8 Development of free ion concentration in pure lime pastes.

It can be inferred from Figures 9.5+6 that, the tendency of pozzolanic reaction firstly occurred on the edge of particles for HTK54, whilst the pozzolanic reaction started firstly on the surface of metakaolin for HTK84. These behaviours, analysed by atomic emission spectroscopy, were confirmed in 2009 by [242]. Kaolin (with all residual water) adsorbed calcium hydroxide not only at the edges of the clay particles but also on the basal faces, while metakaolin (fully dehydroxylated, no residual water) showed a quick formation of hydrated phases at the interfaces between metakaolin and lime solutions [242].

9.6 Concluding remarks

The following results were obtained:

(1) The more metakaolin is replaced for cement, the greater resistance to ASR is gained. This is due to the behaviour of ion binding caused by the pozzolanic reaction of metakaolin. An amount of 10 Wt.-% metakaolin is enough to mitigate ASR according to the German Alkali-Guideline (2007) alternative method.

(2) The pozzolanic reaction of metakaolin can be divided in three activity parts as follows: Firstly, alkali ion consumption by new hydration phases that are created from metakaolin. Secondly, dissolution of Al^{3+}/Si^{4+} from metakaolin. Thirdly, ion absorption of Ca^{2+} and alkali on the surface of metakaolin.

(3) The presence of residual water in the structure of metakaolin is favorable for high binding capabilities during the first and third activity parts of pozzolanic reaction.

(4) Dissolution structure occurs on metakaolin containing residual water firstly on the edges of particles. Whereas, metakaolin without residual water dissolves primary at the surface.

(5) The main aim of this study is also to determine the possibility of using Vietnamese metakaolin to produce concrete resisting ASR. The results gained show that metakaolin calcinated at low temperature 500 ^{o}C (HTK54/DQK53) reaches a similar resistance in ASR to metakaolin calcinated at high temperature 800 ^{o}C (HTK84/DQK83).

10. Influence of metakaolin in mitigating sulfate and sulfuric acid attacks

10.1 Induction

Vietnam has a long coastline (3.444 km [10]) and as such external sulfate and sulfuric acid attacks on concrete constructions often occur. Internal sulfate attack for concrete may also be an issue if sea sand or mixing water containing sea water is used in concrete production. External sulfate attack from sea water (ca. 2800 mg SO_4^{2-}/l, [150]) for concrete constructions is simulated by tests where mortar bars are immersed in the solution of Na_2SO_4 (3000 mg SO_4^{2-}/l). Sulfuric acid attack may occur due to the influence of waste water from industries processing seafood. This influence is simulated by tests where mortar bars are exposed to the solution of H_2SO_4 1 Wt.-%.

The decomposition of seafood creates sulfide ion (S^{2-}) in the form of hydrosulfuric acid (H_2S) with the presence of H_2O [243, 244, 245]. In this way, H_2S concentration offen exceeds the maximum level of Vietnam standards by 4.2 times [246]. In the presence of Cl^- (availability in Vietnam due to the long coastline) in combination with H_2O and H_2S, the transformation as shown by the following reaction: $H_2S + 4Cl_2 + 4H_2O \rightarrow H_2SO_4 + 8HCl$ [247] takes place. The vary acidic environment caused by this reaction destroyed portland cement concrete as seen in Figure 10.1.

Figure 10.1 Effectiveness of waste water on concrete in Vietnam [248]

10.2 Expansion change due to external sulfate attack

Figure 10.2 presents the influence of metakaolin on the appearance of mortar bars exposed to Na_2SO_4 solution (3000mg SO_4^{-2}/l) at 20 ^oC. After 18 months of the hydration process, in total 7 bars which were made by mortar with 10 Wt.-% metakaolin, 4 bars were visually destroyed as shown in Figure 10.2. The edges of 4 destroyed bars were decomposed by the corrosion resulting in the softening and fractured phenomena. Expansion measurements on 4 destroyed bars could not be carried out due to the absence of actual probe length. After 22 months of the hydration process, total 7 bars containing 10 Wt.-% metakaolin were fractured with the presence of softening phenomena. However, all mortar bars with 20 Wt.-% metakaolin did not show any signs of disintegration due to external sulfate attack. The edges of the control mortar bars (only

with VPC 40) were also slightly corroded. This is observed that sands were exposed instead of the protection cement for surface layer in these edges as shown in Figure 10.2.

(a) The control mortar, 100%VP 40 (b) Mortar with 10%HTK84 and 90%VPC 40

Figure 10.2 Appearance of mortar bars (binder:sand:water = 1:3:0.6, 10×40×160 mm^3) after 18 hydration months in the solution Na_2SO_4 (3000mg SO_4^{-2}/l) at 20 °C.

Figure 10.3 shows the results of expansion measurement on mortar bars exposed to external sulfate attack in Na_2SO_4 solution (3000mg SO_4^{-2}/l) at 20 °C up to 22 months. After 18 months of the hydration process, the length of the mortar bars containing 10 Wt.-% of metakaolin strongly increased, i.e. the expansion of these mortar bars went up to 2.77 mm/m, causing cracks and fractures. In contrast, these serious changes of length were not detected in mortars containing 20 Wt.-% metakaolin and the control mortar bars VPC 40. They showed no serious changes of length as shown in Figure 10.3.

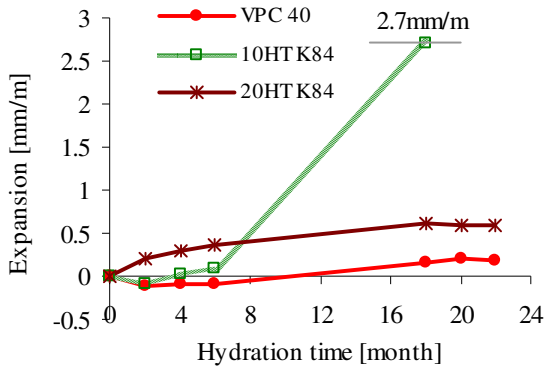

Figure 10.3 Expansion of mortar bars (VPC 40:metakaolin=100:0 / 90:10 / 80:20 Wt.-%, binder: sand: water = 1:3:0.6, 10×40×160 mm^3) after 22 hydration months in the solution Na_2SO_4 (3000mg SO_4^{-2}/l) at 20 °C.

As shown in Figures 10.2+3, the resistance of sulfate attack was promoted in order as follows: mortar with 10Wt.-% metakaolin << mortar with 20Wt.-% metakaolin < the control mortar.

10.3 Strength change due to sulfuric acid attack

Figure 10.4 shows the influence of metakaolin on the appearance of mortar bars exposed to H_2SO_4 solution (1 Wt.-%) at 20 °C after 19 months of the hydration process. The edges of all

mortar prisms (3 prisms) containing 0 - 10 Wt.-% of metakaolin were visually fractured. However, all mortar prisms containing 20 - 30 Wt.-% metakaolin were not eroded.

(a) Control mortar, 100%CEM I52.5 N

c) Mortar with 20%HTK84+80%CEM I52.5 N

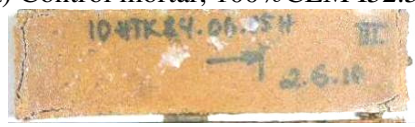

b) Mortar with 10%HTK84+90%CEM I52.5 N

d) Mortar with 30%HTK84+70%CEM I52.5 N

Figure 10.4 Appearance of mortar prisms (binder:sand:water = 1:3:0.6, 40×40×160 mm^3) after 19 hydration months in the solution H_2SO_4 1Wt.-% at 20 °C.

The compressive strength of mortar prisms with 0 - 10 Wt.-% metakaolin was not tested due to their deteriorated status as shown in Figure 10.4. However, the strength of all other samples was determined, and the results are shown in Figure 10.5. This reveals that mortars containing 20 – 30 Wt.-% of metakaolin showed a very strength maintenance during sulfuric acid attack.

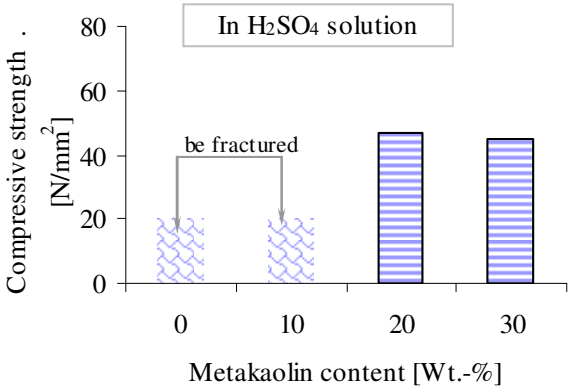

Figure 10.5 Compressive strength of HTK84 mortar prisms (binder:sand:water=1:3:0.6, 40×40×160 mm^3) after 19 months in H_2SO_4 1Wt.-% at 20 °C, the control CEM I 52.5 N.

As shown in Figures 10.4+5, the resistance of sulfuric acid attack was promoted in order as follows: the control mortar ≈ mortar with 10 Wt.-% metakaolin < mortar with 20 Wt.-% metakaolin ≈ mortar with 30 Wt.-% metakaolin.

10.4 Ion binding in cement and lime pastes

It can be inferred from Figures 10.2-5 that, the content of 20 Wt.-% metakaolin is effective enough to resist external sulfate and sulfuric acid attacks. The reason why 20 Wt.-% metakaolin can mitigate sulfate attack and sulfuric acid attack is due to ion binding of metakaolin as

analysed in section 9.5, Figure 9.2. Moreover, after 7 days of the hydration process, almost all the SO_4^{2-} from the cement hydration process was consumed by the pozzolanic reaction of metakaolin in the cement paste with 20 Wt.-% metakaolin as shown in Figure 10.6.

The results in Figure 10.7 indicate that metakaolin can quickly absorb a great amount of SO_4^{2-}. Even after 2 days of the hydration process, almost 447 mmol SO_4^{2-}/l (i.e. 44.5 g/l or 15 times more than the SO_4^{2-}concentration of seawater) was consumed by metakaolin in lime pastes. This indicates a potential of using sea sand or water containing sea water in the composition of metakaolin concrete.

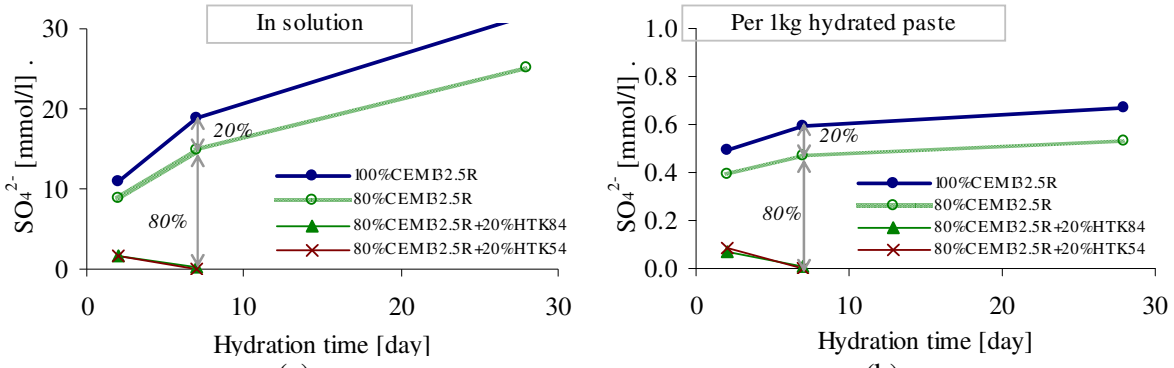

(a) (b)

Figure 10.6 Development of ion concentration in cement pastes. (a) in the extracted solution, (b) per 1kg hydrated cement pastes (CEM I 32.5 R:metakaolin=100:0/80:20Wt.-%, w/b0.35, 100% RH, 20 °C).

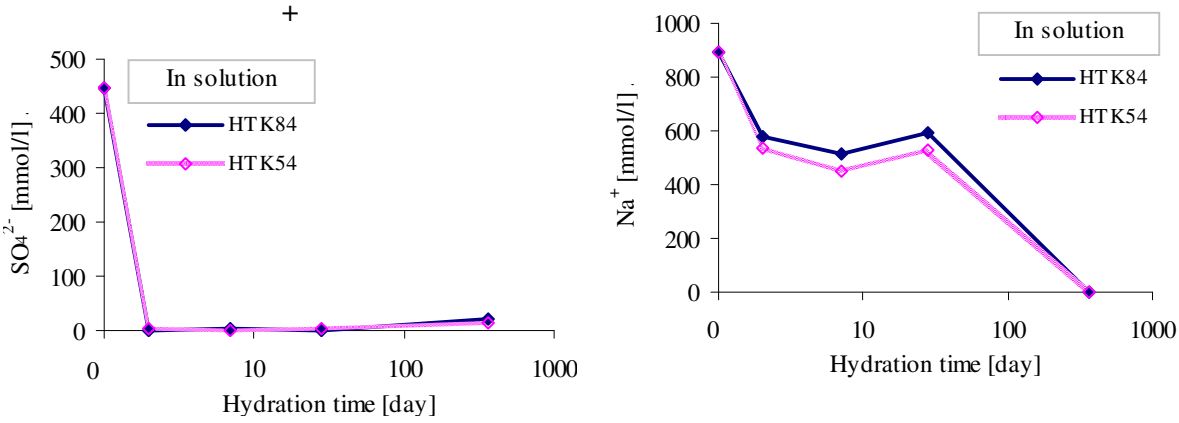

(a) (b)

Figure 10.7 Development of ion concentration in hydrated lime pastes (metakaolin: $Ca(OH)_2$: Na_2SO_4 = 1:1:0.1, w/b 0.75, 100% RH, 20 °C).

10.5 Surface structure of metakaolin and formed hydration products

In order to clearly observe the microstructural development of metakaolin during sulfate attack, SEM analysis (Nova NanoSEM 230, FEI, Netherlands) was performed.

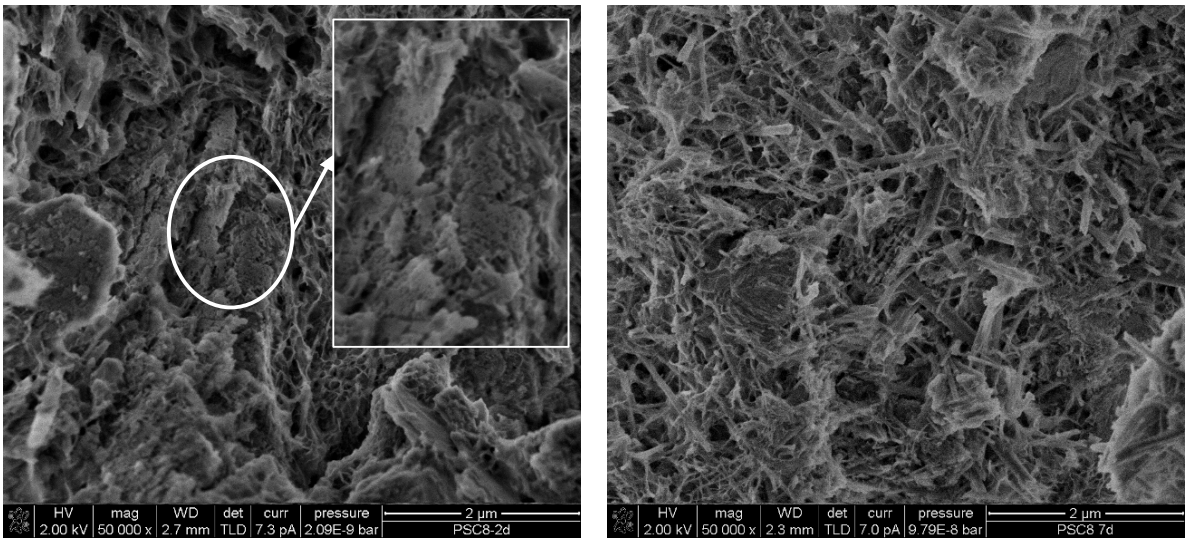

(a) at 2 days of hydration (b) at 7 days of hydration

Figure 10.8 SEM-SE imaging technique of hydrated lime pastes (metakaolin HTK84 :$Ca(OH)_2$:Na_2SO_4= 1:1:0.1, w/b 0.75, 100% RH, 20 ^oC)

The dissolution quickly occurred on the surface and edges of metakaolin after 2 -7 days of the hydration process as shown in Figure 10.8 in comparison with Figures 9.4+6. Dissolution voids indicate that ions were released from metakaolin surface and as such a strong ion exchange (*second activity part*) took place, destroying the surface structure of metakaolin (see Figure 10.8.a). Also, the hydration products were created quickly. Thus, on the day 7 of the hydration process the structure dissolution of metakaolin surface is almost not visible due to the obscuration of surface by hydration products such as AFt, which densifies the structure [249].

Table 10.1 Hydration products analysed by XRD for hydrated pastes$^+$
(metakaolin HTK84:$Ca(OH)_2$:Na_2SO_4= 1:1:0.1, w/b 0.75, 20 ^oC)

2days	C-S-H / SiO_2 Portlandite - $Ca(OH)_2$	2 months	C-S-H / SiO_2 Portlandite - $Ca(OH)_2$ Ettringite – $Ca_6Al_2(SO_4)_3(OH)_{12}.26H_2O$ Stratlingite - $Ca_2Al_2SiO_7{\cdot}H_2O$ Katoite – $Ca_3Al_2(SiO_4)_{3-x}(OH)_{4x}$ (x=1.5-3.0)
7days	C-S-H / SiO_2 Portlandite - $Ca(OH)_2$ Monosulfate - $C_4Al_2SO_{10}{\cdot}12(H_2O)$	18 months	C-S-H / SiO_2 Ettringite – $Ca_6Al_2(SO_4)_3(OH)_{12}.26H_2O$ Stratlingite - $Ca_2Al_2SiO_7{\cdot}H_2O$ Katoite – $Ca_3Al_2(SiO_4)_{3-x}(OH)_{4x}$ (x=1.5-3.0)

+ pastes after squeezing device has used

Table 10.1 shows the hydration products v.s time of lime pastes with the presence of Na_2SO_4. Al^{3+}/Si^{4+}, released from the metakaolin surface, reacted with Ca^{2+} and SO_4^{2-} to create mono-sulfate, ettringite, katoite, and stratlingite phases. Mono-sulfate was formed in early days, but its presence was absent in further hydration period. Which could be in turn changed into ettringite

over further hydration duration. A new hydration product katoite and stratlingite also appeared when the reaction continued, while most of portlandite was consumed after 18 months of the hydration process. The absence of portlandite indicates that 18 months is long enough for the determination of sulfate and acid attacks. This matches achieved results in Figures 10.3+5.

10.6 Porosity of mortar prisms

The porosity factor can cause the destroying of mortar bars during sulfate and sulfuric acid attacks. Therefore, an investigation of porosity on mortar prisms before sulfate and sulfuric acid attacks take place to them was conducted. The results are shown in Table 10.2. The volume of total porosity was similar in mortar prisms containing 0 – 20 Wt.-% metakaolin. However, the volume of pores (> 50 nm) for metakaolin mortar prisms was decreased in order as follows: control mortar > mortar with 10 Wt.-% metakaolin ≈ mortar with 20Wt.-% metakaolin. This indicates that the resistance to sulfate and sulfuric acid attacks should be promoted in order as follows: the control mortar < mortar with 10 Wt.-% metakaolin ≈ mortar with 20 Wt.-% metakaolin. This order does not match to the gained results in increasing expansion of bars by sulfate attack (Figures 10.2+3) and reducing compressive strength of prisms by sulfuric acid attack (Figures 10.4+5). Deterioration significantly occurred for mortar bars with 10 Wt.-% metakaolin. This indicates that, porosity factor does not play a role for sulfate and sulfuric acid attacks in this study.

Table 10.2 Porosity of mortar prisms in water at 20 ^{o}C after 28 days.
(binder:sand:water = 1:3:0.6, 40×40×160 mm^3)

	Total porosity [V.%]	Porosity >50nm [V.%]	Average Pore Radius [µm]
100 Wt.-% VPC 40	14.50	7.02	0.014
90 Wt.-% VPC 40+10 Wt.-% HTK84	14.68	2.68	0.009
80 Wt.-% VPC 40+20 Wt.-% HTK84	13.85	2.73	0.009

10.7 Microstructure and XRD analysis

Expansion hydration products often causes the deterioration of mortar and concrete products during sulfate and sulfuric acid attacks in the formation of softening and cracking phenomena, expansion, and strength reduction. SEM (Nova NanoSEM 230, FEI, Netherlands and Philips, XL 30 SEM-FEG) analysis is used to monitor the formation of secondary hydration products at micro-cracks as shown in Figures 10.9+10. Hydration products that are found are a together

formation of ettringite and thaumasite, gypsum, and thaumasite. The formation of gypsum and ettringite has been well documented in these particular conditions. The formation of gypsum is due to the high concentration of SO_4^{2-}, which may in turn cause expansion [250]. Ettringite with the addition of 32 water molecules in its crystal structure clearly plays a role in volume expansion. However, the formation of thaumasite during study investigations is surprising as this does not usually occur. Details for formation of thaumasite is explained later.

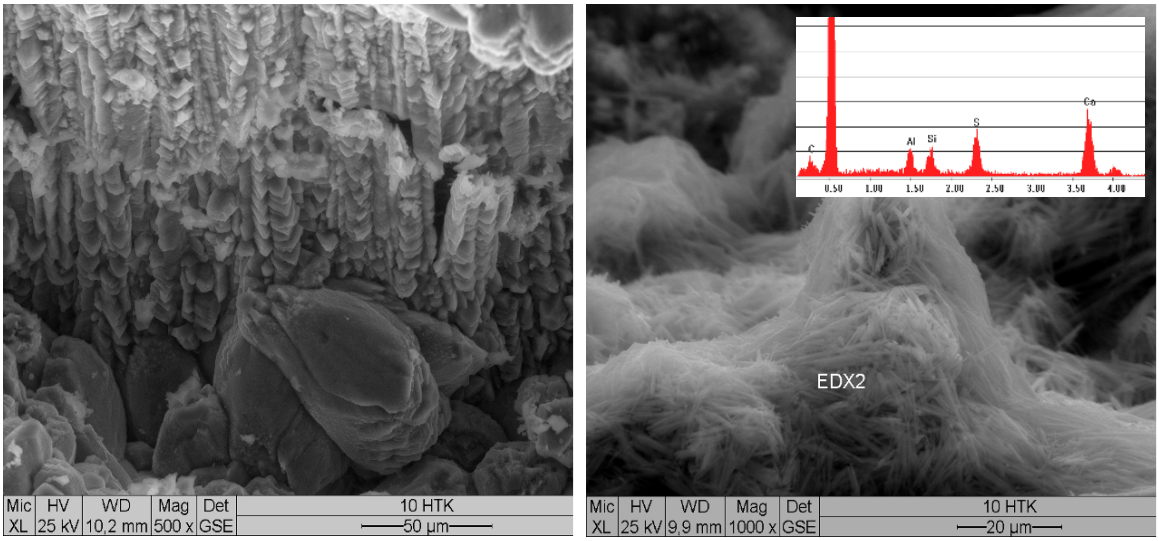

(a) overview on a micro-crack (b) ettringite and thaumasite

Figure 10.9 SEM (Philips, XL 30 SEM-FEG) of mortar (VPC 40:metakaolin HTK84= 90:10 Wt.-%, binder: sand: water = 1:3:0.6, 10×40×160 mm^3) after 18 hydration months in solution Na_2SO_4 (3000mg SO_4^{-2}/l) at 20°C.

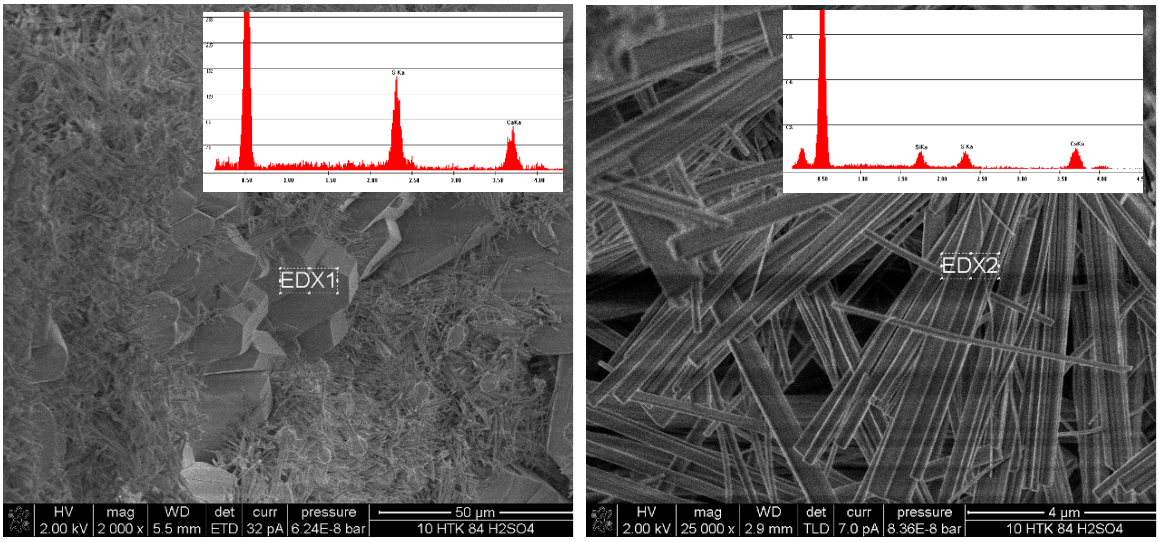

(a) Gypsum (b) Thaumasite

Figure 10.10 SEM (Nova NanoSEM 230, FEI, Netherlands) of micro-cracks in mortar (CEM I 52.5 N:metakaolin HTK84= 90:10 Wt.-%, binder: sand: water = 1:3:0.6, 40×40×160 mm^3) after 19 hydration months in solution H_2SO_4 (1 Wt.-%) at 20 °C.

In order to see clearly whether or not the hydration products cause expansion, a XRD examination of the control cement paste and metakaolin pastes was conducted in Figure 10.11. Mono-sulfate (converting to ettringite) was not present in the control cement paste, while the paste with 10 Wt.-% metakaolin contained mono-sulfate. The peak intensity of mono-sulfate was very weak (almost invisible) in the paste with 20 Wt.-% metakaolin.

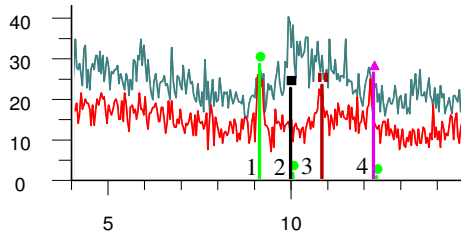

(a) Cement paste with 10 Wt.-% HTK84 (above)
The control cement paste VPC 40 (below)

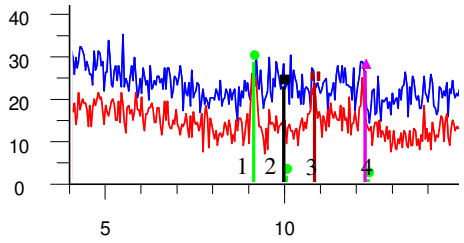

(b) Cement paste with 20 Wt.-% HTK84 (above)
The control cement paste VPC 40 (below)

Figure 10.11 XRD analysis of cement paste (VPC 40:metakaolin =100:0/80:20 Wt.-%, binder:water=1:0.5) after 28 days at 100% RH in 20 ^{o}C.

1-ettringite, 2-mono-sulfate, 3_mono-carbonate, 4_Brownmillerite.

10.8 Discussion

10.8.1 Dependence of deterioration on the level of metakaolin content

It is generally known that deterioration due to sulfate and sulphuric acid attacks results from the formation of AFt/AFm phases and the dissolution of C-S-H phases [150]. These processes are governed by the concentration of Ca^{2+}, Al^{3+} / $Al(OH)_4^-$, SO_4^{2-} ions and alkali content in aqueous phase as well as porosity status [48, 157, 251, 252]. Also it is known that harmful large pores, with a size larger than 50 nm, can increase the permeability parameter [135], which leads to the increase in the permeability of solution (SO_4^{-2}/l) from outside to form expansion hydration products [253]. As more metakaolin is used in the mixture, the frequency of harmful large pores decreased [138, 72, 140].

This section of the study considers the reasons why during sulfate and sulfuric acid attacks on mortars with 10 Wt.-% metakaolin, its resistance was not sufficient. On the other hand, the control mortar (VPC 40, CEM I 52.5 N) and mortar with 20 Wt.-% metakaolin showed a sufficient resistance. Within the line of this discussion, the results of the current study show that:

(1) The usage of 10 Wt.-% metakaolin in the composition of mortar bars/prisms provided a less resistance to sulfate and sulfuric acid attacks (Figures 10.2-5).

(2) The volume of harmful large pores (larger than 50 nm) is similar in mortar prisms containing 10 - 20 Wt.-% metakaolin (see Table 10.2).

(3) The secondary hydration products such as a formation of ettringite - thaumasite together and gypsum were found in micro-cracks of mortar bars/prisms containing 10 Wt.-% metakaolin (Figures 10.9+10)

(4) Mono-sulfate was present in the cement paste with 10 Wt.-% metakaolin, whereas it is almost absent in cement paste with zero or with 20 Wt.-% metakaolin as shown in Figure 10.11.

(5) Mono-sulfate was transformed into ettringite in further hydration period as seen in Table 10.1. Furthermore, it is known that both ettringite and mono-sulfate are formed more quickly in the system of cement – metakaolin – calcite than in the control cement [254]. As such, in further hydration period if SO_4^{2-} is present, the transformation of mono-sulfate into ettringite is possible.

Taken together, five results above indicate that (1) the destruction of mortar bars / prisms with 10 Wt.-% metakaolin is not in dependence of porosity status (2) this destruction of mortar bars/prisms with 10 Wt.-% metakaolin could be due to the more transformation of mono- sulfate into ***ettringite*** in further hydration time (mono- sulfate/***more ettringite*** formation) as follows.

Both cements VPC 40 and CEM I 52.5 N have the same Na_2O_{eq} value of 0.79, which is a normal alkali content. As a result, the speed of hydration reaction for cement and of pozzolanic reaction for metakaolin is normally gradual. It is known that, the speed rate of ettringite formation from Al^{3+} of metakaolin is faster than that from $Al(OH)_4^-$ (C_3A and C_4AF) of cement at the temperature of 20 ^oC [128, 255, 256]. Thus, the formation of mono-sulfate/more ettringite from Al^{3+} of metakaolin takes place continuously unless there is not enough SO_4^{2-} (contributing to the mono-sulfate/more ettringite formation) and Ca^{2+} available (activating metakaolin). Based on the dates of porosity shown in Table 10.2, it is assumed that the transport of SO_4^{2-} (from outside, Na_2SO_4 or H_2SO_4) is similar in samples with 10 and 20 Wt.-% metakaolin. Therefore, the available content of Ca^{2+} (from C_3S, C_2S, C_3A and C_4AF) and SO_4^{2-} (from $CaSO_4$) mainly influences the variation in mono-sulfate/more ettringite content for samples with 10 and 20 Wt.-% metakaolin. Compared to the mortar with 20 Wt.-% metakaolin, the lesser the metakaolin

content (10 Wt.-%) added into mortar, the greater the possibility of mono-sulfate/more ettringite formation. This is due to the greater availability of SO_4^{2-}, Ca^{2+} and Al^{3+} / $Al(OH)_4^-$ from mortar with 10 Wt.-% metakaolin as shown in Table 10.3. The control mortars VPC 40/CEM I 52.5 N, however, possess only $Al(OH)_4^-$ (without Al^{3+} from metakaolin) so less mono-sulfate/more ettringite formation is created as compared to the mortar with 10 Wt.-% metakaolin. As analysed, significant deterioration during sulfate attack occurred for mortars with 10 Wt.-% metakaolin as a result of the greater formation of mono-sulfate/more ettringite as shown in Table 10.3 and Figure 10.11.

Table 10.3 The predicted mass of ions during the hydration process

	SO_4^{2-} (Na_2SO_4 or H_2SO_4)	SO_4^{2-} ($CaSO_4$)	Ca^{2+} (C_3S, C_2S, C_3A and C_4AF)	$Al(OH)_4^-$ (C_3A, C_4AF)	Al^{3+} ($Al_2O_3.2SiO_2$)
The control mortar	XXX	XXX	XXX	XXX	X
Mortar with 10Wt.-%MK	XX	XX	XX	XX	XX
Mortar with 20Wt.-%MK	XX	X	X	X	XXX

Therefore the 20 Wt.-% metakaolin level is required to provide good resistance against sulfate and sulphuric acid attacks for Vietnamese metakaolin mortar. A similar level of metakaolin is observed for a mortar in the study of [157], which indicates that at least 15 Wt.-% metakaolin is considered necessary to provide good sulfate resistance. The 20 Wt.-% level of Vietnamese metakaolin for sulfate resistance is higher than of some other metakaolin in the world (7-10 Wt.-%) studied by [159, 158, 161]. The reason for such a difference in the metakaolin level may be caused by experimental conditions chosen. In this study, normal mortar (w/b 0.6) was used, whereas samples in other studies [159, 158, 161] are normal concretes and HPC (w/b < 0.6).

In summary, the composite cement containing less than 20 Wt.-% metakaolin has a lesser resistance to external sulfate attack than compared to pure cement, while the composite cement containing 20 Wt.-% metakaolin has a better resistance against sulphuric acid attack than pure cement.

10.8.2 Thaumasite formation

Normally in cement system [162, 163, 164, 257], thaumasite is formed in cool temperatures (0 – 15 ^oC). Investigations at a temperature of 20 ^oC for a year could not show a proof for the presence of thaumasite [163]. However it has been suggested that a small quantity of thaumasite

can be formed even at room temperature [258, 259] due to the degree of carbonation, type and concentration of sulfate solutions as well as pH of the pore solution [260, 261]. Thaumasite may also be produced in field exposures at normal temperatures [262, 261, 263]. Furthermore studies suggest that thaumasite appears to be stable and to remain in the concrete regardless of subsequent temperature changes [263].

Mortar prisms containing 10 Wt.-% of metakaolin show the presence of thaumasite at a cure condition of 5 ^{o}C, whereas the presence of thaumasite is not observed in cure conditions of 25 ^{o}C and up to 60 months [260]. However in this current study, as seen in Figures 10.9+10, thaumasite formation in micro-cracks of mortar bars (cured in SO_4^{2-} 3000mg/l) containing 10 Wt.-% metakaolin was obvious at 20 ^{o}C after 18 months of cure time. Additionally, thaumasite was also formed in micro-cracks of mortar prisms (cure in H_2SO_4 1 Wt.-%) containing 10 Wt.-% metakaolin at 20^{o}C after 19 months of cure time.

Table 10.4 Mol rate of $CaCO_3$ to Al^{3+} and $Al(OH)_4^-$ in cement pastes containing metakaolin

	Portland cement (C_3A, C_4AF)	Composite cement (C_3A, C_4AF, $Al_2O_3.2SiO_2$)
	$[CaCO_3]$ / $[Al_2O_3]$	$[CaCO_3]$ / $[Al_2O_3]$
100 Wt.-% VPC 40	0.74	0.74
90 Wt.-% VPC 40+10 Wt.-% HTK84	0.74	0.40
80 Wt.-% VPC 40+20 Wt.-% HTK84	0.74	0.25

The formation of thaumasite in mortar bars / prisms containing 10 Wt.-% metakaolin can be due to the influence of Al^{3+} content. Mono-carbornat content (contributing to the thaumasite formation) in cement paste was reduced with increasing of metakaolin content as well as Al^{3+} (see Figure 10.11 and Tables 10.3+4). Furthermore, as shown in Figure 8.6, the available Al^{3+} content from metakaolin can activate $CaCO_3$ as a Al_2O_3-$CaCO_3$ network (hemi/mono-carbonate). Additionally, after 18 months of the hydration process, almost portlandite can be consumed by pozzolanic reaction to metakaolin as seen in Table 10.1. Thus, Al^{3+} from unreacted metakaolin can not release anymore, and as such the $[CaCO_3]/[Al^{3+}]$ ratio increases, creating a favor of thaumasite formation.

Taken together, in combination with SO_4^{2-} a phase of Al_2O_3-SiO_2-$CaCO_3$-SO_4^{2-} (together formation of ettringite and thaumasite, see Figure 10.10) is possible to be created.

10.9 Concluding remarks

The following results were obtained:

(1) In general, the resistance to external sulfate attack of composite cement with metakaolin is decreased as compared to the pure cement. The composite cement with 20 Wt.-% metakaolin show drastically an increased resistance to sulfate and sulfuric acid attacks as compared to composite cement with 10 Wt.-% metakaolin.

(2) The destruction of mortar bars / prisms containing 10 Wt.-% Vietnamese metakaolin during sulfate and sulfuric acid attacks caused by the mono-sulfate/more ettringite formation.

(3) Thaumasite can be created at 20 ^{o}C in mortars containing 10 Wt.-% metakaolin during sulfate and sulfuric acid attacks.

11. Conclusions and recommendations

11.1 Conclusions

The research objectives of the study were reached as the obtained results from the study opened up a potential of producing and using the composite cement made from metakaolin in Vietnam. In addition, the role of experimentally pozzolanic-activity tests as well as their impact was identified. The results of study showed the role of residual water as well as BET surface in the kinetic behaviour of metakaolin and its influence on the durability and product properties. The following conclusion can be drawn:

The calciantion of kaolin

The low quality Vietnamese kaolin can be converted in to a good quality metakaolin by an optimal thermal treatment process. With respect to this, the heating temperature and the calcination duration of the optimal thermal treatment process was found. The mass loss determined by TGA analysis can be used to assess the complete transformation of kaolin into metakaolin. The testing results of Vietnamese kaolin in laboratory show that the transformation of kaolin into metakaolin from a minimum temperature of 600 °C is independent of calcination duration. However, the temperature of 500 °C at least 3 – 4 hour is required to convert kaolin into metakaolin. At the temperature of 800 °C lasting for 3 - 4 hour, the achieved metakaolin possess the highest pozzolanic reactivity as compressive strength index (CSI).

Pozzolanic testing method

(1) The lime consumption tested by the saturated lime method, TGA-CaO method, and mCh does not agree with the reference test CSI, although TGA-CaO method can be seen to be the most suitable method to characterise the pozzolanic activity of metakaolin and to provide the best agreement between metakaolin and the performance of cement and concrete products.

(2) BET surface has a significant impact on lime consumption evaluation tested by TGA-CaO method, whilst D_{50} shows its more dominant effect on the value of lime consumption testd by mCh.

(3) The mCh method shows the highest lime consumption from the samples tested, whilst the saturated lime method shows the smallest value; with the TGA-CaO method resulting in a medium rate of consumption.

The properties of metakaolin

With achieved metakaolin, a composite cement (based CEM I 42.5 R, which is also served as a comparison cement) with various metakaolin content (20 - 40 Wt.-%) are produced. The following results are drawn:

(1) The presence of metakaolin creates an increase in water demand and mainly affects the initial setting time although the final setting time is slightly influenced. An increase in BET surface of metakaolin increased the initial setting time of cement pastes, but this influence of BET surface is absent in final setting time.

(2) Depending on the results of water demand (normally smaller than 35 Wt.-%), 20 - 40 Wt.-% DQK53/DQK83 can be used for producing composite cement, while a solution to reduce the water demand is needed for producing composite cement containing more than 20 Wt.-% HTK54/HTK84.

(3) The temperature strongly influences the compressive strength of metakaolin mortar on the early days of the hydration process, while in later days of the hydration process this influence is only limited.

- At 8 °C hydration: The early strength of all composite cements after 2 days and 7 days is generally lower than that of the pure cement (CEM I 42.5 R). After 28 days, however, the composite cement show higher strength values than the pure cement.
- At 20 °C hydration: The early strength values after 2 days are the same behaviour as before (8 °C hydration), i.e. a lower strength of composite cements as compared to the pure cement. In contrast, after 7 days composite cements show a similar strength values to the pure cement. After 28 days, both cement types in general are on the same level of strength.
- At 40 °C hydration: The temperature rising up to 40 °C has an significant impact on the pozzolanic reaction of metakaolin. As a consequence, the composite cements already show in the early hydration stage of 2 days and 7 days a distinct higher strenght values than the pure cement. In fact, after 7 days the compressive strength of composite cements reach up to 15 N/mm² higher strength value than that of the pure cement. After 28 days, a comparable strength is reached for all composite cements.

(4) Vietnamese metakaolin contribute to the increase in strength of HPM. The porosity of HPM seemed not to be significantly influenced by different metakaolins in comparison between Vietnamese metakaolins and the commercial product.

(5) The main purpose of this study is to determine the possibility of producing Vietnamese metakaolin as a replacement for other additives in the manufacture of composite cement. Depending on the intended use of composite cement and weather conditions of cure, each Vietnamese metakaolin (HTK54, HTK84, DQK53, DQK83) can be used appropriately as follows:

- A composite cement with a low water demand should be combined with DQK53 or DQK83;
- A high strength of composite cement is gained by using HTK84. However, in the case of high cure temperature (40 ^{o}C) HTK54, DQK53 and DQK83 achive a similar strength to HTK84;
- A composite cement that aims to reduce CO_2 emissions and to improve economics of cement products should added metakaolin and calcite. It is proposed that by adding HTK54 or HTK84, it allows a reduction in 45 Wt.-% Portland cement clinker without the strength reduction.

The influence of metakaolin on durability

(1) The more metakaolin is replaced for cement, the greater resistance to ASR is gained. This is due to the behaviour of ion binding caused by the pozzolanic reaction of metakaolin. An amount of 10 Wt.-% metakaolin is enough to mitigate ASR according to the German Alkali-Guideline (2007) alternative method.

(2) The presence of residual water in the structure of metakaolin is favorable for high binding capabilities during the first and third activity parts of pozzolanic reaction.

(3) The main aim of this study is also to determine the possibility of using Vietnamese metakaolin to produce concrete resisting ASR. The results gained show that metakaolin calcinated at low temperature 500 ^{o}C (HTK54/DQK53) reaches a similar resistance in ASR to metakaolin calcinated at high temperature 800 ^{o}C (HTK84/DQK83).

(4) In general, the resistance to external sulfate attack of composite cement with metakaolin is decreased as compared to the pure cement. The composite cement with 20 Wt.-% metakaolin show drastically an increased resistance to sulfate and sulfuric acid attacks as compared to composite cement with 10 Wt.-% metakaolin.

(5) The destruction of mortar bars or mortar prisms containing Vietnamese metakaolin during sulfate and sulfuric acid attacks caused by the more mono-sulfate/more ettringite formation.

(6) The presence of thaumasite can be occurred at 20 ^{o}C in mortars containing 10 Wt.-% metakaolin during sulfate and sulfuric acid attacks.

Additional results obtained

(1) The thermal treatment of kaolin is a process of mass loss due to the removal of the H_2O^-/ H_2O^+/OH^- groups. Thus, the factor of mass loss determined by Equation 6.1 can be used for determining the complete conversion of kaolin in to metakaolin.

(2) During the calcination, because of the removal of the H_2O^+/OH^- groups and the collapse of kaolinite layer structure, the mass and BET surface of calcinated kaolin tends to decrease, while its density tends to increase. It can be concluded that the presence of residual water as well as the not fully collapsed layer structure in calcinated kaolin causes an increased BET surface during the calcinations.

(3) The peak of dissipation mass in TGA analysis can be used for determining the characteristic peaks from the residual water in kaolinite/metakaolinite.

(4) A save indicator for complete conversion of kaolinite into metakaolinite is the absence of kaolinite peaks in XRD pattern.

(5) The pozzolanic reaction of metakaolin can be divided in three activity parts as follows: Firstly, alkali ion consumption by new hydration phases that are created from metakaolin. Secondly, dissolution of Al^{3+}/Si^{4+} from metakaolin. Thirdly, ion absorption of Ca^{2+} and alkali on the surface of metakaolin.

(6) Dissolution structure occurs on metakaolin containing residual water firstly on the edges of particles. Whereas, metakaolin without residual water dissolves primary at the surface.

11.2 Recommendations

Based on the achieved results in the study, the following recommendations have been drawn:

Additional further researches to facilitate the application of Vietnamese metakaolin

(1) Based on the achieved results of the calcination process, two principal manufacturing possibilities are as the following:

- A normal qualitative metakaolin, i.e. it is sufficient for applications in normal concretes, is calcinated at temperatures of 500 °C for extended calcination duration.

- High qualitative metakaolin, i.e. it is possible for applications in special purpose (e.g, HPC and UHPC), is calcinated at temperatures over 700 °C

(2) The evaluation of pozzolanic activity for metakaolin according to Vietnamese standard (the saturated lime method) needs to study the duration of test time. It is concluded that hydration period should be long enough to achieve a constant value of lime consumption.

(3) The capacity of binding Cl^- by metakaolin needs to be investigated in order to avoid the deterioration of steel due to seawater coming from the long coastline of Vietnam.

(4) The combination between metakaolin and calcite in composite cement should be conducted with different Porland cements (with high and low alkali contents) to find the best combination level. Additionally, the presence of thaumasite needs a clear explanation using different combination levels of metakaolin and calcite in order to resist external sulfate attack.

(5) Metakaolinite with and without residual water needs further investigation to describe its amorphous status as well as its behaviour in pozzolanic reaction.

(6) Ion binding of metakaolin is needed to study further to describe the behaviour of alkali ion.

(7) A study of using metakaolin as SCM in HPC and UHPC should be considered.

The application of research results in the production of metakaolin in Vietnam

(1) It is suggested that the Vietnam International Education Development (Project 322) / Ministry of Education and Training of Vietnam (MOET) should transfer the results of this study to Vietnam Institute for Building materials / Ministry of Construction for the application of metakaolin. However, the companies that use the results of the study should be agreed by F.A.Finger- Institute for Building Materials Science (FIB).

(2) The manufacture of metakaolin should be combined with the production of cement because the waste heat from the manufacturing process of cement can be used for the production of metakaolin. Moreover, it is convenient for composite cement production if transport is limitted. It should be avoided that many mining companies produce metakaolin and sell it to cement manufacturing companies. This would lead to increase the applicability between cement and metakaolin because of lower production variability.

12. References

[1] The decision 567/QD-TTg: The development program of no-heating construction materials up to 2020, Vietnamses Government (2010).

[2] The directive 10/CT-TTg: The increasing use of no-heating construction materials and the limit of production and use for clay brick, Vietnamses Government (2012).

[3] Vu, D. D.; et al: Research for producting metacaolin in Viettnam for using as an active admixture in high performance concrete, National university of civil engineering (2005), H. B200-34-58.

[4] Tran, Q. T.: Research into the completed technology of manufacturing Metakaolin, Vietnam Institute for Building Materials (2006), S. 31.

[5] Tran, Q. T.: The research and production of metakaolin used in the manufacture of high quality concrete, Vietnam Institute for Building Materials (1999).

[6] Vu, D. D.: Strength properties of metakaolin-blended paste mortar and concrete, PhD Thesis in Technische Universiteit Delft, Netherlands (2002).

[7] Vu, D. D.; Stroeven, P.; Bui, V. B.: Strength and durability aspects of calcined kaolin-blended Portland cement mortar and concrete, Cement and Concrete Composites 23 (2001), H. 6, S. 471–478.

[8] Nguyen, M. T.: The study evaluates the ability to use raw materials to produce clinker Portland cement for the projects investing in cement factories., Study collection from the science and technology of building materials, 2005-2009 .

[9] TCVN 6071:1995 (The Vietnamese standard): Raw materials for the production of portland cement clinke. Clay. (1995).

[10] Wedsite: Central intelligence agency: Vietnam, https://www.cia.gov/ (Retrieved 16/2/2012).

[11] Luong, D. L.: Main features of developing plan of Vietnam cement industry in the period 2011-2020 and orientation to 2030, Journal of building material research and development (2011), H. 1, S. 10–14.

[12] Sabir, B. B.; Wild, S.; Bai, J.: Metakaolin and calcined clays as pozzolans for concrete: a review, Cement and Concrete Composites 23 (2001), H. 6, S. 441–454.

[13] Siddique, R.: Metakaolin, waste materials and by-products in concrete, Springer-Verlag, Berlin, Heidelberg (2008).

[14] Siddique, R.; Klaus, J.: Influence of metakaolin on the properties of mortar and concrete: A review, Applied Clay Science 43 (2009), H. 3-4, S. 392–400.

[15] Murray, H. H.: Overview — clay mineral applications, Applied Clay Science 5 (1991), H. 5-6, S. 379–395.

[16] Murray, H. H.: Traditional and new applications for kaolin, smectite, and palygorskite: a general overview, Applied Clay Science 17 (2000), H. 5-6, S. 207–221.

[17] Reeves, G. M.; Sims, I.; Cripps, J. C.: Clay materials used in construction, The Geological Society, London (2006).

[18] Worrall, W. E.: Clays their nature, origin and general properties, Maclaren, London (1968).

[19] Srivastava, V.: Clays: Types and applications, Bulletin of the Catalysis Society of India 11 (2012), S. 56–77.

[20] Ďurovič, S.; Krishna, P.; Pandey, D.: Layer stacking, International Tables for Crystallography C (2006), H. 9.2, S. 752–773.

[21] Fernandez, R.; Martirena, F.; Scrivener, K. L.: The origin of the pozzolanic activity of calcined clay minerals: A comparison between kaolinite, illite and montmorillonite, Cement and Concrete Research 41 (2011), S. 113–122.

[22] Castellano, M.; Turturro, A.; Riani, P.; Montanari, T.; Finocchio, E.; Ramis, G.; Busca, G.: Bulk and surface properties of commercial kaolins, Applied Clay Science 48 (2010), S. 446–454.

[23] Wedsite: Mineralogy Database: http://webmineral.com/data/Kaolinite.shtml (Retrieved 05/2009).

[24] Bell, F. G.: Engineering geology, 2. ed., Butterworth-Heinemann, Amsterdam (2007).

[25] Eberl, D. D.: Clay mineral formation and transformation in rocks and soils, Philosophical transactions (The royal society) A 311 (1984), S. 241–257.

[26] Fialips, C. -I; Petit, S.; Decarreau, A.: Hydrothermal formation of kaolinite from various metakaolins, Clay Minerals 35 (2000), S. 559–572.

[27] The final project report: Master plan for the industry of Vietnamese building materials to 2010 and orientations to 2020, Vietnam Institute for Building Materials (2000).

[28] Le, D. T.; Nguyen, P.; Nguyen, T. T.: Potential of kaolin in Vietnam and orientation of exploratory works and exploitation serving the socio-economic development, Vietnam Department of Geology and Mineral (2008).

[29] Doan, H. C.; Nguyen, P.; Le, D. T.: Potential of kaolin in North - East Vietnam and application in industries, Vietnamese Journal of Geology 297 (2006), H. series A, S. 30–37.

[30] Kušnír, I.: Mineral resources of Vietnam, Acta Montanistica Slovaca 5 (2000), H. 2, S. 165–172.

[31] Gruber, K. A.; Ramlochan, T.; Boddy, A.; Hooton, R. D.; Thomas, M. D. A.: Increasing concrete durability with high-reactivity metakaolin, Cement and Concrete Composites 23 (2001), H. 6, S. 479–484.

[32] Guideline: DMS – 4635 Metakaolin of Texas Department of Transportation (2004).

[33] Gerrard, J.: Fundamentals of soils, Reprinted., Routledge, London (2003).

[34] Malhotra, V. M.; Mehta, P. Kumar: Pozzolanic and cementitious materials, Gordon and Breach, Amsterdam (1996).

[35] Piga, L.: Thermogravimetry of a kaolinite-alunite ore, Thermochimica Acta 265 (1995), S. 177–187.

[36] Gastuche, M. C.; Toussaint, F.; Fripiat, J. J.; Touilleaux, R.; Meersche, M. (1962)Study of intermediate stages in the kaolin -> metakaolin transformation, Universite' de Louvain, Belgium.

[37] Balek, V.; Murat, M.: The emanation thermal analysis of kaolinite clay minerals, Thermochimica Acta 282-283 (1996), S. 385–397.

[38] Badogiannis, E.; Kakali, G.; Tsivilis, S.: Metakaolin as supplementary cementitious material: Optimization of kaolin to metakaolin conversion, Journal of Thermal Analysis and Calorimetry 81 (2005), S. 457–462.

[39] Chakraborty, A. K.: New date on thermal effects of kaolinite in the high temperature region, Journal of Thermal Analysis and Calorimetry 71 (2003), S. 799–808.

[40] Querol, X.; Fernandez Turiel, J. L.; Lopez Soler, A.: The behaviour of mineral matter during combustion of Spanish sub-bituminous and brown coals, Mineralogical Magazine 58 (1994), S. 119–133.

[41] Chakraborty, A. K.: DTA study of preheated kaolinite in the mullite formation region, Thermochimica Acta 398 (2003), H. 1-2, S. 203–209.

[42] Frost, R. L.; Cheng, H.; Yang, J.; Liu, Q.; He, J.: Thermogravimetric analysis-mass spectrometry (TG-MS) of selected Chinese kaolinites, Thermochimica Acta 507 (210), S. 106–114.

[43] Brindley, G. W.; Nakahira, M.: The Kaolinite-MuIIite Reaction Series: II. Metakaolin, Journal of The American Ceramic Society 42 (1959), H. 7, S. 314–318.

[44] Drits, V.A.; Kashaev, A.A: An X-ray study of a single crystal of kaolinite, Soviet Physics - Crystallography 5 (1960), S 207-210.

[45] Fischer, R. X.; Schneider, H.; Schmucker. M: Crystal structure of Al-rich mullite, American Mineralogist (1994), H. 79, S. 983-990.

[46] Popovic, J.; Tkalcec, E.; Grzeta, B.; Kurajica, S.; Schmauch, J.: Cobalt incorporation in mullite, American Mineralogist (2007), H. 92, S. 408–411.

[47] Müller, C. J.: Pozzolanic activity of natural clay minerals with respect to environmental geotechnics, Thesis of Doctor of Technical Science in Zurich (2005).

[48] Taylor, H. F. W.: Cement chemistry, 2. ed.,, Telford Publ., London (2003).

[49] Bredy, P.; Chabannet, M.; Pera, J.: Microstructure and porosity of metakaolin blended bements, Materials Research Society V137. USA (1988), S. 431–436.

[50] He, C.; Makovicky, M.; Osbæck, B.: Thermal stability and pozzolanic activity of calcined kaolin, Applied Clay Science 9 (1994), S. 165–187.

[51] Shvarzman, A.; Kovler, K.; Schamban, I.; Grader, G.; Shter, G. E.: Influence of chemical and phase composition of mineral admixtures on their pozzolanic activity, Advances in Cement Research 14 (2002), H. 1, S. 35–41.

[52] Bich, Ch; Ambroise, J.; Péra, J.: Influence of degree of dehydroxylation on the pozzolanic activity of metakaolin, Applied Clay Science 44 (2009), H. 3-4, S. 194–200.

[53] Plešingerová, B.; Súčik, G.; Fabián, M.: Surface area change of kaolin causing annealing, Acta Metallurgica Slovaca 17 (2011), H. 3, S. 169–176.

[54] Drzal, L. T.; Rynd, J. P.; Fort, T.: Effects of calcination on the surface properties of kaolinite, Journal of Colloid and Interfaces Sciences 93 (1982), H. 1, S. 129–139.

[55] Cristóbal, A. G. S.; Castelló, R.; Luengo, M. A. M.; Vizcayno, C.: Acid activation of mechanically and thermally modified kaolins, Materials Research Bulletin 44 (2009), H. 11, S. 2103–2111.

[56] Murat, M.: Hydration reaction and hardening of calcined clays and related minerals. I. Preliminary investigation on metakaolinite, Cement and Concrete Research 13 (1983), H. 2, S. 259–266.

[57] Baronio, G.; Binda, L.: Study of the pozzolanicity of some bricks and clays, Construction and Building Materials 11 (1997), H. 1, S. 41–46.

[58] DIN EN ISO 3262-9 (The european standard) (1997)Füllstoffe für Beschichtungsstoffe - Anforderungen und Prüfverfahren - Teil 9: Calcinierter kaolin,

[59] ASTM C 618 - 08a (The american standard) (1968)Standard specification for coal fly ash and raw or calcined natural pozzolan for use in concrete,

[60] The Vietnam standard: TCVN 6882 : 2001: Mineral admixture for cement (2001).

[61] Frias, M.; Rodriguez, O.; Vegas, I.; Vigilz, R.: Properties of calcined clay waste and its influence on blended cement behavior, Journal of the American Ceramic Society 91 (2008), H. 4, S. 1226–1230.

[62] Donatello, S.; Tyrer, M.; Cheeseman, C. R.: Comparison of test methods to assess pozzolanic activity, Cement and Concrete Composites 32 (2010), H. 2, S. 121–127.

[63] The Vietnam standard: TCVN 3735 : 1982: Active pozzolanic admixtures (1982).

[64] Rodríguez, O.; Frías, M.; Sánchez Rojas, M. I. de: Influence of the calcined paper sludge on the development of hydration heat in blended cement mortars, Journal of Thermal Analysis and Calorimetry 92 (2008), H. 3, S. 865–871.

[65] Salvador, S.: Pozzolanic properties of flash-calcined kaolinite: A comparative study with soak-calcined products, Cement and Concrete Research 25 (1995), H. 1, S. 102–112.

[66] Kakali, G.; Perraki, T.; Tsivilis, S.; Badogiannis, E.: Thermal treatment of kaolin: the effect of mineralogy on the pozzolanic activity, Applied Clay Science 20 (2001), H. 1-2, S. 73–80.

[67] Samet, B.; Chakchouk, A.; Mnif, T.; Tagnit-Hamou, A.: Influence of mineralogy of Tunisian clays on pozzolanic activity—assessment by different methods, Advances in Cement Research 19 (2007), H. 2, S. 57–65.

[68] Jørgensen, M. R.; Holger, L.; Jakobsen, H. J.; Skibsted, J.: Activation of kaolinite for use as a supplementary cementitious material in Portland cement mixtures (2009).

[69] Gava, G. P.; Prudêncio Jr, L. R.: Pozzolanic activity tests as a measure of pozzolans' performance. Part 2, Magazine of Concrete Research 59 (2007), H. 10, S. 735–741.

[70] Curcio, F.; DeAngelis, B. A.; Pagliolico; S.: Metakaolin as a pozzolanic microfiller for high-performance mortars, Cement and Concrete Research 28 (1998), H. 6, S. 803–809.

[71] Serry, M. A.; Taha, A. S.; El-Hamaly, S. A. S.; El-Didamony, H.: Metakaolin - lime hydration products, Thermochimica Acta 79 (1984), S. 103–110.

[72] Frías, M.; Cabrera, J.: Pore size distribution and degree of hydration of metakaolin–cement pastes, Cement and Concrete Research 30 (2000), H. 4, S. 561–569.

[73] Frías, M.; Sánchez, M. I.: Influence of metastable hydrated phases on the pore size distribution and degree of hydration of metakaolin-blended cements cured at 60 °C, Cement and Concrete Research 35 (2005), H. 7, S. 1292–1298.

[74] Shvarzman, A.; Kovler, K.; Grader, G. S.; Shter, G. E.: The effect of dehydroxylation/amorphization degree on pozzolanic activity of kaolinite, Cement and Concrete Research 33 (2003), H. 3, S. 405–416.

[75] Murat, M.: Hydration reaction and hardening of calcined clays and related minerals.: II. Influence of mineralogical properties of the raw-kaolinite on the reactivity of metakaolinite, Cement and Concrete Research 13 (1983), H. 4, S. 511–518.

[76] Murat, M.; Comel, C.: Hydration reaction and hardening of calcined clays and related minerals III. Influence of calcination process of kaolinite on mechanical strengths of hardened metakaolinite, Cement and Concrete Research 13 (1983), H. 5, S. 631–637.

[77] Sayanam, R. A.; Kalsotra, A. K.; Mehta, S. K.; et al: Studies on thermal transformations and pozzolanic activities of clay from Jammu region (India), Journal of Thermal Analysis 35 (1989), S. 99–106.

[78] NFP 15-402 (The French standard): Elaboration de liants pouzzolaniques à moyenne température et études de leurs propriétés physico-chimiques et mécaniques. Doctorat ès Sciences, Institut National des Sciences Appliqués de Lyon, France (in French). .

[79] TCXDVN 395: 2007 (The Vietnamese construction standard): Mineral Admixtures for Roller-Compacted Concrete (2007).

[80] TCXDVN 311: 2004 (The Vietnamese construction standard): Highly activity puzzolanic admixtures for concrete and mortar: Silicafume and rice husk ash (2004).

[81] Sinthaworn, S.; Nimityongskul, P.: Quick monitoring of pozzolanic reactivity of waste ashes, Waste Management 29 (2009), S. 1526–1531.

[82] Pourkhorshidi, A. R.; Najimi, M.; Parhizkar, T.; et al: Applicability of the standard specifications of ASTM C618 for evaluation of natural pozzolans, Cement and Concrete Composites 32 (2001), S. 794–800.

[83] Metin, A.; Konstantin, S.; Tomris, E.; Asim, Y.; Pelin, T.: Properties of blended cements with thermally activated kaolin, Construction and Building Materials 23 (2009), H. 1, S. 62–70.

[84] Habert, G.; Choupay, N.; Escadeillas, G.; Guillaume, D.; Montel, J. M.: Clay content of argillites: Influence on cement based mortars, Applied Clay Science 43 (2009), S. 322–330.

[85] Yimin, C.; Shuangxi, Z.; Wensheng, Z.: Effect of coal gangue with different kaolin contents on compressive strength and pore size of blended cement paste, Journal of Wuhan University of Technology - Materials Science Edition 23 (2008), H. 1, S. 12–15.

[86] Changling, H.; Bjarne, O.; Emil, M.: Pozzolanic reactions of six principal clay minerals: Activation, reactivity assessments and technological effects, Cement and Concrete Research 25 (1995), H. 8, S. 1691–1702.

[87] Ambroise, J.; Murat, M.; Péra, J.: Hydration reaction and hardening of calcined clays and related minerals V. Extension of the research and general conclusions, Cement and Concrete Research 15 (1985), H. 2, S. 261–268.

[88] Kuo, W. Y.; Huang, J. S.; Lin, C. H.: Effects of organo-modified montmorillonite on strengths and permeability of cement mortars, Cement and Concrete Research 36 (2006), H. 5, S. 886–895.

[89] Zibouche, F.; Kerdjoudj, H.; Lacaillerie, J. B. E.; Damme, H. V.: Geopolymers from Algerian metakaolin. Influence of secondary minerals, Applied Clay Science 43 (2009), H. 3-4, S. 453–458.

[90] Kaloumenou, K.; Badogiannis, E.; Tsivilis, S.; Kakali, G.: Effect of the kaolin particle size on the pozzolanic behaviour of the metakaolinite produced, Journal of Thermal Analysis and Calorimetry 56 (1999), S. 901–907.

[91] Lagier, F.; Kurtis, K. E.: Influence of Portland cement composition on early age reactions with metakaolin, Cement and Concrete Research 37 (2007), H. 10, S. 1411–1417.

[92] Mostafa, N. Y.; El-Hamaly, S. A. S.; Al-Wakeel, E. I.; El-Korashy, S. A.; Brown, P. W.: Characterization and evaluation of the pozzolanic activity of Egyptian industrial by-products: I: Silica fume and dealuminated kaolin, Cement and Concrete Research 31 (2001), H. 3, S. 467–474.

[93] Janotka, I.; Puertas, F.; Palacios, M.; Kuliffayová, M.; Varga, C.: Metakaolin sand–blended-cementnext term pastes: Rheology, hydration process and mechanical properties, Construction and Building Materials 24 (2010), H. 5, S. 791–802.

[94] Damidot, D.; Bellmann, F.; Möser, B.; et al: Measurement and simulation of the dissolution rate of minerals in conditions close to cement paste: From gypsum to tricalcium silicate, 17 Ibausil (2009), B 2.81.

[95] Justice, J. M.; Kurtis, K. E.: Influence of metakaolin surface area on properties of cement-based materials, Journal of Material in Civil Engineering (2007), S. 762–771.

[96] Said-Mansour, M.; Kadri, E.; Kenai, S.; Ghrici, M.: Influence of fineness of active addition on concrete equivalent mortar properties, ICCBT 2008 (2008), S. 539–547.

[97] Pavlov, V. F.; Shalamova, I. V.: Effect of the mineralogical composition on sintering at a rapid firing, Glass and Ceramics 37 (1980), H. 3, S. 134–137.

[98] Albuquerque, F. R.; Parente, B.; Lima, S. J. G.; Paskocimas, C. A.; Longo, E.; Souza, A. G. et al.: Thermal transformations of tile clay before and after kaolin addition, Journal of Thermal Analysis and Calorimetry 75 (2004), S. 677–685.

[99] Mayoral, M. C.; Izquierdo, M. T.; Andrés, J. M.; Rubio, B.: Aluminosilicates transformations in combustion followed by DSC, Thermochimica Acta 373 (2001), H. 2, S. 173–180.

[100] Vorno, B.: Experimental determination of muscovite polymorph stabilities, American Mineralogist 50 (1965), S. 436–449.

[101] Rahier, H.; Wullaert, B.; van Mele, B.: Influence of the degree of dehydroxylation of kaolinite on the properties of aluminosilicate glasses, Journal of Thermal Analysis and Calorimetry 62 (2000), S. 417–427.

[102] Roberto, G.: ynthesis, dealumination, and adsorption behaviour of mordenite extrudates, PhD Thesis, Swiss Federal Institute of Technology, Zurich (1999).

[103] Ibrahim, D. M.; Kabish, A. M.; Ghoneim, N.: Thermal behaviour of some raw materials and ceramic mixes, Thermochimica Acta 75 (1984), H. 1-2, S. 43–50.

[104] Traoré, K.; Gridi-Bennadji, F.; Blanchart, P.: Significance of kinetic theories on the recrystallization of kaolinite, Thermochimica Acta 451 (2006), H. 1-2, S. 99–104.

[105] Yeskis, D.; Gross, A. F. K.; Guggenheim, S.: The dehydroxylation of kaolinite, American Mineralogist 70 (1985), S. 159–164.

[106] Kienow, S.; Harders, F.: Feuerfestkunde (Herstellung, Eigenschaften und Verwendung feuerfesten Baustoffe), Springer, Berlin 1960 .

[107] Salmang, H.; Scholze, H.: Keramik Teil I. Allgemeine, Grundlagen und wichtige Eigenschaften, Springer, Berlin (1962).

[108] Sa´nchez-Soto, P. J.; Jime´nez Haro, M. del C.; Pe´rez-Maqueda, L. A.; Varona, I.; Pe´rez-Rodrı´guez, J. L.: Effects of Dry Grinding on the Structural Changes of Kaolinite Powders, Journal of the American Ceramic Society 83 (2000), S. 1649–1657.

[109] Horváth, E.; Frost, R. L.; Makó, E.; Kristóf, J.; Cseh, T.: Thermal treatment of mechanochemically activated kaolinite, Thermochimica Acta 404 (2003), H. 1-2, S. 227–234.

[110] Takahashi, H.: Effect of dry grinding on kaolin minerals, In Clays and Clay Minerals, Sixth National Conference on Clays and Clay Minerals 6 (1959), S. 279–291.

[111] Murat, M.; Driouche, M.: Conductimetric investigations on the dissolution of metakaolinite in dilute hydrofluoric acid. Structure implications., Clay Minerals 23 (1988), S. 55–67.

[112] Day, R. L.; Shi, C.: Influence of the fineness of pozzolan on the strength of lime natural-pozzolan cement pastes, Cement and Concrete Research 24 (1994), H. 8, S. 1485–1491.

[113] Mathurin, D.; Murat, M.: Analyse de l'etat d'amorphisation de la metakaolinite. Etude par calorimetrie de dissolution, Thermochimica Acta 98 (1986), S. 49–55.

[114] Bondar, D.; Lynsdale, C. J.; Ramezanianpour, A. A.: Alkali activation of natural pozzolan for geopolymer cement production, 2nd International Conference on Concrete & Development (April 30th–May 2nd, Tehran, Iran 2005).

[115] Silva, F. J.; Oliveira, M. C.; Thaumaturgo, C.: Oil-well alkali-activated pozzolanic cements, NOCMAT/3-Vietnam International Conference on Non-Conventional Materials and Technologies (2005).

[116] Shi, C.; Day, R. L.: Pozzolanic reaction in the presence of chemical activators: Part I. Reaction kinetics, Cement and Concrete Research 30 (2000), H. 1, S. 51–58.

[117] Shi, C.; Day, R. L.: Pozzolanic reaction in the presence of chemical activators: Part II — Reaction products and mechanism, Cement and Concrete Research 30 (2000), H. 4, S. 607–613.

[118] Xu, H.; Deventer, J. S. J.; Lukey, G. C.: Effect of alkali metals on the preferential geopolymerization of stilbite/kaolinite mixtures, Journal of Industrial & Engineering Chemistry Research 40 (2001), H. 17, S. 3749–3756.

[119] Granizo, M. L.; Maria, S. A.; Varela, T. B.; Palomo, A.: Alkaline activation of metakaolin: effect of calcium hydroxide in the products of reaction, Journal of The American Ceramic Society 85 (2002), H. 1, S. 225–231.

[120] Qian, G.; Li, Y.; Yi, F.; Shi, R.: Improvement of metakaolin on radioactive Sr and Cs immobilization of alkali-activated slag matrix, Journal of Hazardous Materials B92 (2002), S. 289–300.

[121] Shi, C.; Day, R. L.: Acceleration of strength gain of lime-pozzolan cements by thermal activation, Cement and Concrete Research 23 (1993), H. 4, S. 824–832.

[122] Shi, C.; Day, R. L.: Chemical activation of blended cements made with lime and natural pozzolans, Cement and Concrete Research 23 (1993), H. 6, S. 1389–1396.

[123] Li, C.; Sun, H.; Li, L.: A review: The comparison between alkali-activated slag (Si+Ca) and metakaolin (Si+Al) cements, Cement and Concrete Research 40 (2010), S. 1341–1349.

[124] Shi, C.; Day, R. L.: Comparison of different methods for enhancing reactivity of pozzolans, Cement and Concrete Research 31 (2001), H. 5, S. 813–818.

[125] Mehta, P. K.: Mechanism of Expansion Associated with Ettringite Formation, Cement and Concrete Research 3 (1973), S. 1–6.

[126] Frías, M.; Cabrera, J.: Influence of metakaolin on the reaction kinetics in metakaolin/lime and metakaolin-blended cement systems at 20°C, Cement and Concrete Research 31 (2001), H. 4, S. 519–527.

[127] Frías Rojas, M.; Sánchez Rojas, M. I. de: The effect of high curing temperature on the reaction kinetics in MK/lime and MK-blended cement matrices at 60 °C, Cement and Concrete Research 33 (2003), H. 5, S. 643–649.

[128] Talero, R.: Performance of metakaolin and Portland cements in ettringite formation as determined by ASTM C 452-68: kinetic and morphological differences, Cement and Concrete Research 35 (2005), H. 7, S. 1269–1284.

[129] Oriol, M.; Pera, J.: Pozzolanic activity of metakaolin under microwave treatment, Cement and Concrete Research 25 (1995), H. 2, S. 265–270.

[130] Stark, J.; Wicht, B.: Zement und Kalk, Der Baustoff als Werkstoff, Birkhäuser, Basel (2000).

[131] Silva, P. S.; Glasser de, F. P.: Phase relations in the system CaO-Al2O3---SiO2---H2O relevant to metakaolin - calcium hydroxide hydration, Cement and Concrete Research 23 (1993), H. 3, S. 627–639.

[132] Cabrera, J.; Frías Rojas, M. de: Mechanism of hydration of the metakaolin-lime-water system, Cement and Concrete Research 31 (2001), H. 2, S. 177–182.

[133] Frías Rojas, M.; Cabrera, J.: The effect of temperature on the hydration rate and stability of the hydration phases of metakaolin–lime–water systems, Cement and Concrete Research 32 (2002), H. 1, S. 133–138.

[134] Frías Rojas, M.: Study of hydrated phases present in a MK–lime system cured at 60 °C and 60 months of reaction, Cement and Concrete Research 36 (2006), H. 5, S. 827–831.

[135] Mehta, P. K.; Monteiro, P. J. M.: Concrete: Microstructure, Properties, and Materials, College Custom Series, Germany (1993).

[136] Page, C. L.; Page, M. M.: Durability of concrete and cement composites, CRC Press; Woodhead Publ., Cambridge (2007).

[137] Aligizaki, K. K.: Pore structure of cement-based materials, Testing interpretation and requirements, Taylor & Francis, London (2006).

[138] Khatib, J. M.; Wild, S.: Pore size distribution of metakaolin paste, Cement and Concrete Research 26 (1996), H. 10, S. 1545–1553.

[139] Schmidt, M.: Ultra high performance concrete (UHPC), Kassel (2004. p 213-222).

[140] Güneyisi, E.; Gesogˇlu, M.; Mermerdas, K.: Improving strength, drying shrinkage, and pore structure of concrete using metakaolin, Materials and Structures 41 (2008), S. 937–949.

[141] Wild, S.; Khatib, J. M.: Portlandite consumption in metakaolin cement pastes and mortars, Cement and Concrete Research 27 (1997), H. 1, S. 137–146.

[142] Wild, S.; Khatib, J. M.; Jones, A.: Relative strength, pozzolanic activity and cement hydration in superplasticised metakaolin concrete, Cement and Concrete Research 26 (1996), H. 10, S. 1537–1544.

[143] Parande, A. K.; Ramesh Babua, B.; Aswin Karthik, M.; Deepak Kumaar, K. K.; Palaniswamy, N.: Study on strength and corrosion performance for steel embedded in metakaolin blended concrete/mortar, Construction and Building Materials 22 (2008), H. 3, S. 127–134.

[144] Poon, C. -S; Lam, L.; Kou, S. C.; Wong, Y. -L; Wong, R.: Rate of pozzolanic reaction of metakaolin in high-performance cement pastes, Cement and Concrete Research 31 (2001), H. 9, S. 1301–1306.

[145] Roy, D. M.; Arjunan, P.; Silsbee, M. R.: Effect of silica fume, metakaolin, and low-calcium fly ash on chemical resistance of concrete, Cement and Concrete Research 31 (2001), H. 12, S. 1809–1813.

[146] Badogiannis, E.; Papadakis, V. G.; Chaniotakis E.; Tsivilis, S.: Exploitation of poor Greek kaolins: strength development of metakaolin concrete and evaluation by means of k-value, Cement and Concrete Research 34 (2004), H. 6, S. 1035–1041.

[147] Poon, C. S.; Kou, S. C.; Lam, L.: Compressive strength, chloride diffusivity and pore structure of high performance metakaolin and silica fume concrete, Construction and Building Materials 20 (2006), H. 10, S. 858–865.

[148] Kim, H. S.; Lee, S. H.; Moon, H. Y.: Strength properties and durability aspects of high strength concrete using Korean metakaolin, Construction and Building Materials 21 (2007), H. 6, S. 1229–1237.

[149] Tafraoui, A.; Escadeillas, G.; Lebaili, S.; Vidal, V.: Metakaolin in the formulation of UHPC, Construction and Building Materials 23 (2009), H. 2, S. 669–674.

[150] Stark, J.; Wicht, B.: Dauerhaftigkeit von Beton, Der Baustoff als Werkstoff, Birkhäuser, Basel (2001).

[151] Ichikawa, T.; Miura, M.: Modified model of alkali-silica reaction, Cement and Concrete Research 37 (2007), S. 1291–1297.

[152] Thomas, M.: The effect of supplementary cementing materials on alkali-silica reaction: A review, Cement and Concrete Research 41 (2011), S. 1224–1231.

[153] Aquino, W.; Lange, D. A.; Olek, J.: The influence of metakaolin and silica fume on the chemistry of alkali–silica reaction products, Cement and Concrete Composites 23 (2001), H. 6, S. 485–493.

[154] Ramlochan, T.; Thomas, M.; Gruber, A. Karen: The effect of metakaolin on alkali–silica reaction in concrete, Cement and Concrete Research 30 (2000), H. 3, S. 339–344.

[155] Bellmann, F.; Möser, B.; Stark, J.: Influence of sulfate solution concentration on the formation of gypsum in sulfate resistance test specimen, Cement and Concrete Research 36 (2006), S. 358–363.

[156] Erlin, B.; Stark, D. C.: Identification and occurrence of tbaumasite in concrete, Highway Research Record (1965 (115)), S. 108–113.

[157] Khatib, J. M.; Wild, S.: Sulphate resistance of metakaolin mortar, Cement and Concrete Research 28 (1998), H. 1, S. 83–92.

[158] Smallwood, I.; Wild, S.; Morgan, E.: The resistance of metakaolin – Portland cement concrete to the thaumasite-type of sulfate attack —Programme of research and preliminary results, Cement and Concrete Composites 25 (2003), H. 8, S. 931–938.

[159] Al-Akhras, N. M.: Durability of metakaolin concrete to sulfate attack, Cement and Concrete Research 36 (2006), H. 9, S. 1727–1734.

[160] Gonçalves, J. P.; Toledo Filho, R. D.; Fairbairn, E. M. R.: Evaluation of magnesium sulphate attack in mortar-metakaolin system by thermal analysis, Journal of Thermal Analysis and Calorimetry 94 (2008), H. 2, S. 511–516.

[161] Vejmelková, E.; Pavlíková, M.; Keppert, M.; Keršner; Z; Rovnaníková, P. et al.: High performance concrete with Czech metakaolin: Experimental analysis of strength, toughness and durability characteristics, Construction and Building Materials 24 (2010), S. 1404–1411.

[162] Hartshorn, S. A.; Sharp, J. H.; Swamy, R. N.: Thaumasite formation in Portland-limestone cement pastes, Cement and Concrete Research 29 (1999), S. 1331–1340.

[163] Pipilikaki, P.; Papageorgiou, D.; Teas, Ch; Chaniotakis, E.; Katsioti, M.: The effect of temperature on thaumasite formation, Cement and Concrete Composites 30 (2008), S. 964–969.

[164] Bensted, J.: Thaumasite—background and nature in deterioration of cements, mortars and concretes, Cement and Concrete Composites 21 (1999), S. 117–121.

[165] Justice, J. M.; Kennison, L. H.; Mohr, B. J.; Beckwith, S. L.; McCormick, L. E.; Wiggins, B. et al.: Comparison of two metakaolins and a silica fume used as supplementary cementitious materials, Proc.

Seventh International Symposium on Utilization of High-Strength/High Performance Concrete; Washington D.C (2005).

[166] Phungthithu, H.; Ludwig, H. M.; Kletti, H.: Utilizing Vietnamese kaolin for manufacturing metakaolin as an additive in HPC, AdIPoC, International RILEM Conference on Material Science - Volume III, AdIPoC, Aachen, Germany (2010), S. 329–344. Online verfügbar unter http://www.gbv.de/dms/tib-ub-hannover/662038886.pdf.

[167] Quercia Bianchi, G.; Brouwers, H. J. H.; Hüsken, G.: Water layer thickness of silica fines and their effect on the workability of cement pastes, Proceedings 12th International Congress on the Chemistry of Cement, Madrid, 3-8th July 2011. Spain. (2011), S. 386.

[168] Quercia, G.; Hüsken, G.; Brouwers, H. J. H.: Water demand of amorphous nano silica and its impact on the workability of cement paste, Cement and Concrete Research 42 (2012), S. 344–357.

[169] Roy, D. M.; Jiang, W.; Silsbee M. R.: Chloride diffusion in ordinary, blended, and alkali-activated cement pastes and its relation to other properties, Cement and Concrete Research 30 (2000), H. 12, S. 1879–1884.

[170] Asbridge, A. H.; Page, C. L.; Page, M. M.: Effects of metakaolin, water/binder ratio and interfacial transition zones on the microhardness of cement mortars, Cement and Concrete Research 32 (2002), H. 9, S. 1365–1369.

[171] Badogiannis, E.; Tsivilis, S.: Exploitation of poor Greek kaolins: Durability of metakaolin concrete, Cement and Concrete Composites 31 (2009), H. 2, S. 128–133.

[172] Dhir, R. K.; Hewlett, P. C.; Csetenyi, L. J.: Innovations and developments in concrete materials and construction, Proceedings of the International Conference held at the University of Dundee, Scotland, UK on 9-11 September. p354-364., University.Thomas Telford, London (2002).

[173] Coleman, N. J.; Page, C. L.: Aspects of the pore solution chemistry of hydrated cement pastes containing metakaolin, Cement and Concrete Research 27 (1997), H. 1, S. 147–154.

[174] Asbridge, A. H.; Chadbourn, G. A.; Page, C. L.: Effects of metakaolin and the interfacial transition zone on the diffusion of chloride ions through cement mortars, Cement and Concrete Research 31 (2001), H. 11, S. 1567–1572.

[175] Wild, S.; Khatib J. M.; Roose L. J.: Chemical shrinkage and autogenous shrinkage of Portland cement-metakaolin pastes, Advances in Cement Research 10 (1998), H. 3, S. 109–119.

[176] Brooks, J. J.; Megat Johari, M. A.: Effect of metakaolin on creep and shrinkage of concrete., Cement and Concrete Composites 23 (2001), H. 6, S. 495–502.

[177] Gleize, P. J. P.; Cyr, M.; Escadeillas, G.: Effects of metakaolin on autogenous shrinkage of cement pastes, Cement and Concrete Composites 29 (2007), H. 2, S. 80–87.

[178] Frías, M.; Sánchez Rojas, M. I. de; Cabrera, J.: The effect that the pozzolanic reaction of metakaolin has on the heat evolution in metakaolin-cement mortars, Cement and Concrete Research 30 (2000), H. 2, S. 209–216.

[179] Snelson, D. G.; Wild, S.; O'Farrell, M.: Heat of hydration of Portland cement–metakaolin–fly ash blends, Cement and Concrete Research 38 (2008), H. 6, S. 832–840.

[180] Gani, M. S. J.: Cement and concrete, 1. ed., Chapman & Hall, London (1997).

[181] Diamond, S.; Sahu, S.: Densified silica fume: particle sizes and dispersion in concrete, Materials and Structures 39 (2006), S. 849–859.

[182] Elsayed, A. A.: Influence of Silica Fume, Fly Ash, Super Pozz and High Slag Cement on Water Permeability and Strength of Concrete, Jordan Journal of Civil Engineering 5 (2011), H. 2, S. 245–257.

[183] Mostafa, N. Y.; Mohsen, Q.; El-Hemaly, S. A. S.; El-Korashy, S. A.; Brown, P. W.: High replacements of reactive pozzolan in blended cements: Microstructure and mechanical properties, Cement and Concrete Composites 32 (2010), S. 386–391.

[184] Christina, K. Yip; Grant, C. L.; John, L. P.; Jannie S. J.D.: Effect of calcium silicate sources on geopolymerisation, Cement and Concrete Research 38 (2008), H. 4, S. 554–564.

[185] Duxson, P.; Lukey, G. C.; Deventer J. S. J.: The thermal evolution of metakaolin geopolymers: Part 2 – Phase stability and structural development, Journal of Non-Crystalline Solids 353 (2007), S. 2186–2200.

[186] Duxson, P.; Lukey, G. C.; Deventer, J. S. J.: Thermal evolution of metakaolin geopolymers: Part 1 – Physical evolution, Journal of Non-Crystalline Solids 352 (2006), S. 5541–5555.

[187] Duxson, P.; Fernández-Jiménez, A.; Provis, J. L.; Lukey, G. C.; Palomo, A.; Deventer, J. S. J.: Geopolymer technology: the current state of the art, Journal of Materials Science 42 (2007), S. 2917–2933.

[188] Day, R. L.: Pozzolans for use in low-cost housing, International Development Research Centre, Ottawa, Canada (1990).

[189] Marsh, B. K.; Day, R. L.: Pozzolanic and cementitious reactions of fly ash in blended cement pastes, Cement and Concrete Research 18 (1988), S. 301–310.

[190] Haines, P. J.: Principles of thermal analysis and calorimetry, The Royal Society of Chemistry (2002).

[191] Adamiec, P.; Benezet, J. C.; Benhassaine, A.: Pozzolanic reactivity of silico-aluminous fly ash, Particuology 6 (2008), H. 2, S. 93–98.

[192] Steven, M. R.; James, W. R.: Crystal structure of a pink muscovite from Archer's Post, Kenya: implications for reverse pleochroism in dioctahedral micas, Mineralogical Magazine 67 (1982), S. 69–75.

[193] Milan, R.; Giancarlo, C.; D'yakonov, Y. S.; Kamenetski, V. F.; Gottardi, G.; Guggenheim, S. et al.: Nomenclature of the micas, The Canadian Mineralogist 36 (1998), S. 41–48.

[194] TCVN 1770 : 1986 (The Vietnamese standard): Sand for construction - Technical requirement (1986).

[195] Sika Deutschland GmbH: Sicherheitsdatenblatt: http://deaddconst01.webdms.sika.com/fileshow.do?documentID=646 (Retrieved 05/2010).

[196] Chandra, S.: Waste materials used in concrete manufacturing, Noyes Publications, Westwood, NJ (1997).

[197] Helena, S. S.; Teresa, W. C.: Thermal phase sequences in gibbsite/kaolinite clay: electron microscopy studies, Ceramics International 31 (2005), S. 1077–1084.

[198] Chmielova´, M.; Weiss, Z.: Determination of structural disorder degree using an XRD profile fitting procedure. Application to Czech kaolins, Applied Clay Science 22 (2002), S. 65–74.

[199] Aparicio, P.; Galan, E.: Mineralogical interference on kaonilite crystallinity index measurement, Clays and Clay Minerals 47 (1999), H. 1, S. 12–27.

[200] Hinckley, D. N.: Variability in ‘‘crystallinity’’ values among the kaolin deposits of the coastal plain of Georgia and South Carolina, Clays and Clay Minerals 11 (1963), S. 229–235.

[201] Krause, E.; Berger, I.; Kröckel, O.; Maier, P.: Technologie der Keramik, 3 Bände, Druckhaus "Maxim Gorki", Berlin, Germany (1985 (4).

[202] Adylov, G. T.; Kulagina, N. A.; Menosmanova, G. S.; Rumi, M. Kh; Faiziev, Sh A.: Ceramogranite made from natural minerals found in Uzbekistan, Glass and Ceramics 64 (2007), H. Nos. 11 – 12, S. 413–415.

[203] Yoder, H. S.; Eugster, H. P.: Synthetic and natural muscovites, Geochimica et Cosmochimica Acta 8 (1955), H. 5-6, S. 225–230.

[204] Gridi-Bennadji, F.; Beneu, B.; Laval, J. P.; P. Blanchart, P.: Structural transformations of Muscovite at high temperature by X-ray and neutron diffraction, Applied Clay Science 38 (2008), S. 259–267.

[205] Mazzucato, E.; Artioli, G.; Gualtieri, A.: High temperature dehydroxylation of muscovite-2M1: a kinetic study by in situ XRPD, Physics and Chemistry of Minerals 26 (1999), S. 375–381.

[206] Dow, C.; Glasser, F. P.: Alkali releases from crushed minerals and thermally activated constituents of metakaolin, Advances in Cement Research 15 (2003), H. 4, S. 137–143.

[207] Dreher, P.; Niederbudde, E. -A: Potassium release from micas and characterization of the alteration products, Clay Minerals 29 (1994), S. 77–85.

[208] Hanu, L. G.; Simon, G. P.; Cheng, Y. B.: Preferential orientation of muscovite in ceramifiable silicone composites, Materials Science and Engineering A 398 (2005), S. 180–187.

[209] Gridi-Bennadji, F.; Chateigner, D.; Di Vitaa, G.; Blanchart, P.: Mechanical properties of textured ceramics from muscovite–kaolinite alternate layers, Journal of the European Ceramic Society 29 (2009), S. 2177–2184.

[210] Lundgren, L. W.: Muscovite reactions and partial melting in south-eastern connecticut, Journal of Petrology 7 (1966), H. 3, S. 421–453.

[211] Brearley, A. J.; Rubie, D. C.: Effects of H2O on the disequilibrium breakdown of muscovite + quartz, Journal of Petrology 31 (1990), H. 4, S. 925–956.

[212] Chermak, J. A.; Rimstidt, J. D.: The hydrothermal transformation rate of kaolinite to muscovite / illite, Geochimica et Cosmochimica Acta (1990), H. 54, S. 2979–2990.

[213] Kletti, H.: Petrogonese des Obsidians von Hindere, PhD Thesis in the University of Jena, Germany (2002).

[214] Moodi, F.; Ramezanianpour, A. A.; Safavizadeh, A. Sh: Evaluation of the optimal process of thermal activation of kaolins, Scientia Iranica A 18 (2011), H. 4, S. 906–912.

[215] Said-Mansour, M.; Kadri, E. H.; Kenai, S.; Ghrici, M.; Bennaceur, R.: Influence of calcined kaolin on mortar properties, Construction and Building Materials 25 (2011), S. 2275–2282.

[216] DIN EN 196-5: Methods of testing cement - Part 5: Pozzolanicity test for pozzolanic cement (2005).

[217] Schindler, A. K.; Folliard, K. J.: Influence of supplementary cementing materials on the heat of hydration of concrete, Advances in cement and concrete, IX Conference Copper Mountain Conference Resort in Colorado, 10-14 August (2003).

[218] Sha, W.; Pereira, G. B.: Differential scanning calorimetry study of ordinary Portland cement paste containing metakaolin and theoretical approach of metakaolin activity, Cement and Concrete Composites 23 (2001), H. 6, S. 455–461.

[219] Gava, G. P.; Prudêncio Jr, L. R.: Pozzolanic activity tests as a measure of pozzolans' performance. Part 1, Magazine of Concrete Research 59 (2007), H. 10, S. 729–734.

[220] Nguyen, S. M.; Nguyen, D. T.; Hoang, M. D.; Phungthithu, H.: Research into manufacture of high-early-strength concrete (Rn28=60-80MPa) used for building of constructions in Hanoi capital, Science and Technology Programme, code 01C-04/03-2005-1, Hanoi capital (2005).

[221] Pham, D. A.: Research in technology development for ultra high performance concrete in bridge structures, University of Transport and Communications (2010).

[222] Bui, D. D.: Rice husk ash as a mineral admixture for HPC, PhD Thesis in Technische Universiteit Delft, Netherlands (2001).

[223] Nguyen, V. T.: Rice husk ash as a mineral admixture for UHPC, PhD Thesis in Technische Universiteit Delft, Netherlands 2011 .

[224] Wedsite (Nation hydro-meteorological service, Nation centre for hydro-meteorological forecasting): Intense heat waves for July and August in 2010, http://www.nchmf.gov.vn (Retrieved 9/2010).

[225] Wedsite (Nation hydro-meteorological service, Nation centre for hydro-meteorological forecasting): Cold weather damage for January and February in 2008, http://www.nchmf.gov.vn (Retrieved 9/2010).

[226] Matschei, T.; Lothenbach, B.; Glasser, F. P.: The role of calcium carbonate in cement hydration, Cement and Concrete Research 37 (2007), H. 4, S. 551–558.

[227] Antoni, M.; Rossen, J.; Martirena, F.; Scrivener, K.: Cement substitution by a combination of metakaolin and limestone, Cement and Concrete Research 42 (2012), S. 1579–1589.

[228] ASTM C1293 C1293-08b (The american standard): Standard test method for determination of length change of concrete due to Alkali-Silica Reaction .

[229] CAN/CSA A23.2 – 14A (The Canadian standards association): Potential expansivity of aggregates (procedure for length change due to Alkali-Aggregate Reaction in concrete prisms) .

[230] Giebson, C.; Seyfarth, K.; Stark, J.: Influence of acetate and formate-based deicers on ASR in airfield concrete pavements, Cement and Concrete Research 40 (2010), S. 537–545.

[231] CAN/CSA A23.2 – 25A (The Canadian standards association): Test method for detection of Alkali-Silica Reactive Aggregate by accelerated expansion of mortar bars .

[232] Grattan-Bellew, P. E.; Cybanski, G.; Fournier, B.; Mitchell, L.: Proposed universal accelerated test for alkali-aggregate reaction: the concrete microbar test, Cement Concrete and Aggregates 25 (2003), H. 2, S. 29–34.

[233] DAFSTH (The German test method): The German Alkali-Guideline (2007) alternative method for ASR .

[234] Diamond, S.: Effects ofmicrosilica (silica fume) on pore-solution chemistry of cement pastes, Communications of the American Ceramics Society (1983), S. 82–84.

[235] Kollek, J. J.; Varma, S. P.; Zaris, C.: Measurement of OH− concentrations of pore fluids and expansion due to alkali-silica reaction in composite cement mortars, The 8th International Congress on the Chemistry of Cement (1986), H. 3, S. 183–189.

[236] Kagimoto, H.; Sato, M.; Kawamura, M.: Threshold OH- ion concetnration in pore solution of mortar using 2 to 3 types of alkali reactive aggregate, Transactions of the Japan Concrete Institute (2001), H. 23, S. 171–178.

[237] Bentur, A.; Diamond, S.; Berke, N. S.: Steel corrosion in concrete, Fundamentals and civil engineering practice, 1. ed., E & FN Spon, London (1997).

[238] Stark, J.; Seyfarth, K.; Giebson, C.: Beurteilung der Alkali-Reaktivität von Gesteinskörnungen ung AKR-Performance-Prüfung Beton, Ibausil, 16. Internationale Baustofftagung , 20-23 september (2009), H. 2, S. 399–434.

[239] Hong, S. Y.; Glasser, F. P.: Alkali binding in cement pastes. Part I. The C-S-H phase, Cement and Concrete Research 29 (1999), S. 1893–1903.

[240] Hong, S. Y.; Glasser, F. P.: Alkali sorption by C-S-H and C-A-S-H gels. Part II. Role of alumina, Cement and Concrete Research 32 (2002), S. 1101–1111.

[241] Chen, W.; Brouwers, H. J. H.: Alkali binding in hydrated Portland cement paste, Cement and Concrete Research 40 (210), S. 716–722.

[242] Konan, K. L.; Peyratout, C.; Smith, A.; Bonnet, J. -P; Rossignol, S.; Oyetola, S.: Comparison of surface properties between kaolin and metakaolin in concentrated lime solutions, Journal of Colloid and Interface Science (2009), H. 339, S. 103–109.

[243] Wedsite: Vietnam environment administration – Ministry of natural resources and environment: Companys processing seafood - the culprit causing pollution, http://vea.gov.vn/ (Retrieved 26/5/2010).

[244] Wedsite (Hoang Mai cement): The corrosion destroying cement Portland in the environment of waste water, http://www.ximanghoangmai.vn/ (Retrieved 26/3/2010).

[245] College board. Advanced Placement Programe: AP Chemistry, 2006–2007 Professional Development - Workshop Materials (2007).

[246] Le, Q. T.: Water pollution and its consequences, Faculty of environment and resources- Nonglam University (2009).

[247] American Water Works Association: Basic science concepts and applications, 3. ed., American Water Works Association, Denver, Colo. (2003).

[248] Vietnam News. vnexpress.net: The people accuse the Sonadezi company of repeatedly discharged waste-water into the environment, http://vnexpress.net/ (Retrieved 9/12/2011).

[249] Shi, C.; Krivenko, P.; Roy, D.: Alkali-activated cements and concrete, Taylor & Francis, London (2006).

[250] Tiana, B.; Cohen, M. D.: Does gypsumformation during sulfateattack on concrete lead to expansion?, Cement and Concrete Research 1 (2000), H. 30, S. 117–123.

[251] Torii, K.; Taniguchi, K.; Kawamur, M.: Sulfate resistance of high fly ash content concrete, Cement and Concrete Research 25 (1995), H. 4, S. 759–768.

[252] Malhotra, V. M.; Caretter, G. G.; Sivasundaram, V.: Role of silica fume in concrete: A review, Proceedings. International Symposium on Advantage in Concrete Technology. Athens, 1992. .

[253] Collepardi, M.: A state-of-the-art review on delayed ettringite attack on concrete, Cement and Concrete Composites 25 (2003), S. 401–407.

[254] Makar, J.; Chang G.; Torresf, F.; et al: Effect of n-CaCO3 and metakaolin on hydrated Portland cement, Advances in Cement Research 24 (2012), H. 4, S. 211–219.

[255] Talero, R.: Expansive synergic effect of ettringite from pozzolan (metakaolin) and from OPC, co-precipitating in a common plaster-bearing solution: Part I: By cement pastes and mortars, Construction and Building Materials 24 (2010), H. 9, S. 1779–1789.

[256] Talero, R.: Expansive synergic effect of ettringite from pozzolan (metakaolin) and from OPC, co-precipitating in a common plaster-bearing solution. Part II: Fundamentals, explanation and justification, Construction and Building Materials 25 (2011), H. 3, S. 1139–1158.

[257] Bensted, J.: Thaumasite—direct, woodfordite and other possible formation routes, Cement and Concrete Composites 25 (2003), H. 8, S. 873–877.

[258] Lee, S. T.; Hooton, R. D.; Jung, H. S.; Park, D. H.; Choi, C. S.: Effect of limestone filler on the deterioration of mortars and pastes exposed to sulfate solutions at ambient temperature, Cement and Concrete Research 38 (2008), S. 68–76.

[259] Irassar, E. F.; Bonavetti, V. L.; Trezza, M. A.; Gonzalez, M. A.: Thaumasite formation in limestone filler cements exposed to sodium sulphate solution at 20 oC, Cement and Concrete Composites 27 (2005), S. 7–84.

[260] Skaropoulou, A.; Tsivilis, S.; Kakali, G.; Sharp, J. H.; Swamy, R. N.: Thaumasite form of sulfate attack in limestone cement mortars: A study on long term efficiency of mineral admixtures, Construction and Building Materials 23 (2009), S. 2338–2345.

[261] Sahu, S.; Badger, S.; Thaulow, N.: Mechanism of thaumasite formation in concrete slabs on grade in Southern California, Cement and Concrete Composites 25 (2003), S. 889–897.

[262] Sahu, S.; Badger, S.; Thaulow, N.: Evidence of thaumasite formation in Southern California concrete, Cement and Concrete Composites 24 (2002), S. 379–384.

[263] Diamond, S.: Thaumasite in Orange County, Southern California: an inquiry into the effect of low temperature, Cement and Concrete Composites 25 (2003), S. 1161–1164.

[264] Wedsite:: http://www.quangninh.industry.gov.vn/ (Retrieved 05/2009).

[265] Wedsite:: http://edu.go.vn/ (Retrieved 05/2011).

[266] Wedsite:: http://www.baophutho.org.vn/ (Retrieved 12/2008).

[267] Wedsite:: http://www.yenbai.gov.vn/ (Retrieved 05/2009).

[268] Wedsite:: http://tnmtvinhphuc.gov.vn/ (Retrieved 12/2008).

[269] Wedsite:: http://www.monre.gov.vn/ (Retrieved 11/2008).

[270] Nguyen, D. C.; Pham, V. H.; Le, H. C.: Findings of geological and mineral resources in Hai Duong, Journal No. 4 / 2008 - Science and Technology in Hai Duong (12/2008).

[271] Nguyen, H. M.: Phenpat, kaolin in Da Lat City - Lam Dong, Information of science and technology, Lam Dong No. 3. (1993).

[272] Wedsite:: http://www.dalat.gov.vn/ (Retrieved 6/2011).

[273] Do, C. D.: The quality and specifications of Aluoi kaolin in Thua Thien Hue, Hanoi University of Mining and Geology .

[274] Wedsite:: http://www.binhduong.gov.vn/ (Retrieved 12/2008).

[275] Wedsite: http://www.thuvienbinhdinh.com (Retrieved 05/2009).

[276] People's committee of Quang Binh province: Decision of People's committee about "Approve the development plan of the mining industry in Quang Binh period 2001 -2010 ", 03/2002/QĐ-UB (2002).

13. Appendix

13.1 The quality of kaolin

Table 13.1 The quality of some kaolin in the world

	Chemical [Wt.-%]												
	SiO_2	Al_2O_3	Fe_2O_3	SO_3	TiO_2	CaO	MgO	K_2O	Na_2O	P_2O_5	Cl^-	LOI	Minerals
Denmark kaolin [50]	46	35	1.01	+	0.05	0.06	0.27	1.62	0.06	0.12	+	12	Kaolinite Mica Quartz Microcline
Greece kaolin [38]	39-73	18-35	0.6	2-10	+	0.36 - 0.54	0.03 - 0.06	0.8-2.51	+	+	+	8-22	Kaolinite Alunite Quartz Illite
France kaolin [65, 37]	43-49	34-37	0.79-1.36	+	0.1-3.54	0.01 - 0.07	0.08 -0.2	0.04 - 1.45	0.01	0.07 - 0.11	+	13-16	Kaolinite Anatase Iron oxide Quartz
UK kaolin [37]	48	36	0.71	+	0.05	-	0.26	1.76	0.05	+	+	13	Kaolinite Muscovite Quartz
Hungary kaolin [109]	47	34	3.1	+	0.06	0.53	0.71	0.35	0.16	+	+	15	Kaolinite Feldspar Quartz
USA kaolin [51, 31]	52	43-45	0.25-0.06	0	1.64 - 4.21	0-0.05	0	0-0.16	0-0.21	0-0.01	0	0.5 1	Kaolinite Quartz Anatase
Turkey kaolin [83]	55-67	22-32	0.3-2.7	-	0.1-1.2	0.1-0.2	0.1-0.7	0.1-2.5	0.1	0.1-0.2	+	8-11	Kaolinite Quartz Alunite Tridymite Halloysite
Tunisian [67]	58-63	16-29	1.89-8.02	0.05-1.03	+	0.27 - 2.15	0.24 - 2.38	1.28 - 2.71	0.03-0.18	+	+	+	Kaolinite Quartz Anatase Montmorillonite Muscovite Albite Illite Calcite Haematite Dolomite

- inappreciable content. + no information

Table 13.2 Deposit and quality of Vietnamese kaolin

Mines of kaolin	Deposit, million ton	Chemical Compositions, % wt		Current capacity of manufacturing technology
Quang Ninh [28,264, 265]	- mineral resource: 150 - sound deposit: 15.375 (Tan Mai)	SiO_2	43.88-47.81	
		Al_2O_3	34.60-37.43	
		Fe_2O_3	0.18-0.74	
		TiO_2	0-0.03	
		CaO	0.21-0.76	
		MgO	0-0.15	
		K_2O	0.05-0.10	
		Na_2O	0.03-0.16	
		P_2O_5	0.09	
		LOI	12.51	
Phu Tho* (Thach Khoan, Huu Khanh) [266, 265]	- mineral resource: 16.8 - sound deposit: 3.2 (Thach Khoan)	SiO_2	47.5 - 76.1	35.000 ton/year
		Al_2O_3	22.9 - 35.8	
		Fe_2O_3	0.11 - 2.9	
		LOI	9.81	
Yen Bai* [267]	sound deposit: 1.1 – 1.5 (Yenbai, Tanthinh,Trucbinh, Langcan)	Al_2O_3	29-34	20.000 ton/year
		Fe_2O_3	0.8-4.2	
Vinh Phuc [268]	mineral resource: 4.025	SiO_2	42-83	
		Al_2O_3	10-25	
		Fe_2O_3	0.8-8	
		LOI	6-8	
Thai Nguyen [269]	mineral resource: 20 million cubic meters			
Hai Duong [270]	sound deposit: 0.38 (Chi Linh palce), 10.04 (Phao Son and Minh Tan)			
Lam Dong (Prenn, Trai Mat) [271, 272]	- mineral resource: 520 - sound deposit: 4-6 (Trai Mat), 5-7 (Prenn)	SiO_2	22.8 - 65	
		Al_2O_3	18 - 49	
		Fe_2O_3	0.5 - 7.9	
		LOI	0.16 - 22.5	
Thua Thien Hue* [273]		SiO_2	46.65-73.05	7.000 ton/year
		Al_2O_3	15.27-34.75	
		Fe_2O_3	0.07-10.56	
		TiO_2	0.03-0.66	
		MgO	0.04-1.03	
		K_2O	1.66-4.11	
		Na_2O	3.31-5.63	
		LOI	11.88	
Binh Duong* (Đat Cuoc, Chanh Luu, Binh Hoa) [28, 274]	- mineral resource: 300-320 - sound deposit: 6 (Chanh Luu)			
Binh Dinh [28, 275]	- mineral resource: 37 million cubic meters - sound deposit: 10.1 (Long My)			
Quang Binh [276]	- mineral resource: 30.4 - sound deposit: 18.825 (Bac Ly)	SiO_2	74.55	
		Al_2O_3	17-19	
		Fe_2O_3	1.5	
		TiO_2	0.4	

* The Vietnamese Ministry of Industry has promulgated the plan for 110.000 ton kaolin/year capacity of manufacturing technology that will be invested in 2010-2012 in Thua Thien Hue, Phu Tho, Yen Bai, and Binh Duong.

13.2 Calculation for the Equations 4.3-4

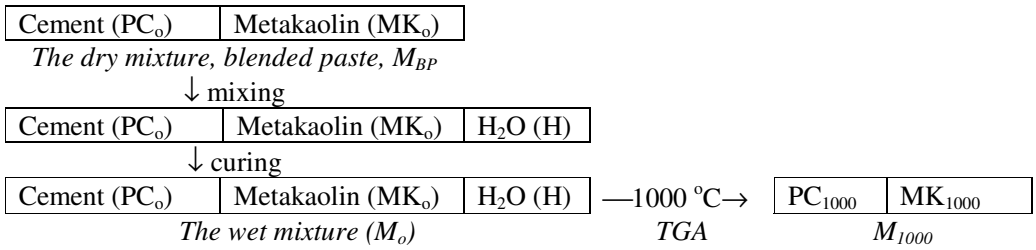

Definitions:

FL_{PC}/FL_{BP}	free lime content in the cement paste/blended paste [mg/g]
M_o/M_{1000}	the mass of samples at a beginning temperature/1000°C during TG analysis [mg]/[g]
M_{CO2}	mass loss of CO_2 content from $CaCO_3$ [g]. $M_{CO2} = 0.01M_ox^*$. Where x^* is mass loss of CO_2 [Wt.-%], x^* was determined like x factor.
x	mass loss of water content from $Ca(OH)_2$ [Wt.-%].
y	the mass loss of metakaolin at 1000 °C during TG analysis [Wt.-%]
α	the mass rate of metakaolin replaced for cement.
M_{BP}	the mass of blended paste

In the dry mixture:

$M_{BP} = PC_o + MK_o$

$PC_o = (1-\alpha)M_{BP}$

$MK_o = \alpha M_{BP}$

In the wet mixture:

$M_o = PC_o + MK_o + H$

After TG analysis:

$PC_o = PC_{1000} + M_{CO2}$

$MK_o = MK_{1000} + MK_o(y/100)$

$M_{1000} = PC_{1000} + MK_{1000}$

Calculation of M_{BP}:

$$\begin{aligned} M_{1000} &= PC_{1000} + MK_{1000} \\ &= (PC_o - M_{CO2}) + [MK_o - MK_o(y/100)] \\ &= (PC_o - M_{CO2}) + MK_o(1-y/100) \\ &= (1-\alpha)M_{BP} - M_{CO2} + \alpha M_{BP}(1-y/100) \end{aligned}$$

$$\Rightarrow M_{BP} = \frac{M_{1000} + M_{CO_2}}{1 - \frac{\alpha.y}{100}}$$

Free lime content:

$Ca(OH)_2$	⟶	CaO_{free}	$+ H_2O$
		56	18
		$56M_ox/1800$	$M_ox/100$

$$FL_{PC} = CaO_{free} / PC_o = \frac{56M_o x}{1800(M_{1000} + M_{CO_2})} \qquad \text{(with } \alpha = 0\text{)}$$

$$FL_{BP} = CaO_{free} / M_{BP} = \frac{56M_o x(1-\frac{\alpha.y}{100})}{1800(M_{1000}+M_{CO_2})} \qquad \text{(in this study: } \alpha = 0.1 - 0.4\text{)}$$

Calculation of x:

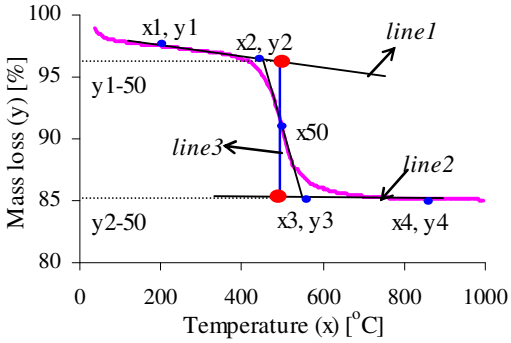

Figure 13.2 The calculation x as [189] and [190].

Line 1:

$y_1 = ax_1 + b$

$y_2 = ax_2 + b$

$b = (x_1y_2 + x_2y_1)/(x_1 + x_2)$

$a = \{[(x_1y_2 + x_2y_1)/(x_1 + x_2)] - y_1\}x_1$

Line 2:

$y_3 = cx_3 + d$

$y_4 = cx_4 + d$

$d = (x_3y_4 + x_4y_3)/(x_3 + x_4)$

$c = \{[(x_3y_4 + x_4y_3)/(x_3 + x_4)] - y_3\}x_3$

Line 3:

$x_{50} = 0.5(x_2 + x_3)$

$y^1_{50} = ax_{50} + b$

$y^2_{50} = cx_{50} + d$

The value of x:

$x = y^1_{50} - y^2_{50}$

13.3 An overview of extraction for Vietnamese kaolin from raw material

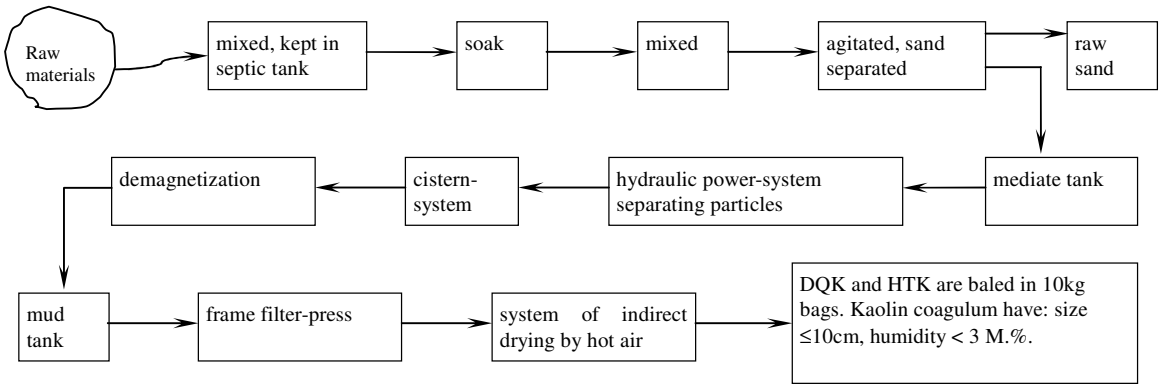

Figure 12.1 extraction for Vietnamese kaolin from raw material

13.4 Particle size distribution of calcinated kaolin

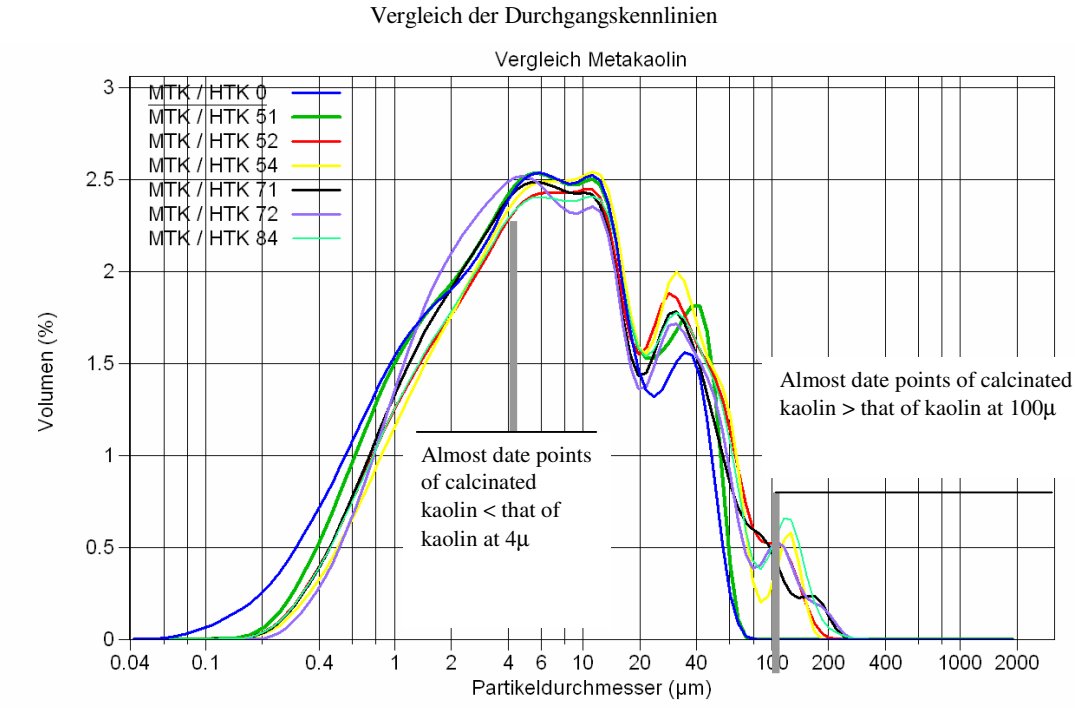

Figure 13.3 Particle size distribution of calcinated HTK kaolin

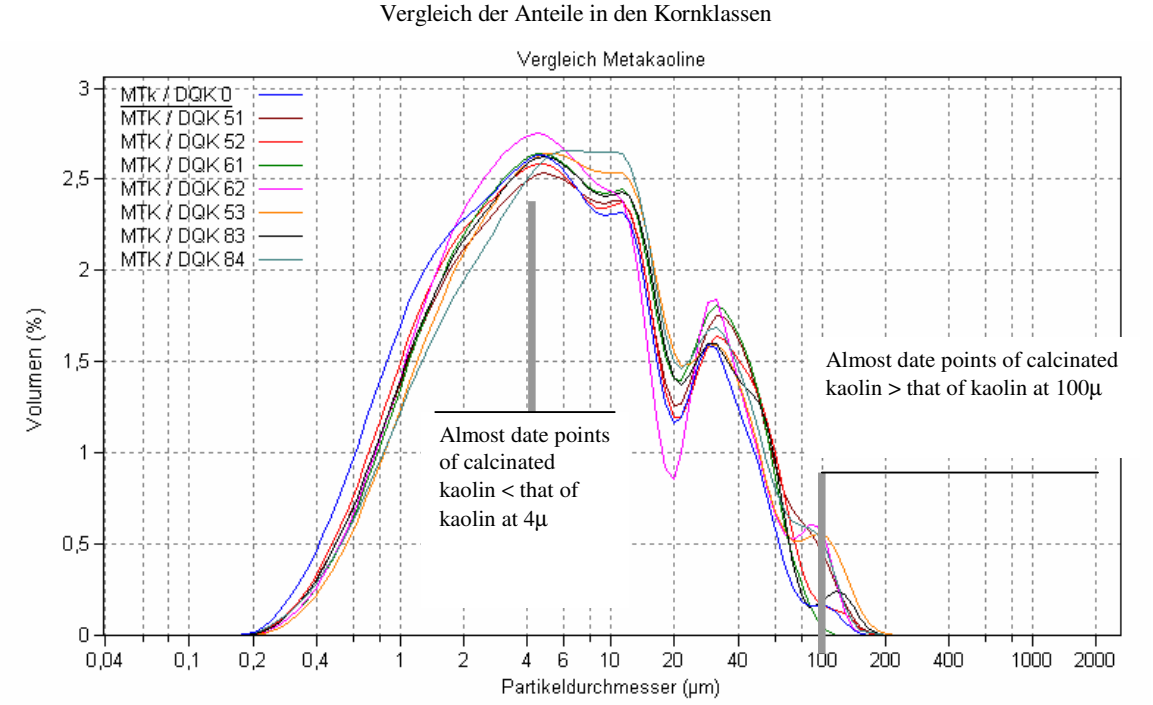

Figure 13.4 Particle size distribution of calcinated DQK kaolin

13.5 Strength development

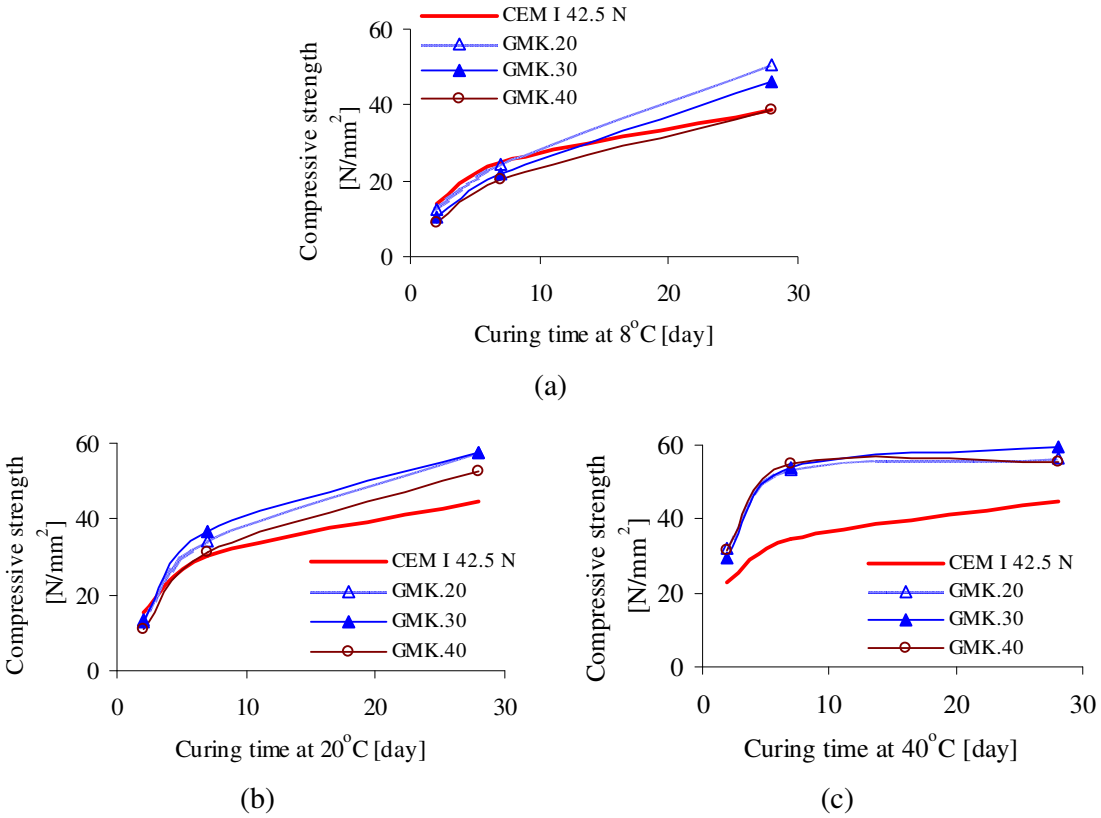

Figure 13.5. Strength development of mortars (form 40×40×160 mm^3, CEM I 42.5 N:metakaolin = 100:0 / 80:20 / 70:30 /60:40 Wt.-%, binder:sand = 1:3, w/b of 0.6, in water at 8-40 °C, the control CEM I 42.5 N)

13.6 Expansion of mortar barsfor ASR

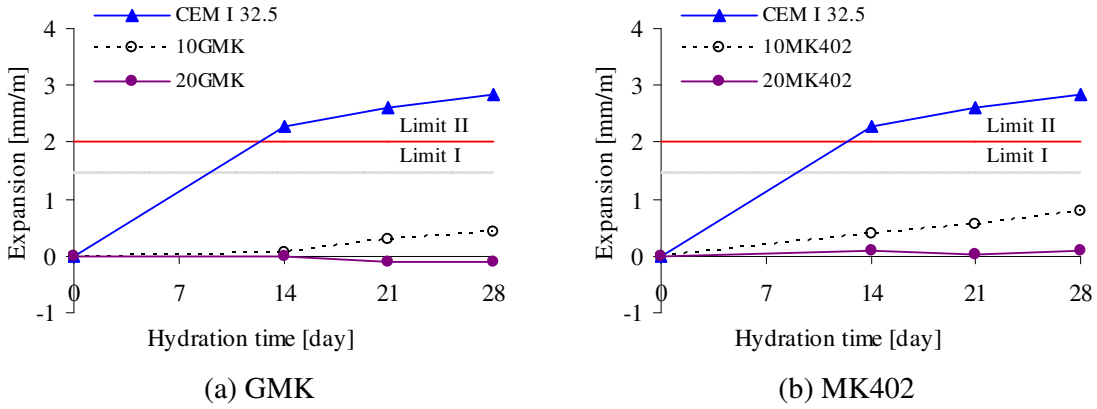

Figure 13.6. The expansion of mortar bars (CEM I 32.5 R:metakaolin=100:0/90:10/80:20Wt.-%, Binder:reactive quartz:solution=1:3:0.5, Water:NaOH:K_2SO_4=1:0.031:0.017, 100%RH, 70°C)